The Institute of Paper Chemistry

Appleton, Wisconsin

Doctor's Dissertation

The Application of the Verwey and Overbeek Theory to the Stability of Kaolinite-Water Systems

William Holtzman

June, 1959

THE APPLICATION OF THE VERWEY AND OVERBEEK THEORY TO THE STABILITY OF KAOLINITE-WATER SYSTEMS

A thesis submitted by

William Holtzman

B.S. 1953, Pennsylvania State College
M.S. 1955, Lawrence College

in partial fulfillment of the requirements
of The Institute of Paper Chemistry
for the degree of Doctor of Philosophy
from Lawrence College,
Appleton, Wisconsin

June, 1959

TABLE OF CONTENTS

INTRODUCTION

The ability of soils and clay minerals to exchange cations with solutions containing other cations has been recognized for many years. Thompson (1) is credited with the first systematic study of cation exchange and voluminous literature has since been published on the subject. In recent years, the possibility of anion exchange in clay minerals has gained recognition and a fund of evidence affirming this possibility has been presented (2, 3, 4). In many cases, these investigations have been oriented to studies of exchange by the crystalline region of the clay particle.

This thesis will be concerned primarily with the manner in which an aqueous kaolinite suspension responds to the addition of dispersing agents or other salts. Because the proposed theory for dispersing agent action depends upon a selective adsorption of anions by the kaolinite particle, the phenomenon of anion exchange at the clay surface—an adsorption phenomenon rather than a crystalline substitution phenomenon—will be considered in detail. This adsorption of anions will be studied under various conditions known to affect the rheological properties of the kaolinite-water system and, as we shall see later, the results of this study will permit us to establish a quantitative theory of dispersing agent action. However, before the theory for dispersing agent action can be presented in an intelligible manner, it is necessary to consider the structure and physical properties of kaolinite and the kaolinite-water system.

THE STRUCTURE OF KAOLINITE

The aluminum-oxygen octahedron and the silicon-oxygen tetrahedron are the basic building units of kaolinite (Figure 1). The silicon-oxygen tetrahedron forms a network having the composition $Si_4O_6(OH)_4$. A simplified model of this network (hydrated silica) is shown in Figure 2. The aluminum-oxygen octahedron, on the other hand, can form a saturated structure consisting only of aluminum and hydroxyl groups. This material, commonly known as gibbsite, is depicted in simplified fashion in Figure 3. These two structural units combine, with the elimination of water, to form kaolinite (Figure 4). It is important to note that the net electrical charge of the structure is zero.

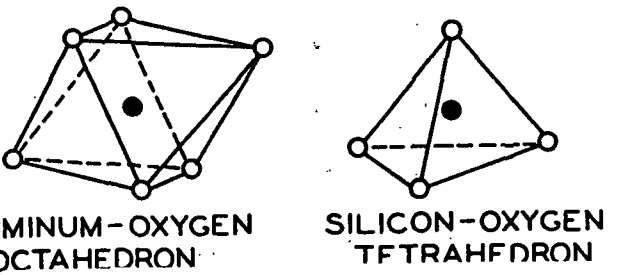

Figure 1.

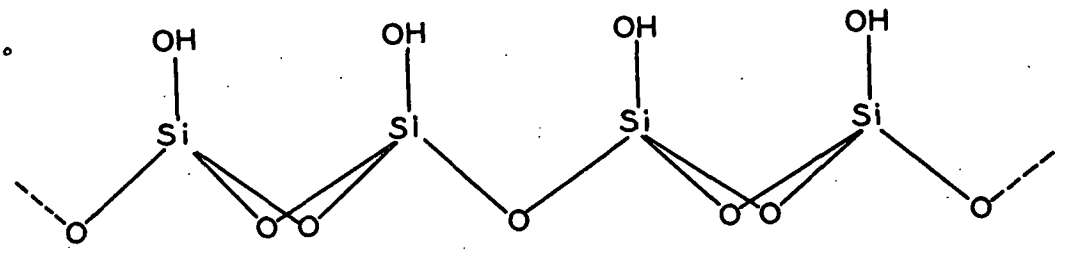

Figure 2. Hydrated Silica Structure

Naturally occurring kaolinite obviously does not consist of a single silica sheet joined to a gibbsite sheet. The exposed hydroxyl

groups of the gibbsite sheet offer an excellent opportunity for hydrogen bonding to occur between a gibbsite layer and a silica layer. Since many such bonds are possible, these layers may be held together very tightly. Thus, kaolinite consists of many alternating layers of silica and gibbsite.

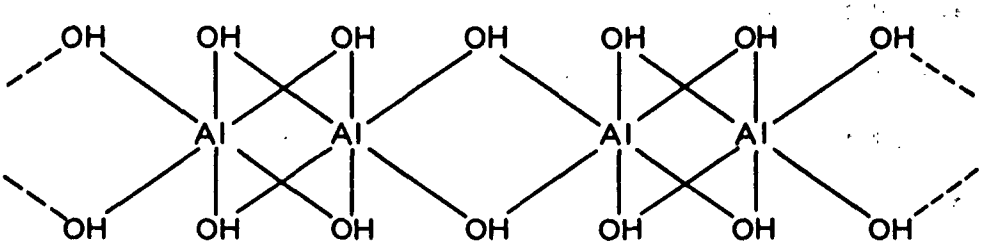

Figure 3. Gibbsite Structure

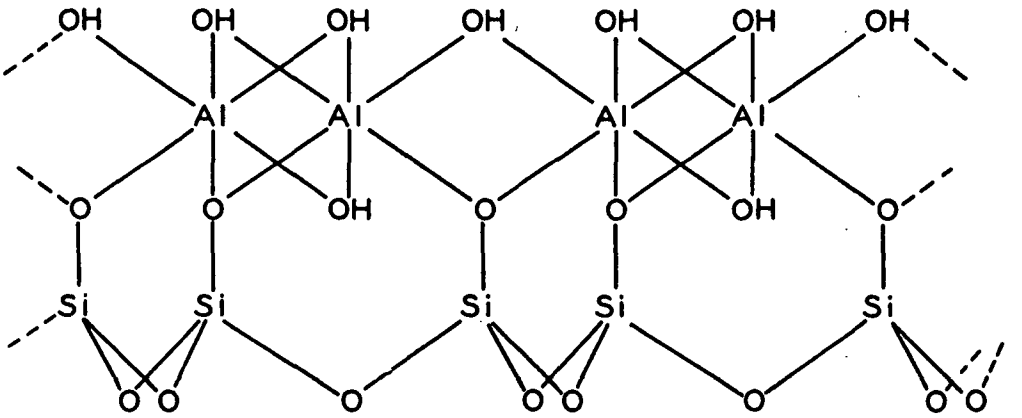

Figure 4. Kaolinite Structure

ORIGIN OF THE ELECTRICAL CHARGE

In general, there are three methods by which clay minerals acquire their charge. The first of these, substitution within the crystal lattice, is of minor importance in kaolinite. Therefore, the crystalline

structure of this mineral is electrically neutral. Presumably, this accounts for the low cation-exchange capacity of kaolinite (3-15 meq. per 100 g.) in comparison with other clay minerals. The montmorillonites, for example, exhibit substitution within the crystal lattice which produces a structure having a net negative charge. As a result, the cation-exchange capacity of these minerals is considerably in excess of that of kaolinite and values greater than 100 meq. per 100 g. clay are not uncommon.

The second and third possible mechanisms for the acquisition of a charge arise from a consideration of the properties of an aqueous kaolinite suspension. If kaolinite is endowed with a neutral crystalline structure, then the electrical charge that the clay particles exhibit in an aqueous medium must, in some manner, be induced by the presence of the water. There are two mechanisms by which this can occur and these differ only in location. The first mechanism was proposed by Johnson and Norton (5) and has since been amplified by Asdell (6, 7), Kingery (8), and others.

Electron micrographs of kaolinite show that the particles of this clay exist as hexagonal plates. The kaolinite particle is most easily cleaved at the plane where the silica layer is hydrogen bonded to the gibbsite layer. Fracture in this plane produces no unsaturation because no primary valence bonds are broken. However, some fracture must occur perpendicular to the basal cleavage plane if hexagonal plates are to be formed. Fracture in this plane does break primary valence bonds and the result is a particle with 'active' areas along the fracture.

These 'active' areas provide sites for the selective adsorption of ions. The ions which can be adsorbed must fit well into the kaolinite lattice and form a substance which is insoluble and slightly dissociated. In an aqueous suspension, no ions are available which could be absorbed on the negative zones of the crystal fragment. Hydroxyl ion, however, readily fulfills the above conditions and is preferentially adsorbed at the positive 'active' areas. The result is a particle coated with negative charges which form the first layer of the so-called electrical double layer.

The third mechanism by which the particle can acquire its charge depends upon a similar adsorption phenomenon occurring at the faces of the crystal instead of at the edges. In this case, however, the selective adsorption of certain anions depends not on a localized unsaturation, but rather on the ability of the anion to hydrogen bond to exposed hydroxyl groups.

The preferentially adsorbed anions are bound firmly to the clay particle and are surrounded by a swarm of counterions which may extend a considerable distance from the surface of the particle. These counterions form the second or diffuse part of the electrical double layer. At distances from the particle greater than the thickness of the Stern layer, the concentration of these ions is believed to increase exponentially as the particle surface is approached. This is in accordance with Boltzmann's theorem. The establishment of the double layer in the manner described above results in a negatively charged kaolinite particle.

THE VERWEY AND OVERBEEK THEORY

The degree of dispersion which a lyophobic colloidal system exhibits has been ascribed to the relative influence of attractive and repulsive forces existing between the colloidal particles. Verwey and Overbeek (9) have considered these forces for several cases, including large parallel plates. The equations derived for this case should govern the kaolinite-water system because individual kaolinite particles are essentially flat plates.

Considering the Van der Waals-London attractive forces, Verwey and Overbeek (10) have shown that the attractive potential energy (V_A) between two parallel plates is equal to

$$V_A = -\frac{A}{48\pi}\left(\frac{1}{d^2} + \frac{1}{(d+\delta)^2} - \frac{2}{(d+\delta/2)^2}\right) \qquad (1)$$

where

d = half the distance of separation of the plates, cm.,

δ = the thickness of the plates, cm., and

A = a constant.

It is important to note that A is constant for a given chemical composition of the mineral. Thus, for a given colloid, the value of A is fixed and V_A will depend only on the separation and the thickness of the plates.

Depending upon the relative values of d and δ, several useful approximations of Equation (1) become apparent, viz.

$$V_A = -\frac{\delta^2 A}{32\pi d^4} \qquad \text{where } d \gg \delta \qquad (2)$$

$$V_A = -\frac{A(1/d^2 - 7/\delta^2)}{48\pi} \qquad \text{where } d < \delta \qquad (3)$$

$$V_A = -\frac{A}{48\pi d^2} \qquad \text{where } d \ll \delta \qquad (4)$$

It will be shown later that the values of d that are of interest are considerably less than those of δ for kaolinite and, consequently, Equation (4) is generally applicable.

The repulsive forces, on the other hand, are not so free from the conditions of the system. The equation derived by Verwey and Overbeek (11) for the repulsive potential energy (V_R) of two parallel plates,[1] each one square centimeter in area, when the double layer interaction is not very extensive is

$$V_R = \frac{32\, nKT\gamma^2}{X}(1 - \tanh Xd) \qquad (5)$$

[1] The development of this equation is based on the following considerations: (a) the Gouy-Chapman model of the electrical double layer with due consideration for Stern's correction to this model, (b) Poisson's equation interrelating the density of the space charge, the electrical potential, and the dielectric constant of the medium, and (c) the free energy of a system of two double layers as a function of their distance of separation. An inherent assumption in the choice of the model is that outside the Stern layer, the distribution of ions is in accordance with the statistical theorem of Boltzmann.

The further mathematical development is based on the implication that the free energy of a system of double layers in interaction is identical with the amount of work associated with some isothermal and reversible process of building up the double layers to that degree of interaction. Hence, the interaction of the double layers is responsible for the repulsion between particles and the free energy change in bringing the particles from an infinite distance of separation to some finite distance of separation is equivalent to the amount of work required to do this.

where

n = the number of ions of opposite charge to the particle contained in one cubic centimeter of intermicellar solution,

K = the Boltzmann constant,

T = the absolute temperature,

X = a parameter related to the reciprocal of the effective thickness of the electrical double layer ($cm.^{-1}$),

d = half the distance of separation of the plates (cm.), and

$$\gamma = \frac{e^{Z/2}-1}{e^{Z/2}+1} \tag{6}$$

and where Z may be expressed by

$$Z = \frac{V\epsilon\psi_o}{300\ KT} \tag{7}$$

in which

V = the valence of the counterions,

ϵ = the charge on the electron (absolute e.s.u.), and

ψ_o = the potential existing between the surface of the particle and the intermicellar solution (volts).

The parameter X in Equation (5) is more precisely defined by the following equation (12):

$$X = \sqrt{\frac{8\pi n\epsilon^2 V^2}{DKT}} \tag{8}$$

where D is the dielectric constant of the intermicellar solution.

We now see that the total potential energy of two flat plates ($V_R + V_A$) is composed of two parts; an attractive potential energy which is fixed for a given colloidal system and a repulsive potential energy which is highly dependent upon the number and type of ions existing in the dispersing

medium. If all the terms in Equations (4) and (5) can be evaluated under a specific set of conditions, it should then be possible to predict the electrical contribution to the rheological properties of the colloidal system at the stated conditions.

PRESENTATION OF THE PROBLEM

It is now evident that a test for the validity of the application of the Verwey and Overbeek theory to kaolinite-water suspensions must be preceded by an evaluation of the terms in Equations (4) and (5). The evaluation of A in Equation (4) and d in Equations (4) and (5) presents special problems which will be considered later in this thesis. The determination of n, on the other hand, is quite simple if the composition of the intermicellar solution is known. This term is obviously the product of the molar concentration of positive ions and the Avogadro number.

The evaluation of n permits the calculation of X quite simply according to Equation (8). This inherently assumes that the dielectric constant of the intermicellar solution (D) remains fixed for all solutions to be considered, regardless of ionic concentration or ionic species present. The plausibility of this assumption is quite simply demonstrated. According to Hasted, Ritson, and Collie (13), the molar depression of the dielectric constant of water is governed by the equation

$$D = D_W + 2\Delta c \qquad (9)$$

where

D = the dielectric constant of the solution,

D_W = the static dielectric constant of water,

Δ = the molar dielectric depression constant for the electrolyte, and

c = the concentration of the electrolyte in moles per liter.

At a pH of 12.5 (the most severe condition to be encountered), the

concentration of sodium hydroxide is 3.2×10^{-2} molar. At 25°C., the value of D_W is 78.5 and the value of Δ given for sodium hydroxide is -10.5. The corresponding value for the dielectric constant of the solution is 77.8, a change of less than one per cent. Consequently, the substitution of the value of the static dielectric constant of water for D in Equation (8) introduces a negligible error.

The quantitative application of the Verwey and Overbeek theory to kaolinite-water suspensions has never been possible primarily because the potential existing between the surface of the particle and the intermicellar solution (ψ_o) has not been measured. However, this measurement may be bypassed if the surface charge density of the particle (σ) is known. Verwey and Overbeek (14) have derived an expression relating the surface charge density to the parameter Z. Thus

$$\sigma = \sqrt{\frac{2 n D K T}{\pi}} \; o \; \sinh \frac{Z}{2} \qquad (10)$$

The problem is now one of evaluating σ.

Since kaolinite acquires its charge by the adsorption of anions from the intermicellar solution, a knowledge of the number of anions adsorbed under a given set of conditions would permit a calculation of the total charge of the mineral under those conditions. This follows directly from the fact that each adsorbed ion would endow the particle with a charge equal to the product of the electronic charge and the valence of the adsorbed ion. Furthermore, if the total surface area of

these particles were known, then the surface charge density—the number of charges per unit surface area—could readily be calculated. Thus, if σ and n are known, Z may be determined from Equation (10); if Z is known, γ may be determined from Equation (6); and if γ is known, its value may be substituted directly in Equation (5).

It is now apparent that a knowledge of the anionic adsorption, particle surface area, and equilibrium composition of the intermicellar solution will permit a calculation of the repulsive potential energy for any given distance of separation of the particles. It is also apparent that if the constant A in Equation (4) is known, it is possible to compute the total potential energy ($V_R + V_A$) for any given distance of separation of the particles. The questions that remain are how and why these potential energies change as dispersing agents, or any other salts for that matter, are added to a suspension of kaolinite in water.

Verwey and Overbeek have considered numerous cases in which the repulsive potential energy varies as a function of the distance of separation of the particles or the parameter Xd. However, in each case some variable or combination of variables has been held constant. The effects of the addition of dispersing agents to aqueous kaolinite suspensions constitute a much more dynamic matter. In the first place, n is constantly changing. In addition, σ is also constantly changing, forcing a continuous change in Z according to Equation (10) and γ (Equation 6). The parameter X must also undergo variation enforced by Equation (8). Furthermore, as we shall demonstrate later, even the range

of values of d which are important in controlling the total potential energy will vary to some degree with the amount of dispersing agent added.

In this paper we will consider the variations of total potential energy experienced by aqueous kaolinite suspensions containing two dispersing agents (sodium citrate and sodium hydroxide) and an inert salt (sodium chloride) in various combinations. It will become apparent that the general principles formulated and the mechanisms of dispersion and flocculation evolved are applicable to any kaolinite-water system, regardless of the number and type of ions present.

NOMENCLATURE

The definitions of all symbols used in the text is indicated below. The units designated are those employed in the various equations to achieve dimensional consistency.

A	a constant in Equation (1) characteristic of the chemical composition of the mineral, ergs.
a	the semidiameter of a disk-shaped particle, cm.
a'	the specific surface area of the colloid, sq. cm./g.
b	the semithickness of a disk-shaped particle, cm.
c	the concentration of the electrolyte, moles/l.
D	the dielectric constant of the intermicellar solution.
D_W	the static dielectric constant of water, 78.9 at 23°C.
d	half the distance of separation of two flat plates, cm.
d_1	the density of a sedimenting particle, g./cc.
d_2	the density of the suspending medium, g./cc.
E.S.D.	the equivalent spherical diameter of a particle, cm.
G	the average acceleration on a particle in the siphoning zone, cm./sec.^{2}
G'	the instantaneous acceleration on a sedimenting particle, cm./sec.^{2}
g	the acceleration due to gravity, 980 cm./sec.^{2}
K	the Boltzmann constant, 1.380×10^{-16} ergs/°K./ion.
$K_{1,2,3}$	the dissociation constants for citric acid.
k	a parameter in the Müller equation defined by Equation (29).
m	the equivalent weight of sodium citrate, 86.03 mg./meq.
N	the speed of the centrifuge, revolutions/sec.

N_o the Avogadro number, 6.023×10^{20} ions/meq.

n the number of ions of opposite charge to the particle contained in one cubic centimeter of intermicellar solution, ions/ml.

n_d^- the average concentration of the anion under consideration at a distance d from the particle.

n_∞^- the concentration of the anion in the intermicellar solution.

P a parameter defined by Equation (31).

R the distance of a particle from the axis of rotation of the centrifuge, cm.

R' the equivalent radius of centrifugation, cm.

R_1 the initial radius of rotation of the particle, cm.

R_2 the radius of rotation of the particle at time t, cm.

r the equivalent spherical radius of a particle, cm.

S the distance of travel of a particle, cm.

T the absolute temperature, 296°K. for all experiments.

t the centrifuging time, sec.

V the valence of the counterions.

V^- the valence of the anion.

V_o the average sedimentation velocity of a particle, cm./sec.

V' the instantaneous sedimentation velocity of a particle, cm./sec.

V_A the attractive potential energy between two parallel plates, ergs/sq. cm.

V_R the repulsive potential energy between two parallel plates, ergs/sq. cm.

w/M the specific adsorption of chloride ions on kaolinite, meq./g. kaolinite.

X a parameter related to the reciprocal of the effective thickness of the electrical double layer and defined by Equation (8), $cm.^{-1}$.

x/M the specific adsorption of citrate ions on kaolinite, mg. sodium citrate/g. kaolinite.

y/M the specific adsorption of hydroxyl ions on kaolinite, meq./g. kaolinite.

y'/M the apparent hydroxyl ion adsorption, meq./g. kaolinite.

Z a parameter defined by Equation (7).

γ a parameter defined by Equation (6).

Δ the molar dielectric depression constant for an electrolyte.

δ the thickness of a flat plate, cm.

ϵ the charge on the electron, 4.802×10^{-10} absolute electrostatic units.

η the absolute viscosity of the suspending medium, poises.

σ the surface charge density of the particle, electrostatic units/sq. cm.

ψ_o the potential existing between the surface of the particle and the intermicellar solution, volts.

ψ_d the difference in potential between that at a distance d from the particle and the intermicellar solution.

ω the angular velocity of the centrifuge, radians/sec.

EXPERIMENTAL PROCEDURES

GENERAL METHOD FOR MEASURING ANION ADSORPTION

In one of the common ways of measuring ionic adsorption, a solution of known concentration is added to the colloidal material. The system is allowed to attain equilibrium and then the suspension is filtered to obtain a colloid-free phase in which the concentration of the various ionic species may be determined. From the differences between the initial and final concentration of a particular ionic species, it is supposedly possible to calculate the amount of the given ion which has been adsorbed by the colloid.

While this procedure measures the ionic adsorption of some sort, it does not measure the ionic adsorption at equilibrium because the separation of the colloid-free phase from the colloid phase (filtration in this case) is a nonequilibrium process. Davis (15) has pointed this out and has shown that unless extreme care is taken, successive portions of the filtrate will show various compositions. The problem is then one of separating the two phases while maintaining an equilibrium between them.

This may be accomplished by using a cell having two compartments separated by a membrane. The colloidal suspension is placed on one side of the membrane (suspension side) and an aqueous solution of appropriate reagents is placed in the other compartment (solution side). In such a system, all ions except those bound to the colloidal particles are free

to distribute themselves throughout the system. When this system has attained equilibrium, the conditions on the solution side are equivalent to the conditions existing in the intermicellar solution of the suspension side.[1] Thus, the amount of a particular ionic species adsorbed may be calculated if the intermicellar concentration of that ion is known both after equilibrium has been established and under a situation in which no adsorption had taken place. Hence, we need know only the amount of ions placed into the system, the total fluid volume of the system, and the concentration of ions in the solution side after equilibrium has been established.

CONSTRUCTION OF THE CELL

The general construction of the cell is depicted in Figure 5. The cell was fabricated from 1/2-inch Lucite and the gaskets were cut from 1/32-inch rubber sheeting. A Millipore Filter (type VC 047) was chosen

---

[1] The intermicellar solution is defined as that portion of the solution which is so remote from the particle surface that its composition is constant and independent of the distance from the particle. In terms of the Boltzmann theorem, this is the solution at an infinite distance from the particle. However, the exponential relationship between concentration and distance from the particle is such that for all practical purposes, an 'infinite' distance from the particle is something less than one micron.

With this point in mind, this system is not in conflict with a system viewed from the standpoint of a Donnan membrane equilibrium if the ions adsorbed by the clay particle and their counterions are considered as nondiffusible ions. As Donnan (16) points out, "The adsorption of certain ions on the surface of a solid wall would provide a constraint, and the 'binding' of these ions would impose a restraint on the free diffusion and mobility of an electrically equivalent amount of oppositely charged ions." Under these conditions, it is obvious that an essential consequence of the Donnan equations, i.e., that the product of the activities of any diffusible ion pair be equal on both sides of the membrane, is not violated.

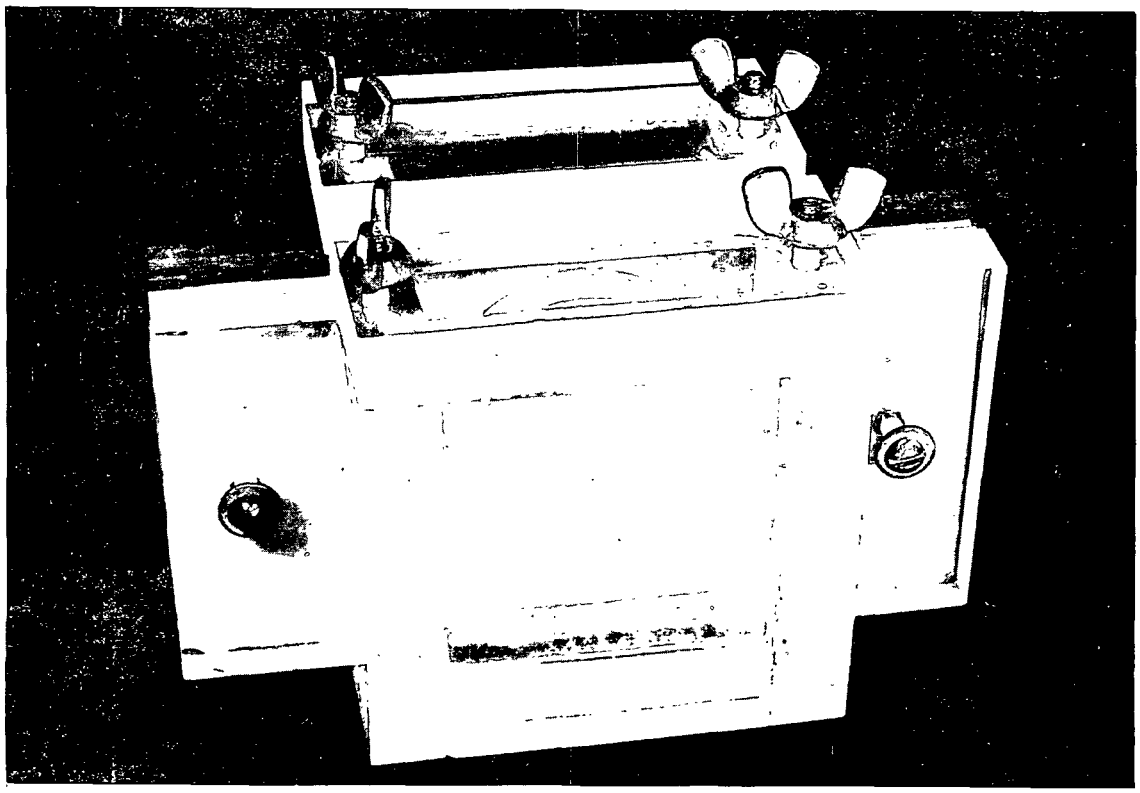

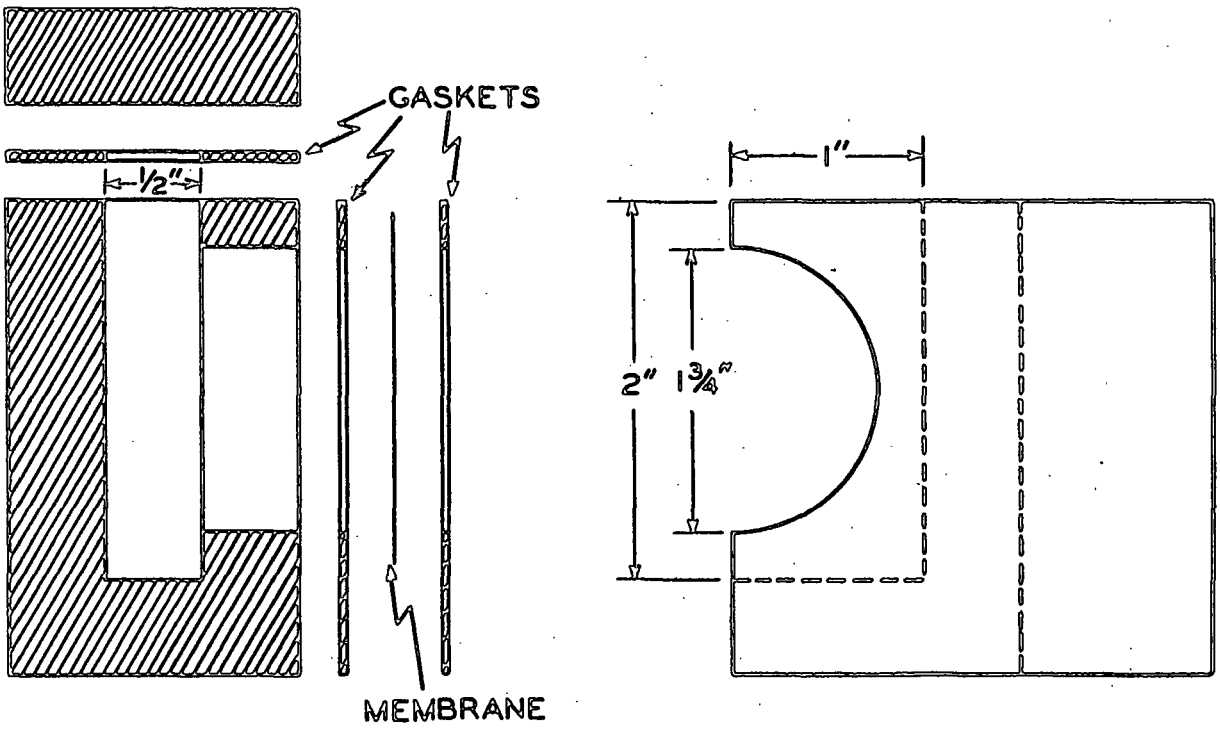

Figure 5. Two-Compartment Adsorption Cell

for the membrane for several reasons. It could be obtained in a very uniform pore size (100 ± 8 millimicrons) small enough to prohibit the passage of any clay particles and yet the material is so highly permeable that equilibrium could be obtained in a reasonable period of time. Furthermore, this membrane exhibits no asymmetry potential (17).

In order to promote the establishment of equilibrium, the cells were agitated on a horizontal shaker. The alignment of the cells in the shaker was such that the fluid motion was parallel to the membrane. The shaker was placed in a room of constant temperature so that the temperature effect could be eliminated in comparing the adsorption results.

MEASUREMENT OF THE ADSORPTION OF CITRATE IONS

It is apparent that to measure the adsorption of citrate ions, one need only know the amount of sodium citrate placed in the system, the total fluid volume, and the concentration of this salt on the solution side after equilibrium has been attained. Thus, it is necessary to have a method of preparing a solution of known sodium citrate content and a method of analyzing solutions for the amount of sodium citrate present.

Standard sodium citrate solutions may be prepared gravimetrically from reagent-grade sodium citrate. A few simple checks on the purity of the reagent were first made. The salt was obtained in a form supposedly containing two molecules of water of hydration ($Na_3C_6H_5O_7 \cdot 2H_2O$). Since

this salt can exist as $Na_3C_6H_5O_7 \cdot 5H_2O$ or $Na_3C_6H_5O_7 \cdot 5\text{-}1/2H_2O$, the reagent was checked for H_2O content. The loss of weight at 105°C. was 0.01%. Dehydration at 172°C. showed 87.65% $Na_3C_6H_5O_7$ compared to a theoretical value of 87.75%. In addition, dry combustion showed a carbon content of 24.58% compared to a theoretical value of 24.50%. These values are well within other experimental errors so the reagent was considered to be 100.0% $Na_3C_6H_5O_7 \cdot 2H_2O$. In the course of this thesis, the occasion will frequently arise when reference is made to a specific amount of sodium citrate. Unless otherwise indicated, the amount of sodium citrate specified will be in terms of anhydrous sodium citrate ($Na_3C_6H_5O_7$).

The analysis of solutions for sodium citrate content presented an entirely different problem. Because it was desirable to keep the sample size as small as possible, a quantitative analytical method was needed which would accurately measure as little as 0.1 mg. of sodium citrate. The answer seemed to lie in a radiochemical technique.

The Van Slyke-Folch method for wet carbon combustion (18, 19) provided a good starting point. In this procedure, carbon-containing compounds are completely oxidized to carbon dioxide by a mixture of wet and dry combustion reagents. The carbon dioxide generated is quantitatively transferred to a gas buret and absorbed in an alkaline solution. After inert gases have been removed, the alkaline solution of carbon dioxide is acidified to liberate the carbon dioxide. The pressure exerted by this gas at a definite volume and temperature is measured and from tables provided, the amount of carbon contained in the original sample may be computed.

Unfortunately, the amount of carbon contained in a desirable sample size was smaller than that which could be accurately analyzed by the procedure. In addition, the procedure would yield a value for total carbon which would include any carbon dioxide absorbed by the sample in its preparation. Since many of the solutions to be analyzed were strongly alkaline, the latter restriction prohibited the use of the manometric procedure for accurate determinations of sodium citrate solutions.

The Van Slyke-Folch procedure has been modified (20) to permit a simultaneous determination of both total carbon and radioactive carbon. Essentially, the modified procedure consists of a method of quantitatively transferring only the carbon dioxide (the amount of which has already been determined by the procedure described above) to a Bernstein-Ballentine counting tube. A methane atmosphere is provided for the carbon dioxide and the beta emission of any C^{14} present is recorded by proportional counting in the gas phase.

To utilize this method for the analysis of small amounts of sodium citrate, it is only necessary to prepare a gravimetrically standardized solution of sodium citrate containing some amount of this salt labelled with C^{14}. The standard solution may then be calibrated by the modified Van Slyke-Folch procedure to determine its specific activity in terms of counts per minute (c.p.m.) per milligram of sodium citrate.

Several preliminary experiments were necessary before the modified Van Slyke-Folch procedure could be adopted for general use. It was first necessary to determine if the combustion reagents suggested for

carbohydrates would quantitatively oxidize the carbon in sodium citrate to carbon dioxide. To show this, samples of $Na_3C_6H_5O_7 \cdot 2H_2O$ were weighed on a microbalance and transferred to the combustion tubes. The oxidation was carried out with the carbohydrate combustion reagents and the amount of carbon found was compared with the theoretical amount. The results are shown in Table I. It is obvious that within experimental error, complete combustion of sodium citrate to carbon dioxide occurs.

TABLE I

COMBUSTION OF $Na_3C_6H_5O_7 \cdot 2H_2O$

Sample Weight, mg. $Na_3C_6H_5O_7 \cdot 2H_2O$	Theoretical Yield, mg. carbon	Actual Yield, mg. carbon	Error, %
6.224	1.525	1.533	+0.5
7.506	1.839	1.831	-0.4
9.022	2.210	2.198	-0.5

It was next necessary to determine the individual characteristics of each of the Bernstein-Ballentine tubes used. The three most important characteristics are the counting plateau, the background count, and the counting efficiency. These will be discussed individually.

A Bernstein-Ballentine tube containing some $C^{14}O_2$ exhibits a counting rate dependent upon the voltage in the manner shown in Figure 6. It is desirable to count within the plateau so that small changes in the voltage will not appreciably affect the counting rate.

To establish the counting plateaus for the various tubes, radioactive

samples were transferred to the tubes and counted over an extensive range of voltages. It was also necessary to determine if variations in the total amount of carbon dioxide in the tubes appreciably shifted the plateau. It was found that while larger amounts of carbon dioxide in the tubes narrowed the plateau, the shift of the midpoint was negligible. From the data gathered, counting voltages were picked which corresponded to the midpoints of the plateaus. These values are listed in Table II. The slope of the curve in the counting plateau is such that a change of 100 volts yields a change in the counting rate of about 0.5%.

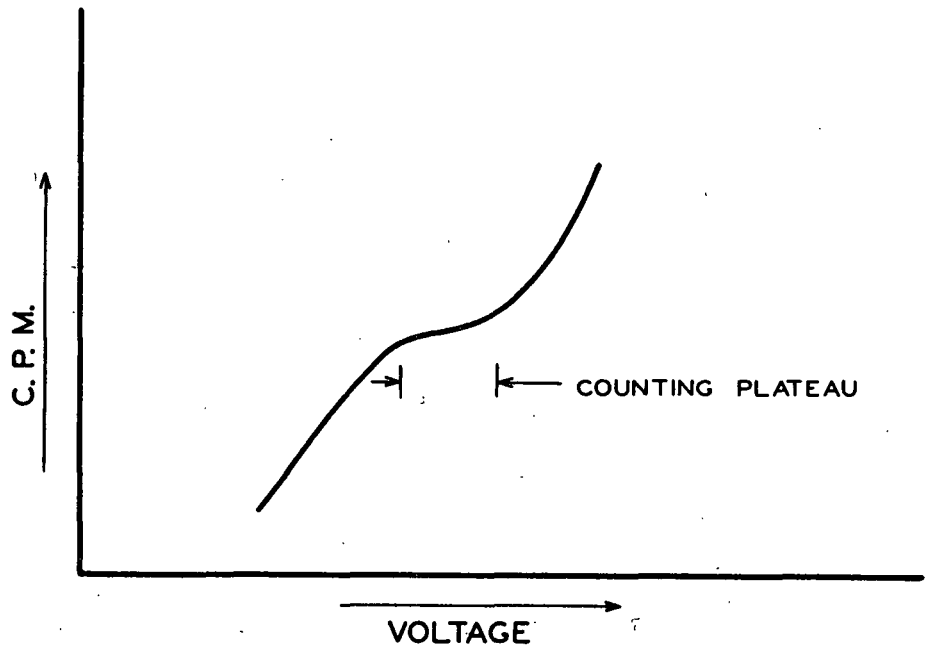

Figure 6. The Relationship Between Counting Rate and Counting Voltage

TABLE II

COUNTING VOLTAGE AND BACKGROUND COUNT

Tube	Voltage	Background, c.p.m.
C	3600	173
E	3600	160
F	3600	157
G	3700	159

The background count was obtained by counting cleaned Bernstein-Ballentine tubes filled only with methane at the voltages corresponding to the midpoints of the plateaus. The results are listed in Table II. A periodic check was made of the background count and over a period of 18 months, the value never varied by more than 5 c.p.m. from that listed in Table II. This variation was insignificant since essentially all the data was gathered at counting rates greater than 1000 c.p.m. above background.

It is not necessary to obtain an absolute value for the counting efficiency[1] (the ratio of the number of counts recorded per unit time to the number of radioactive disintegrations actually taking place per unit time) of each tube, but it is necessary to calibrate each tube to determine the specific activity obtained by a given procedure. To accomplish this, a standard sodium citrate solution was prepared containing 2.998 mg. sodium citrate/ml. and an activity of approximately 44,000 c.p.m./ml.

[1] Counting efficiencies for this method run approximately 98%.

Portions of this solution were quantitatively diluted and 2-ml. samples were pipetted from the diluted solutions into the combustion tubes. The samples were evaporated to dryness by allowing them to stand overnight in a vacuum desiccator. A few crystals of nonradioactive sodium citrate were added to each combustion tube[1] and the samples were subjected to the radioactive carbon analysis. The results are shown in Table III.

The results obtained for tubes E, F, and G were so similar that these tubes were grouped together and assigned a common specific activity for the standard solution of 12,850 c.p.m./mg. sodium citrate. Tube C, which had consistently exhibited a higher counting efficiency than the other tubes, was assigned a specific activity for the standard solution of 12,980 c.p.m./mg. sodium citrate. Thus, by withdrawing a sample of known volume from the solution side and determining the amount of radioactivity within the sample, it is possible to calculate the intermicellar concentration of sodium citrate.

---

[1] Since the determination is based only on radioactive carbon, the addition of inactive carbon causes no difficulty. It should be noted, however, that the total amount of carbon in the combustion tube is well below that recommended for accurate analysis. The few crystals of sodium citrate provide nonradioactive carrier CO_2. Thus, if any trace amounts of CO_2 are lost in the analysis, only a small portion of the $C^{14}O_2$ will be lost.

The addition of inactive sodium citrate became a standard part of all subsequent citrate analyses. It was used whenever the evaporated sample in the combustion tube contained less than 1 mg. of carbon. The amount added was sufficient to bring the total carbon content of the sample to 1-2 mg. This yields an amount of carbon dioxide far below that which causes a serious depression of the counting efficiency (20).

TABLE III

CALIBRATION OF THE BERNSTEIN-BALLENTINE TUBES AND THE STANDARD SODIUM CITRATE SOLUTION

Tube	Sample	Sample Size, mg. $Na_3C_6H_5O_7$	Net Activity, c.p.m.	Specific Activity, c.p.m./mg.
C	A	0.8994	11,650	12,950
	B	0.5396	7014	13,000
	C	0.1799	2338	13,000
E	A	0.8994	11,406	12,680
	B	0.5396	6870	12,730
	C	0.1799	2317	12,880
F	A	0.8994	11,597	12,900
	B	0.5396	6985	12,950
	C	0.1799	2309	12,840
G	A	0.8994	11,607	12,910
	B	0.5396	6936	12,850
	C	0.1799	2323	12,920

Perhaps it is best, at this point, to discuss the reasons why sodium citrate was chosen as a model dispersing agent. In the first place, this salt is known to be an effective dispersing agent (21) and probably has an action very similar to the glassy phosphates commonly used as dispersing agents. Secondly, this material is available in a C^{14}-tagged form which permitted accurate analyses of minute quantities. Finally, the dissociation constants for citric acid are known. Consequently, if the pH of the intermicellar solution is known, the relative proportion of each type of citrate ion present may be calculated. This matter is discussed in greater detail in Appendix I.

MEASUREMENT OF THE ADSORPTION OF HYDROXYL IONS

GENERAL TECHNIQUE

An indirect method of measurement has been chosen for this analysis, the basis of which rests solely upon the principle of electroneutrality of solutions. If a given number of anions are adsorbed by the particle, then an equivalent amount of cations will be present in the ion swarm surrounding the particle. This is necessitated by the fact that the dry kaolinite is electrically neutral and acquires its charge by the adsorption of anions from the solution in which it is immersed. Consequently, a knowledge of the number and type of cations present in the ion swarm will permit a calculation of the total number of charges adsorbed by the particle. Since the adsorbed charges are either citrate anions or hydroxyl ions, the total charges minus the number of charges attributable to the citrate anions will equal the number of hydroxyl ions adsorbed.

If only sodium ions formed the counter charges to the adsorbed anions, then a sodium balance similar to the citrate balance previously described would indicate the total number of charges adsorbed. It must be pointed out, however, that the starting substance will consist of a hydrogen-saturated clay. Consequently, the addition of sodium ion to the system is accompanied by an exchange according to the following reaction:

$$\text{Clay}\text{---}\text{OH}\circ\circ\circ\circ\text{H} + \text{Na}^{+} = \text{Clay}\text{---}\text{OH}\circ\circ\circ\circ\text{Na} + \text{H}^{+}$$

Considering the case where only sodium hydroxide is added to the system, the exchange will be complete, i.e., essentially all hydrogen counterions

will be replaced by sodium counterions, only when the ratio of the concentration of sodium ions to the concentration of hydrogen ions in the intermicellar solution is great enough to overcome the natural tendency for an adsorbed hydroxyl ion to prefer a hydrogen counterion to a sodium counterion. With only sodium hydroxide added, this obviously would occur at some alkaline pH value. When the pH is below this value, the following reaction may occur:

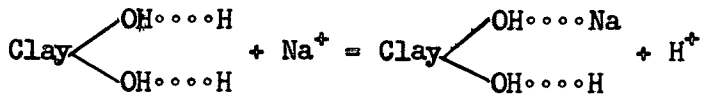

This indicates partial exchange and a sodium balance will yield an apparent hydroxyl ion adsorption less than the amount of hydroxyl ion adsorption actually occurring.

To rectify this matter, it is necessary to have some method of building up the sodium ion concentration at the pH values which show incomplete exchange. This may be accomplished by the addition of an inert salt such as sodium chloride. This salt was chosen not only because it is inert and water soluble, but also because chloride ion lies far below hydroxyl ion in the Hofmeister series of anion adsorbability. Consequently, the chloride ion would probably not compete to any appreciable extent with either the citrate ion or the hydroxyl ion for adsorption sites on the kaolinite surface. However, in view of the possibility that some chloride ion adsorption could occur, the adsorption of this ion was checked and appropriate corrections, if necessary, were applied to the measurements of hydroxyl ion adsorption.

Let us now introduce the concept of an apparent hydroxyl ion adsorption ($\underline{y}'/\underline{M}$). We may define this term as the hydroxyl ion adsorption found by a sodium balance (the number of sodium ions placed into the system minus both those which can be accounted for by analysis of the intermicellar solution and those which are associated with adsorbed citrate and chloride ions) regardless of whether or not complete exchange has taken place. If we now measure this quantity over a range of pH values with no sodium chloride added and repeat this procedure with various amounts of sodium chloride in the system, we may anticipate (Figure 7) a series of curves ($\underline{y}'/\underline{M}$ as a function of pH for each of several concentrations of sodium chloride) exhibiting, at a given pH, higher values of $\underline{y}'/\underline{M}$ for increased concentrations of sodium chloride. The differences in the various curves should be particularly pronounced at the lower pH values where exchange is incomplete.

At any given pH value, we may cross-plot the data to obtain $\underline{y}'/\underline{M}$ as a function of the sodium chloride concentration[1]. This should yield a curve similar to that shown in Figure 8. Extrapolating this curve to high concentrations of sodium chloride should yield a reasonable estimate of the limiting value of $\underline{y}'/\underline{M}$ for that pH. Since this represents a case where exchange is essentially complete, the limiting value of $\underline{y}'/\underline{M}$ should correspond to the true hydroxyl ion adsorption ($\underline{y}/\underline{M}$) occurring at the given pH.

---

[1] In essence, this should be total sodium ion concentration in the intermicellar solution. However, the concentration of sodium chloride serves as an adequate indicator.

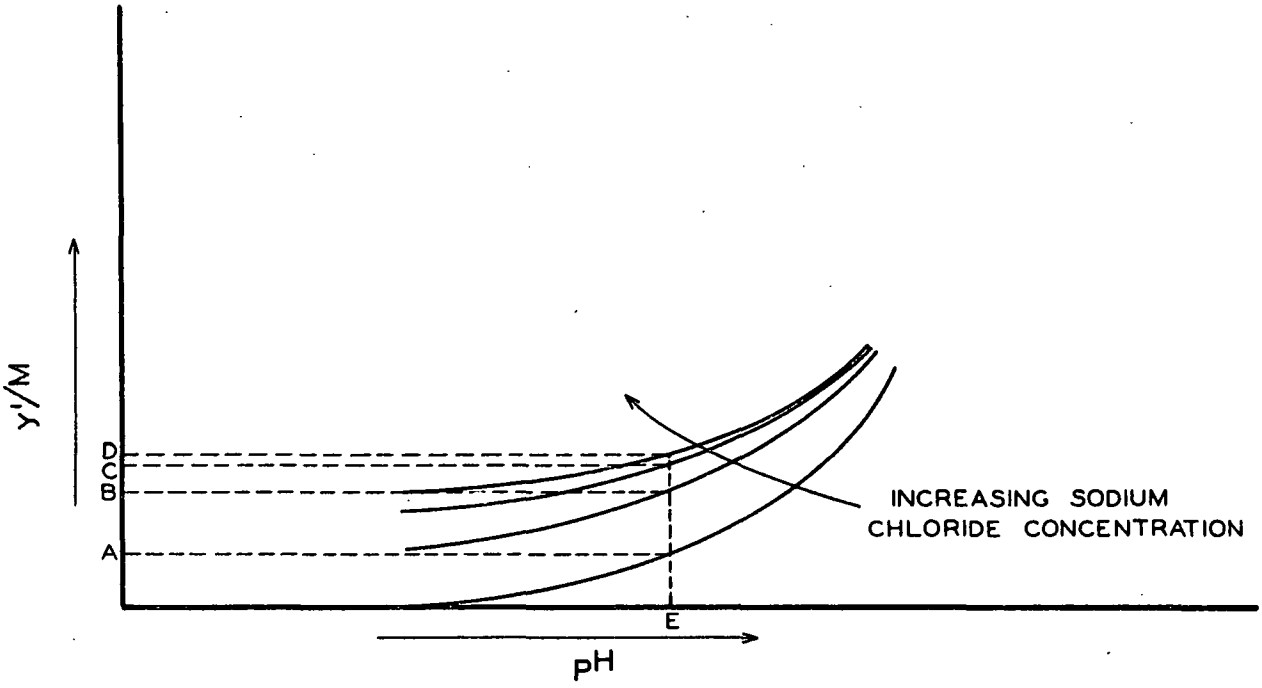

Figure 7. The General Relationship Between the Apparent Hydroxyl Ion Adsorption and pH

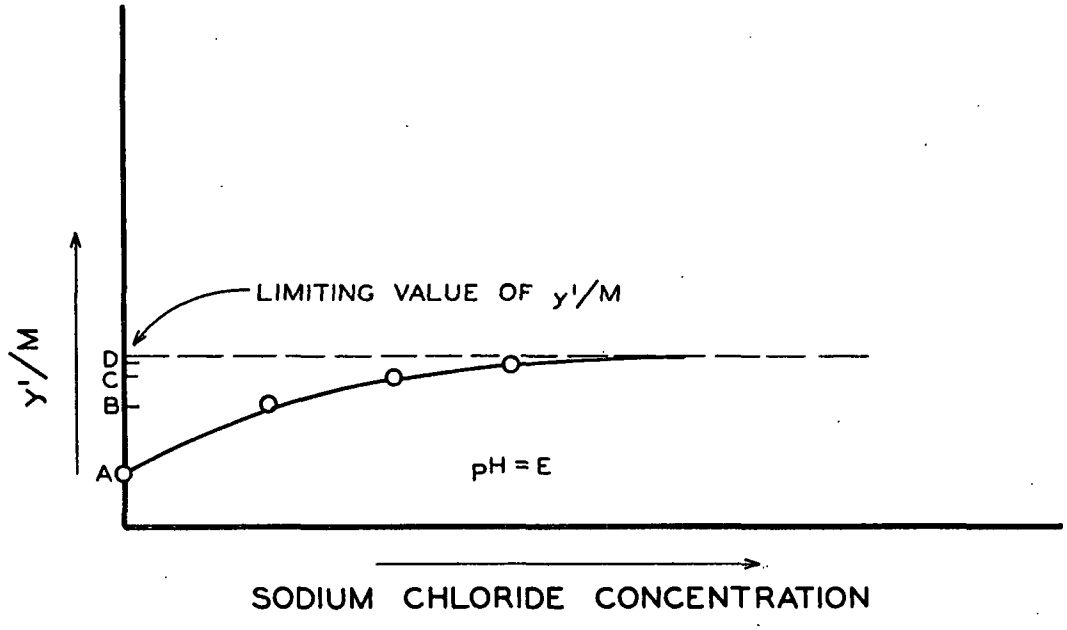

Figure 8. The Relationship Between the Apparent Hydroxyl Ion Adsorption and the Concentration of Sodium Chloride at a Given pH

SODIUM DETERMINATION

The successful application of a sodium balance technique to the determination of hydroxyl ion adsorption requires an accurate method for the determination of sodium ion in rather dilute solutions. The usual gravimetric procedures for the determination of sodium are both time-consuming and insufficiently accurate for some of the more dilute solutions encountered. A method was needed which would be both rapid and accurate and which would require no more than 25 ml. of solution.

Fortunately, the only cations which could be present in the intermicellar solution are hydrogen ion and sodium ion. If all the anions present (chloride, hydroxyl, and the various citrate ions) could be quantitatively exchanged for hydroxyl ion, then a simple acidimetric titration of the solution would reveal its sodium ion content[1]. This suggests an ion-exchange procedure.

Details of the final procedure evolved are given in Appendix II. Essentially, the procedure consists of passing a known amount of the solution to be analyzed through a column containing anion-exchange resin (Amberlite IRA-401) in the hydroxyl form. The column is washed with purified water and the total effluent is titrated with standardized 0.1N sulfuric acid to the phenolphthalien end point. The titration is carried out with either a ten-milliliter buret or a two-milliliter microburet, depending upon the amount of hydroxyl ion present.

[1] All anions associated with hydrogen ions will yield water.

The accuracy of the method was checked by preparing several solutions containing known amounts of sodium citrate, sodium chloride, and sodium hydroxide in various proportions. Samples of each of these solutions were pipetted into the column and the sodium determinations were carried out in the manner previously described. The results are shown in Table IV. It is evident that the accuracy of the analysis is greater than one per cent.

TABLE IV

THE DETERMINATION OF THE SODIUM CONTENT OF KNOWN SAMPLES BY THE ION-EXCHANGE TECHNIQUE

Solution no.	1	2	3	4
Total meq./100 ml.	0.867	1.371	1.189	1.881
Equivs. as NaOH, %	2.8	0.9	1.0	0.4
Equivs. as $Na_3C_6H_5O_7$, %	57.8	24.4	70.3	8.9
Equivs. as NaCL, %	39.4	74.7	28.7	90.7
Sample size, ml.	25.0	25.0	25.0	25.0
Na^+ found, meq.	0.218	0.346	0.298	0.469
Theoretical Na^+ content, meq.	0.217	0.343	0.297	0.470
Error, %	+0.5	+0.9	+0.3	-0.2

CHLORIDE DETERMINATION

In this case, the problem consisted of finding an accurate method of determining the chloride ion content of a solution containing as little as 0.05 meq. of sodium chloride. Two standard chloride determinations were investigated for their applicability to this situation. These were the Fajans adsorption indicator method (using dichlorofluorescein as the indicator) and the Volhard method.

In the Volhard method, the sample is treated with an excess of standardized silver nitrate to precipitate silver chloride. The excess of silver ion is titrated with potassium thiocyanate in the presence of ferric ion. As the potassium thiocyanate is added, silver thiocyanate continuously precipitates until the silver ion is exhausted. The thiocyanate ion then combines with the ferric ion to give a red color indicating the end point. From the amount of silver nitrate added and the amount of potassium thiocyanate required to consume the excess silver nitrate, it is possible to calculate the amount of chloride ion present in the sample.

In the adsorption indicator method, the sample is titrated directly with standardized silver nitrate. At the stoichiometric point, the indicator is adsorbed by the precipitated silver chloride and a sharp change of color results.

It is obvious that the adsorption indicator method has some distinct advantages over the Volhard method. In the first place, it requires only one standard solution. Of more importance is the fact that the end point is generally so distinct that the titration may be carried out with 0.02N silver nitrate solutions, whereas the Volhard end point is rather difficult to discern when the potassium thiocyanate solution is less than 0.1N. However, it was found that the presence of small amounts of sodium citrate destroyed the end point and, consequently, this method was discarded in favor of the Volhard method.

In the Volhard method, the assumption is often made that the blank is negligible. This is indeed justifiable for the usual range of sample sizes (3-6 meq. of sodium chloride), but the assumption can lead to serious error when the sample contains only 0.05 meq. of sodium chloride. If the assumption is made that the true blank is 0.03 ml. of 0.1N potassium thiocyanate, the neglect of the blank leads to an error of -0.1% for a 3.0-meq. sample and an error of -6.0% for a 0.05-meq. sample.

It is difficult to obtain good values for the blank in the Volhard determination. This situation arises because the end point found in the presence of a silver thiocyanate precipitate appears to be somewhat different from that obtained in a mixture of silver thiocyanate and silver chloride precipitates. As a result, a different procedure was used to determine the blank. A standard solution of sodium chloride was prepared by a gravimetric procedure and checked for chloride content by the Fajans determination. The gravimetric and titrimetric standardizations yielded identical values of sodium chloride concentration. This standard solution was then subjected to a Volhard analysis under conditions in which the blank correction was appreciable. From the results obtained, it was possible to calculate the magnitude of the blank necessary to yield the assigned value of the standard sodium chloride solution. The average of several such determinations indicated that the blank was approximately 0.025 ml. of potassium thiocyanate. This correction was applied to all subsequent Volhard chloride analyses.

pH MEASUREMENT

In order to eliminate the difficulties encountered in measuring the pH of suspensions containing charged particles (22), all pH measurements were made on samples withdrawn from the solution side of the cell. In general, the measured pH of the suspension was about 0.1 units lower than that found in the intermicellar solution.

A Beckman Model G pH meter equipped with miniature electrodes was used for the determination of pH. This permitted accurate measurements of pH on as little as three milliliters of solution. Since many of the solutions were rather alkaline, the glass electrode was of the type having a low sodium ion error. Before any measurements were made, the meter was standardized against two different buffer solutions (pH 7.00 and pH 10.00) and used only if the readings obtained on these solutions were within 0.03 units of the assigned values.

PRELIMINARY EXPERIMENTS

MEMBRANE DIFFUSION RATE

The purpose of this experiment was to determine the time required to establish equilibrium under the most drastic conditions. To accomplish this, a clay slurry was placed in one of the cell compartments and reagents, in concentrations greater than those used in the adsorption studies, were placed in the compartment on the other side of the membrane. Small samples were withdrawn from the solution side periodically during the agitation and analyzed for citrate ion. The

results are indicated in Table V. It is evident that equilibrium had been established some time within the first 40 hours. To insure that all adsorption data were obtained at equilibrium, a minimum of 48 hours of agitation was adopted as part of the standard procedure.

TABLE V

DIFFUSION OF SODIUM CITRATE ACROSS THE MEMBRANE

Agitation Time, hours	Net Activity, c.p.m.
0	7740
39.5	3972
62.5	4017
93.5	4058

ADSORPTION BY THE CELL AND MEMBRANE

To minimize any possible adsorption of either sodium ion or citrate ion by the cell and its components, the cell was treated with a solution containing sodium chloride, sodium hydroxide, and radioactive sodium citrate in concentrations approximately equivalent to those which were used in the bulk of the adsorption studies. The treatment was accomplished by placing the solution in the cell and shaking for several days.

The adsorption of sodium ion by the cell and membrane was determined by placing a solution of the various sodium salts in a treated cell, shaking the cell and its contents for three days, and analyzing the solution withdrawn from the cell for sodium content. Duplicate analysis of

the solution placed in the cell showed 0.254 and 0.255 meq. of sodium ion per 25 ml. After the three-day period of agitation, duplicate analyses of the samples withdrawn showed a sodium ion content of 0.254 and 0.254 meq./ml. Consequently, measurements of the adsorption of hydroxyl ion made in a treated cell need not be corrected for sodium ion adsorption by the cell and membrane.

The adsorption of citrate ion by a treated cell and membrane proved rather difficult to measure. This occurred because the citrate adsorption was so small that the final result depended upon a very small difference between two relatively large numbers. To determine the maximum amount of citrate ion adsorption which could conceivably take place, the cell was filled with radioactive sodium citrate solution. After several days of shaking, the solution was removed and the cell was thoroughly rinsed with water. A relatively concentrated solution of inactive sodium citrate was then placed in the cell. The concentration was adjusted so that if complete exchange took place between the adsorbed radioactive sodium citrate and the inactive sodium citrate solution, virtually all the radioactivity would appear in the solution. After the inactive solution had been agitated in the cell for several days, samples were withdrawn and analyzed for radioactivity. The results indicated that 0.12 mg. of sodium citrate had been adsorbed. While this amount may be significant in terms of that which is adsorbed by the clay, it should be pointed out that this represents the adsorption which would occur in an untreated cell and from a solution containing more sodium citrate than was used in any of the experiments. The actual

amount of sodium citrate taken up by a treated cell during any given experiment is undoubtedly far less than this. Consequently, citrate ion adsorption by the cell and membrane may be neglected.

REPRODUCIBILITY OF RESULTS

The analytical determinations have proved both sufficiently precise and accurate to warrant single analyses. The question arises, however, as to whether adsorption measurements made in two separate cells will yield the same result. An experiment was designed to answer this question. Procedures which were different, but which could not affect the result, were intentionally employed in the separate determinations.

The clay used was a 13.56% (by weight) slurry of purified kaolin. The cells were prepared according to the schedule shown in Table VI. In one cell, all reagents were placed on one side of the membrane. In the other cell, the reagents were introduced in such a manner that a part of each reagent was initially present on each side of the membrane. This provided a different initial concentration of the reagents in the vicinity of the clay for each cell. It is of interest to note that while the total fluid volume is essentially the same for both cells, the amount of fluid contained on the solution side is probably quite different in the two cases. As we shall see later, this fact does not enter into the calculation.

The cells were placed on the shaker and after 49 hours of agitation, samples were removed from each cell and analyzed. The results

are recorded in Table VI. From the raw data, it is quite obvious that results can be duplicated easily. However, the agreement found in this experiment is somewhat better than is ordinarily obtained. This fact will become apparent later when the adsorption obtained over a range of pH values is considered.

TABLE VI

COMPARISON OF THE DATA OBTAINED BY TWO DIFFERENT CELLS CONTAINING IDENTICAL INGREDIENTS

	Cell No. 6		Cell No. 9	
	Amount	Placement[a]	Amount	Placement
Sample size, g. at 13.56% solids	36.80	Susp.	36.76	Susp.
Distilled water, ml.	50.0	Split	50.0	Split
NaCl, ml. 0.1004N	1.00	Soln.	1.00	Split
NaOH, ml. 0.1000N	1.00	Soln.	1.00	Split
$Na_3C_6H_5O_7$ stock solution, ml.[b]	2.00	Soln.	2.00	Split
Analysis of samples from the solution side:				
pH	8.4		8.4	
Net c.p.m./2 ml.	1435		1444	
Meq. Na^+/25 ml.	0.0638		0.0639	

[a] Susp. indicates that the material was placed on the suspension side. Soln. indicates that the material was placed on the solution side. Split indicates that the pipetted sample was placed partly on both sides of the membrane.

[b] The concentration of sodium citrate was 2.998 mg./ml. and the specific activity was 12,850 c.p.m./mg.

It is instructive to carry the calculations further to show how sensitive the calculated values of adsorption are to small differences in analytical results. These calculations are detailed in Appendix III. In this case, a 0.6% difference in radioactivity between the two samples

gave a 2.5% difference in the calculated adsorption of sodium citrate. A difference of 0.2% in the determined sodium ion concentration yielded a 0.4% difference in the calculated hydroxyl ion adsorption.

RÉSUMÉ OF THE METHODS OF OBTAINING ADSORPTION DATA

The adsorption of the various anions on kaolinite was determined in the following manner. From a clay slurry of known solids content, a sufficient amount of kaolinite was transferred to the suspension side of the cell to give an ovendry weight of this mineral equivalent to 5.00 ± 0.01 g.[1] The appropriate reagents were added to either the solution side or both sides of the cell by either pipet or buret. Sufficient purified water was added to the cell by buret to bring the total fluid volume of the system to 86.0 ± 0.1 ml.

All reagents were carefully standardized before use. The sodium hydroxide solutions were prepared, stored, and transferred to the cells in such a manner that any carbonate contamination was minimized. The water used in all experiments consisted of distilled water which had been passed through a column containing a mixed bed of ion-exchange resins (Amberlite MB-3). The specific resistance of the water thus prepared was in excess of 400,000 ohms.

The cells were generally prepared in groups of six or twelve. After the cells had been filled and sealed, they were placed on a shaker

[1] In a few cases, it was impossible to get this much clay into the system. Consequently, 3.90 ± 0.01 g. of kaolinite were used.

located in a room of constant temperature (23 ± 2°C). Agitation was allowed to proceed for a minimum of 48 hours. When the cells had attained equilibrium, they were removed from the shaker. Immediately after each cell was opened, samples were withdrawn from both chambers for pH measurement. In addition, a 2.00-ml. sample was pipetted from the solution side and transferred to a combustion tube. The remainder of the material on the solution side was transferred to a two-ounce bottle and stored for subsequent sodium and chloride determinations.

The samples in the combustion tubes were evaporated to dryness in a vacuum desiccator. A few crystals of inactive sodium citrate were added to the combustion tubes and the samples were then subjected to radioactive carbon analysis by the method previously described. From the results, it is possible to calculate the concentration of citrate ion in the intermicellar solution.

For the sodium analysis, samples of either 10, 15, or 25 ml. were pipetted into the anion-exchange column. The effluent was titrated with standardized 0.1N sulfuric acid, using either a ten-milliliter buret or a two-milliliter microburet. The remainder of the stored sample (about 12 ml.) was used for the chloride analysis. A portion was pipetted into a flask to which 2.00 ml. of standardized 0.1N silver nitrate had been added. Five milliliters of 8N boiled and cooled nitric acid together with two milliliters of nitrobenzene and one milliliter of ferric alum indicator were also added to the flask. The solution was cooled to 20-25°C. and titrated with standardized 0.1N potassium thiocyanate

contained in a two-milliliter microburet. From these results, the concentrations of sodium ion and chloride ion in the intermicellar solution could be calculated.

FRACTIONATION OF THE CRUDE KAOLIN

The starting material consisted of crude, pit-run kaolin obtained from the Edgar Division of Minerals and Chemicals Corporation of America in McIntyre, Georgia. This material was chosen because no artificial dispersing agents, which might be irreversibly adsorbed by the kaolin, had come in contact with the clay. This crude material was chopped to about 2-inch chunks and then slurried with water for a few seconds in a Waring Blendor. The result was a crude, undispersed slurry having a solids content of approximately 30%.

Sedimentation according to Stokes' law was used to separate the particles having an equivalent spherical diameter (E.S.D.) of less than one micron from the crude clay. According to Stokes' law, the rate of sedimentation under gravity is

$$\underline{V}_o = \frac{2(\underline{d}_1 - \underline{d}_2)gr^2}{9\eta} \qquad (11)$$

where

$\underline{V}_o$ = the velocity of fall of a particular particle, cm./sec.,

$\underline{d}_1$ = the density of the particle, g./cc.,

$\underline{d}_2$ = the density of the suspending medium, g./cc.,

g = the acceleration due to gravity, cm./sec.^{2},

η = the absolute viscosity of the suspending medium, poises, and

r = the equivalent spherical radius of the particle, cm.

Assuming $d_1 = 2.58$, $d_2 = 1.00$, and $g = 980$, the velocity of fall at 23°C. ($\eta = 0.00936$) is 7.94 centimeters per day for a particle one micron E.S.D. In 18 hours, then, a 1-micron particle will fall 5.95 centimeters.

A siphon of the shape shown in Figure 9 was prepared from 6-mm. glass tubing. This provides a minimum of surface agitation during the siphoning process while siphoning the required amount of slurry in a few minutes. In addition, it is possible to repeatedly siphon a 5-gallon pickle jar to within 0.05 centimeters of a given mark.

A mark was placed on the pickle jar corresponding to the level of the liquid in the jar after siphoning. An additional mark was made 5.95 centimeters above the siphoning mark. The crude clay slurry was diluted to 8% solids with distilled water and dispersed with 1.0N sodium hydroxide to a pH of 10.5-11.0. The jar was then filled with this dispersed slurry until the liquid level coincided with the upper mark on the jar. The slurry was agitated for five hours with a high speed 'Lightnin' stirrer, and at the end of this time, the suspension was allowed to stand until the fluid motion had stopped. The time was noted and after 18 hours had elapsed, the top 5.95 centimeters of the suspension were siphoned off and collected. After siphoning, distilled water was added until the

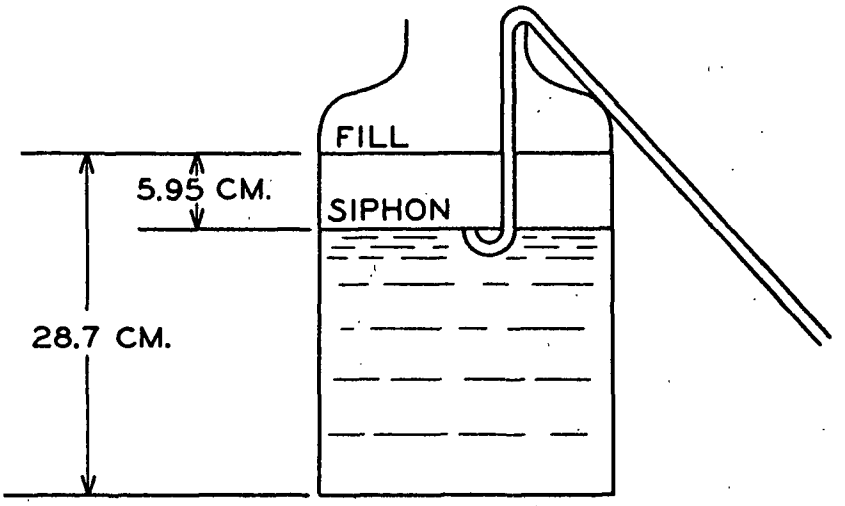

Figure 9. Fractionation by Sedimentation

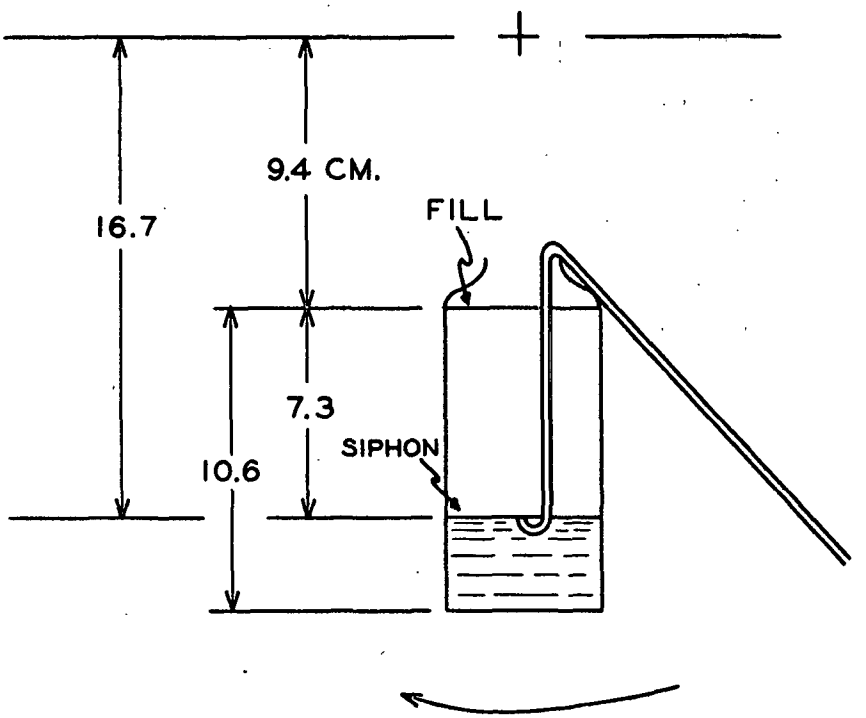

Figure 10. Fractionation by Centrifugation

level was again at the top mark. The slurry was again stirred for 30 minutes, allowed to stand 18 hours, and siphoned. This process was repeated until five siphonings had been obtained from each jar. The siphonings contained material smaller than 1 micron E.S.D. at about 2% solids.

Further fractionation of the siphoned material was accomplished by centrifugation. The application of Stokes' law to sedimentation by centrifugation is complicated by the fact that as a particle moves through the suspension, its radius of rotation changes and this change is accompanied by a change in the force on the particle. Thus, Stokes' law, in differential form, becomes

$$\frac{dR}{dt} = \frac{2 R \omega^2 (d_1 - d_2) r^2}{9\eta} \qquad (12)$$

where

t = the centrifuging time, sec.,

ω = the angular velocity, radians/sec., and

R = the distance of the particle from the axis of rotation of the centrifuge, cm.

Rearranging and integrating

$$\int_0^t dt = \frac{9\eta}{2\omega^2 (d_1 - d_2) r^2} \int_{R_1}^{R_2} \frac{dR}{R} \qquad (13)$$

or

$$\underline{t} = \frac{9\eta \ln (\underline{R}_2/\underline{R}_1)}{2\omega^2 \underline{r}^2 (\underline{d}_1 - \underline{d}_2)} \qquad (14)$$

where

$\underline{R}_1$ = the radius of rotation of the particle, cm., at $\underline{t} = 0$ and

$\underline{R}_2$ = the radius of rotation of the particle, cm., at time $\underline{t}$.

Since $\omega = 2\pi\underline{N}$, where $\underline{N}$ is the number of revolutions per second, Equation (14) reduces to

$$\underline{t} = \frac{9\eta \ln (\underline{R}_2/\underline{R}_1)}{8\pi^2 \underline{N}^2 \underline{r}^2 (\underline{d}_1 - \underline{d}_2)} \quad \text{or} \quad \frac{\eta \log (\underline{R}_2/\underline{R}_1)}{3.81 \underline{N}^2 \underline{r}^2 (\underline{d}_1 - \underline{d}_2)} \qquad (15)$$

This is the general equation for fractionation by centrifugation.

Using the substitutions previously indicated for aqueous suspensions of kaolin at 23°C. ($\eta = 0.00936$, $\underline{d}_1 = 2.58$, $\underline{d}_2 = 1.00$), and substituting values of 16.7 and 9.4 cm. for $\underline{R}_2$ and $\underline{R}_1$, respectively, (see Figure 10), we may calculate a convenient combination of centrifuge speed and centrifuging time to achieve a desired separation. These combinations are tabulated in Table VII. The interpretation of the table is simply this: A kaolin particle of indicated size will travel from a radius of 9.4 centimeters to a radius of 16.7 centimeters in the corresponding time when the centrifuge is rotating at the corresponding speed.

The object was to prepare five fractions of kaolin from the material smaller than one micron (the siphonings obtained from the sedimentation procedure) according to the schedule in Table VIII. Fraction 1 was used for the bulk of the adsorption studies. The remaining fractions were used

TABLE VII

CONDITIONS EMPLOYED FOR FRACTIONATION BY CENTRIFUGATION

Particle Size, mmu E.S.D.	Centrifuging Time, min.	Centrifuge Speed, r.p.m.
200	34.2	2600
400	14.4	2000
600	10.0	1600
800	10.0	1200

to determine the surface of the clay particle on which adsorption takes place.

In order to prepare the siphonings from the sedimentation for efficient centrifugation, it was necessary to raise the solids content of the suspension. To achieve this, some IR-120 cation-exchange resin was converted to the hydrogen form and placed in a funnel fitted with an 80-mesh

TABLE VIII

SCHEDULE OF FRACTIONS

Fraction No.	Nominal Particle Size Range, mmu E.S.D.
1	200 - 1000
2	200 - 400
3	400 - 600
4	600 - 800
5	800 - 1000

screen. The clay slurry was mixed for about one minute with this resin and then drained, leaving the resin behind. As a result, the effluent clay slurry was in a flocculated form and settled out very easily, permitting the clear liquid on top of the clay slurry to be siphoned away. This method made it possible to raise the solids content to about 15% with no adverse effects.

Twenty matched centrifuge bottles, each having a capacity of 250 ml., were marked at a point corresponding to a distance of 9.4 cm. from the axis of the centrifuge during operation. A siphon was constructed (Figure 10) which would siphon each bottle to a level 7.30 $\pm$ 0.05 cm. below this mark. Two International centrifuges having identical heads and cups were used so that R_1 remained 9.4 cm. no matter which combination of bottles and centrifuge was used. The timers and tachometers on both centrifuges were calibrated and the appropriate corrections were applied.

Dispersed 8.0% suspensions of the kaolin smaller than 1 micron E.S.D. were placed in the centrifuge bottles so that the meniscus corresponded to the marks on the bottles. The 200-millimicron cut was first made (34.2 minutes at 2600 r.p.m.) and the siphonings were discarded. The remaining suspension was diluted to the mark with distilled water and agitated to re-establish a uniform suspension. Sufficient 1.0N sodium hydroxide was added to maintain the pH between 10.5 and 11.0. The resuspended material was again centrifuged for the 200-millimicron cut and again the siphonings were discarded. This

process was repeated until six siphonings were made. The material remaining in the centrifuge bottle essentially consisted of particles in the range 200-1000 mmu E.S.D. and was designated Fraction 1.

To prepare the remaining fractions, centrifugation was continued after the 200-millimicron cut had been made. Centrifuging for 14.4 minutes at 2000 r.p.m. yielded siphonings which contained material 200-400 mmu E.S.D. The sediment remaining in the centrifuge bottle was resuspended and dispersed as before until seven siphonings had been made.

In a similar manner, eight siphonings were made for the 600-millimicron cut and nine siphonings for the 800-millimicron cut. The reason six, seven, eight, and nine were chosen will become apparent later. After the 800-millimicron cut was completed, the material remaining in the bottle was collected. It contained particles nominally in the range 800-1000 mmu E.S.D.

In any fractionation by sedimentation, the siphonings will always contain particles smaller than those of a given size. The residue, however, does not contain particles composed solely of those larger than the specified size unless the process of centrifuging, siphoning, and resuspending is carried on endlessly at a given set of conditions. However, probability allows us to estimate the efficiency of the separation after a finite number of siphonings at one set of centrifuging conditions. This estimation is quite simple in the case of gravity sedimentation if the containing vessel has a uniform cross section.

As an example, let us consider the separation that was made at 1 micron E.S.D. At the conditions actually used, we may plot the distance a particular particle travels in 18 hours as a function of its size (Figure 11). Thus, a particle having a diameter of 0.8 microns will travel a distance of 3.81 cm. in the 18-hour period. Referring to the dimensions of the vessel shown in Figure 9, it is obvious that only those particles having an E.S.D. of 0.8 microns which were originally present in the zone extending from the top surface to a depth of 2.14 cm. (5.95 - 3.81) would be siphoned away. If we started with a uniform distribution of particles throughout the jar, then the percentage of 0.8-micron particles removed in a single siphoning would be (2.14/28.7) 100 or 7.5%. Consequently, the vessel would still contain 92.5% of the particles 0.8 microns E.S.D.

When the siphoned vessel is again diluted to the mark, stirred, and siphoned a second time, the percentage of 0.8-micron particles remaining in the jar would be $100(0.925)^2$; and after n siphonings it would be $100(0.925)^n$. Thus, for $n = 5$, we may plot the information shown in Figure 12.

This analysis leads to some broad but important conclusions regarding fractionation by sedimentation procedures. For efficient separation, the ratio of the siphoned volume to the total volume should be as large as is practical. This fact was used to full advantage in the centrifugation procedure. Secondly, after a finite number of siphonings, the extracted portion will contain particles composed solely of those smaller

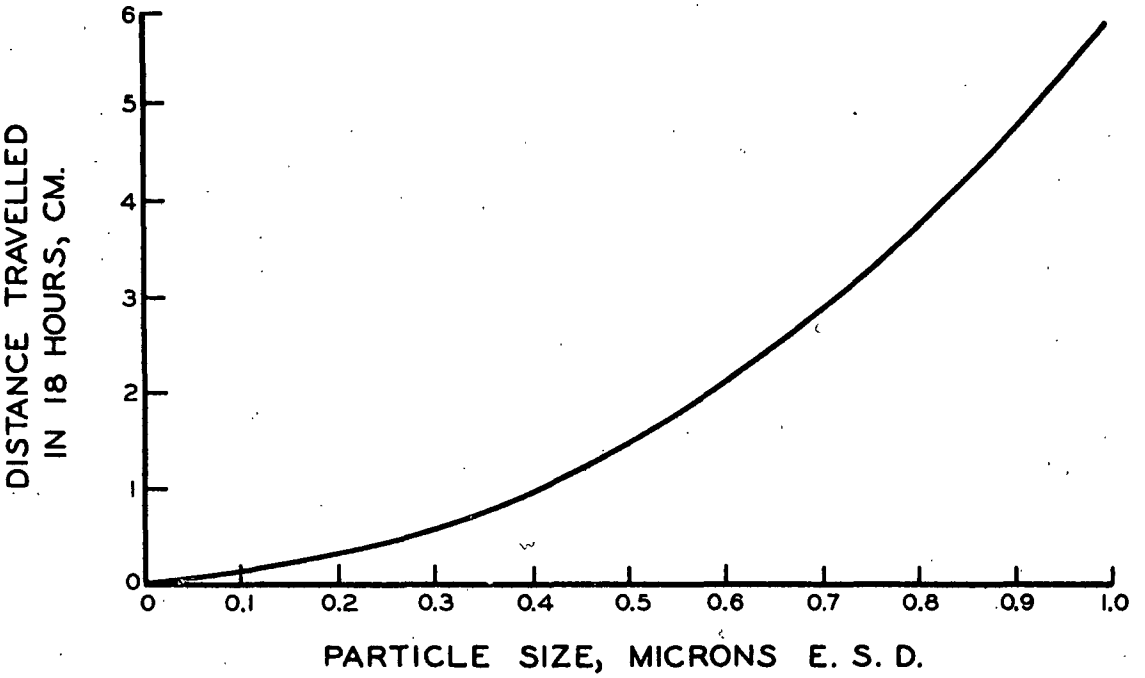

Figure 11. Distance Travelled vs. Particle Size for the 1.0-Micron Cut

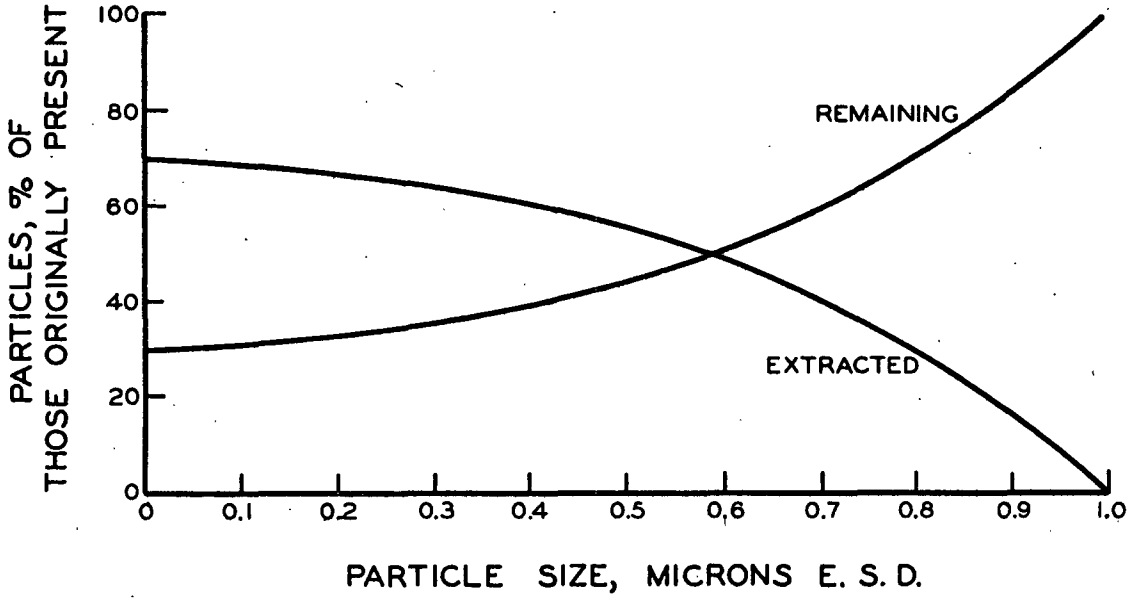

Figure 12. The Efficiency of Separation at the 1.0-Micron Cut

than a given size; however, it will be deficient in the largest particles removed. Finally, the residue will contain some particles of all the sizes originally present, but the contamination will consist largely of particles having sizes slightly smaller than the boundary size. It is quite important that these principles be applied to the isolation of monodisperse fractions, particularly when the upper boundary of the fraction is less than twice the lower boundary.

The estimation of the efficiency of separation in a varying force field (centrifugation) is considerably more complicated than that in a gravity sedimentation. However, the case may be greatly simplified by determining an equivalent centrifuging radius for the siphoning zone ($\underline{R}'$) and assuming that the force at this radius is constant throughout the siphoning zone. Thus, we will view the separation in an identical manner with that of gravity sedimentation, except that the force on the particles will be many times that of gravity.

It can be shown (Appendix IV) that the equivalent centrifuging radius for the siphoning zone is equal to the logarithmic mean radius of centrifugation, i.e.,

$$\underline{R}' = \frac{\underline{R}_2 - \underline{R}_1}{\ln (\underline{R}_2/\underline{R}_1)} \qquad (16)$$

It is also shown in Appendix IV that if the concept of an equivalent centrifuging radius is employed, the distance of travel of a particular particle (S) may be related to its size, the centrifuge speed, and the time of centrifuging by the equation

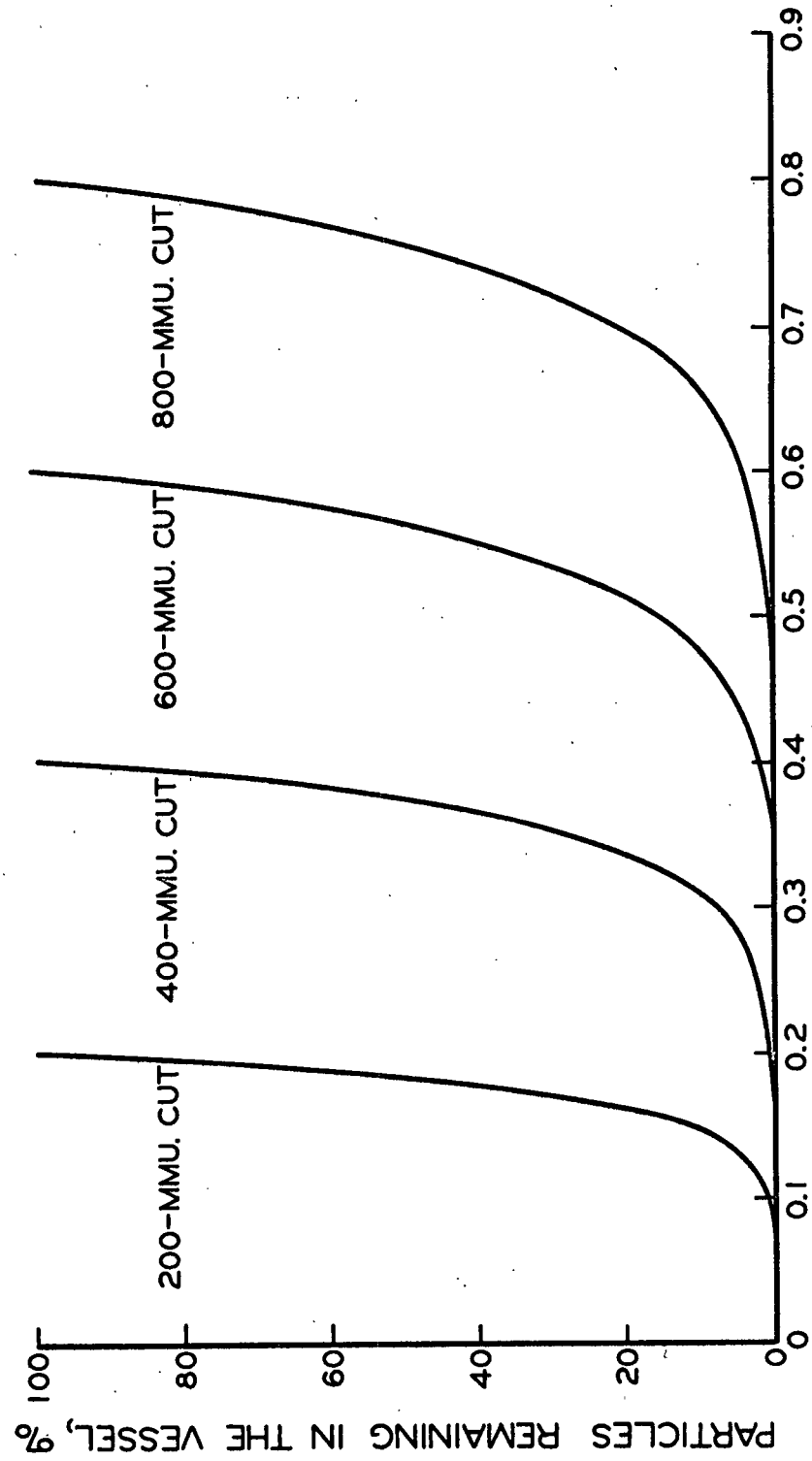

Figure 13. The Efficiency of Separation During Centrifugation

$$\underline{S} = 1.88 \times 10^4 \, \underline{N}^2 \, \underline{r}^2 \, \underline{t} \qquad (17)$$

for the particular conditions chosen in this work. We may now proceed with an analysis identical to that for gravity separation. In this manner, the data in Figure 13 were computed.

It is now possible to obtain a profile of the various fractions isolated. If we assume that the crude, unfractionated kaolin had a distribution[1] according to the curve ABC in Figure 14, then we may construct a curve ADEF which is the product of ABC and the curve in Figure 12 showing the percentage of the various particles extracted at the 1.0-micron cut. This constructed curve represents the profile of the siphonings obtained from the sedimentation procedure and constitutes the fraction of particles 0.0-1.0 microns E.S.D. used as the starting material for the centrifuging procedure. The product of the curve ADEF and the curve in Figure 13 showing the 0.2-micron cut yields the curve AGEF. This represents the profile of the material remaining in the centrifuge bottle after the 0.2-micron cut had been completed and constitutes those particles nominally in the range 0.2-1.0 microns (Fraction 1). In a

---

[1] The ordinates of the curves in Figures 14 and 15 correspond to the product of the number of particles of a particular size and the weight per particle of that size. The curves may be construed as 'differential histograms' where the total weight of particles of sizes $\underline{x} + \underline{dx}$ is plotted against the average particle size $\underline{x} + (\underline{dx}/2)$.

The assumption that the crude kaolin had the distribution described in Figure 14 is taken from the fact that many kaolin clays exhibit a rather uniform distribution between 0.2 and 1.0 microns and that the amount of material smaller than 0.2 microns is generally present in exceedingly small quantity.

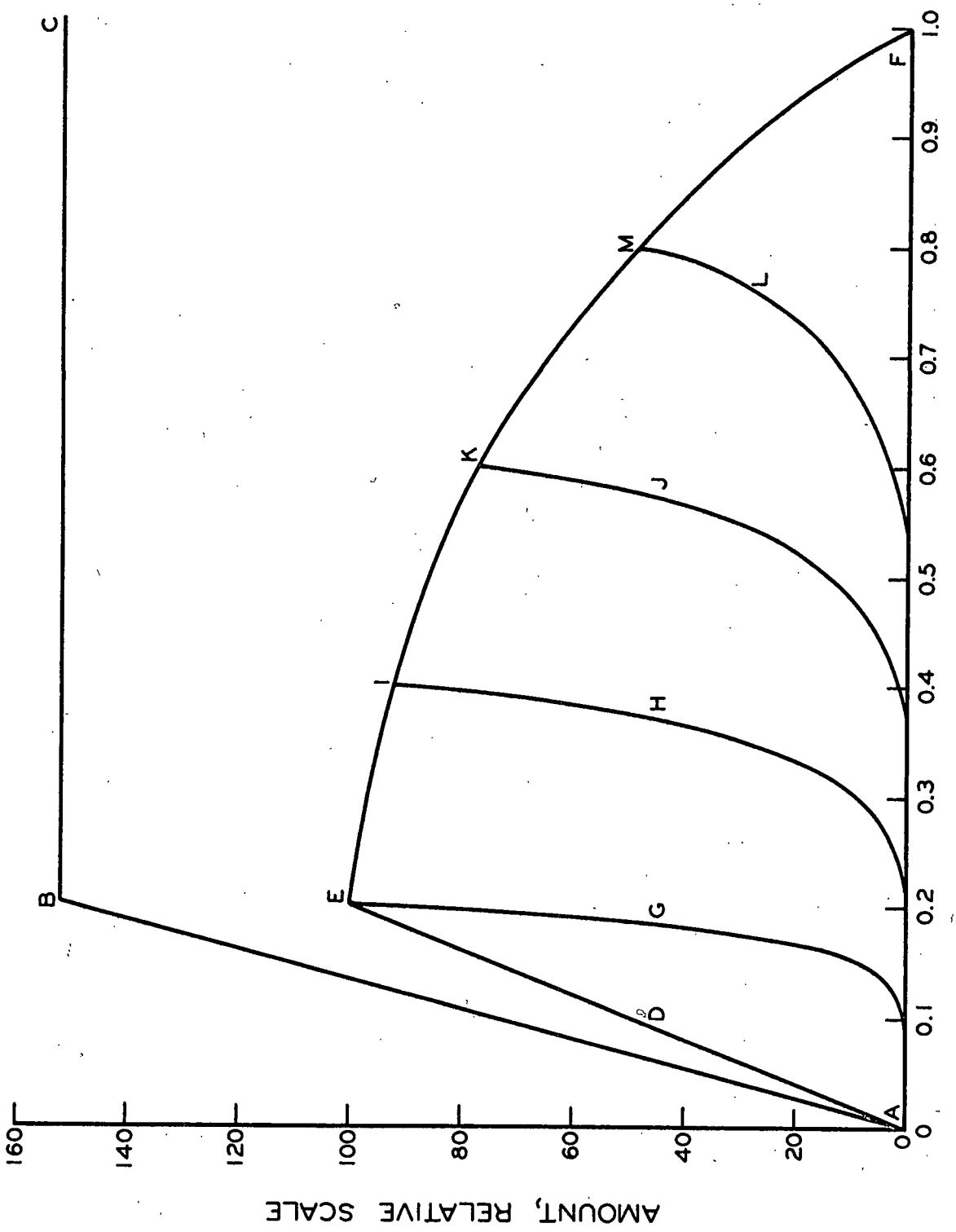

Figure 14. Graphical Method for Obtaining the Profiles of the Various Fractions

similar manner, the curves AHIF, AJKF, and ALMF were constructed and these represent, respectively, the nominal fractions 0.4-1.0, 0.6-1.0, and 0.8-1.0 microns E.S.D.

If we subtract curve AHIF from AGEF, we obtain a profile of the material which was siphoned and collected during the 0.4-micron cut. This material has been designated as Fraction 2. Similarly, the subtraction of AJKF from AHIF and the subtraction of ALMF from AJKF yields Fractions 3 and 4, respectively. The curve ALMF is, of course, Fraction 5. The profiles of these various fractions are shown in Figure 15.

The curves in Figure 15 vividly demonstrate the difficulties encountered in isolating a monodisperse fraction. Fraction 5, for example, contains particles nominally in the range 0.8-1.0 microns E.S.D. Although the particles smaller than 0.8 microns were removed by nine successive siphonings under rather efficient separating conditions (69% of the total volume was siphoned), these particles still constituted an appreciable portion of the particles designated as Fraction 5. The assumption that the average particle size for this fraction is 0.9 microns E.S.D., as is often made in a separation of this sort, can lead to a significant error. The profiles, however, allow us to obtain a more realistic value of the average particle size of each fraction.

PURIFICATION OF THE CLAY FRACTIONS

The clay suspensions were purified by passing them successively through beds of cation-, anion-, and cation-exchange resins. This was

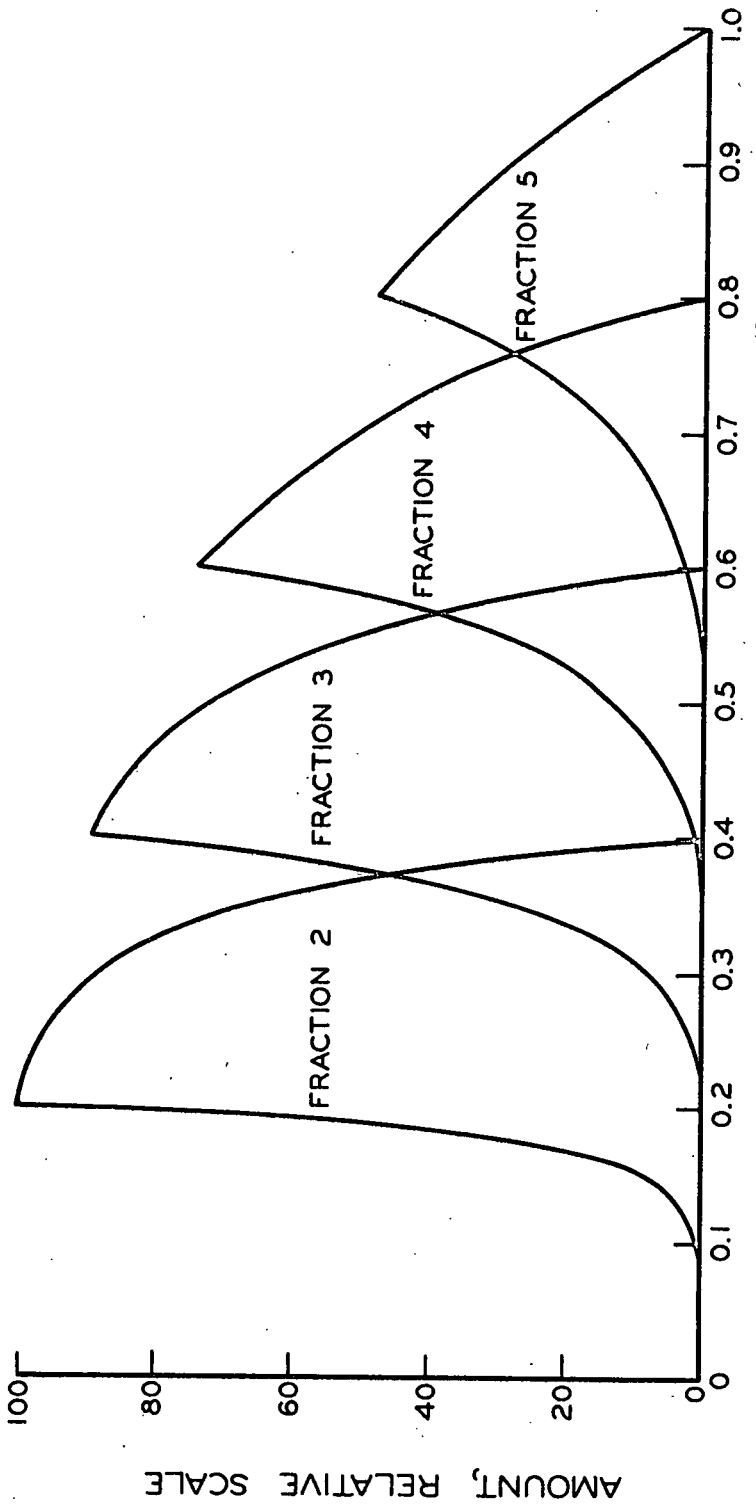

Figure 15. Profiles of the Various Fractions

accomplished by cementing an 80-mesh screen in a funnel and placing the prepared resin on top of the screen. With the funnel outlet closed, the clay slurry was poured into the funnel and stirred with the resin. After a few minutes, the slurry was drained out of the first funnel and passed to the next funnel and resin. The size of the screen was such that virtually all of the resin was retained while the clay slurry passed through freely. After the slurry had passed through the three resin beds, it was filtered through a 150-mesh screen to remove any traces of the resin. The resins employed were Amberlite IR-120 (cation) and Amberlite IR-45 (anion). Before use, the resins were carefully purified.

Purification of the IR-120 resin was accomplished in the following manner. The resin was placed in a column and regenerated with 2N hydrochloric acid using about 20 meq. regenerant/ml. resin. This yields an exchange capacity of about 1.7 meq./ml. resin. Distilled water was then passed through the column until the effluent showed a negative chloride test and had a specific resistance of at least 100,000 ohms. Approximately 380 ml. of this resin was placed in both the first and third funnels. The exchange capacity was consequently about 650 meq. per bed.

About 400 ml. of the IR-45 resin was allowed to stand overnight in 20% sodium hydroxide and then placed in a column through which four liters of 2N sodium hydroxide was passed. Near the end of the regeneration, a chloride test on the caustic effluent was negative. The resin was then washed with distilled water until the column effluent showed a

specific resistance of at least 100,000 ohms. The regeneration procedure yielded an exchange capacity of about 1.85 meq./ml. resin or about 740 meq. for the entire batch. The purified resin was then transferred to the second funnel.

TABLE IX

SPECIFIC RESISTANCE AND pH DURING THE PURIFICATION PROCEDURE

Material	pH	Specific Resistance, ohms
Unpurified Fraction 1 kaolin	10.9	1520
Effluent from the first resin (IR-120)	5.5	127,000
Effluent from the second resin (IR-45)	5.9	216,000
Effluent from the third resin (IR-120)	5.5	212,000

As the clay slurry was passed through the resin beds, some spot measurements of the pH and specific resistance were made. The results

TABLE X

SPECIFIC RESISTANCE OF THE VARIOUS CLAY FRACTIONS

Fraction	Nominal Size, mu E.S.D.	Specific Resistance, ohms
1	0.2-1.0	214,000
2	0.2-0.4	301,000
3	0.4-0.6	309,000
4	0.6-0.8	256,000
5	0.8-1.0	190,000

are shown in Table IX. In addition, specific resistance measurements were made on the purified clay slurries after they had been concentrated and allowed to stand in bottles for several days. These results are presented in Table X.

CHARACTERIZATION OF THE PURIFIED KAOLINITE

Each of the five fractions isolated was subjected to chemical analysis. The results are reported on an ovendry basis in Table XI and represent the average of duplicate determinations. Spectographic analyses for sodium and potassium indicated that these elements were absent in all fractions.

X-ray techniques were also used as an aid in characterizing the purified material. The application of this method to a glycerol solvated sample of the smallest fraction (0.2-0.4 mu E.S.D.) indicated that no detectable amount of bentonite was present. If bentonite were present in any of the fractions, it should occur in greatest quantity in this fraction. The x-ray method was also applied to a random powder sample of Fraction 1. The results indicated that the material was very pure kaolinite and was apparently well crystallized.

The average E.S.D. of each fraction was determined by locating the centroid of each of the profiles shown in Figure 15 and noting the value of the particle size corresponding to the centroid. The results are shown in Table XII. Table XII also shows the specific surface area of

each of the fractions as determined by the application of the Brunauer, Emmett, and Teller equation to nitrogen adsorption data. The values listed are the average of duplicate determinations.

TABLE XI

CHEMICAL COMPOSITION OF THE VARIOUS CLAY FRACTIONS

Fraction	1	2	3	4	5	Theoretical Kaolinite
Al_2O_3, %	38.80	37.25	39.00	39.76	39.18	39.50
SiO_2, %	45.24	44.48	45.76	46.01	44.80	46.50
H_2O, %	13.64	13.48	13.71	13.84	13.84	14.00
TiO_2, %	2.52	4.29	2.25	1.63	2.24	0.00
Fe_2O_3, %	0.28	0.39	0.27	0.24	0.24	0.00
CaO, %	0.12	0.12	0.18	0.16	0.04	0.00
MgO, %	0.00	0.00	0.04	0.00	0.00	0.00

TABLE XII

AVERAGE PARTICLE SIZE AND SPECIFIC SURFACE AREA OF THE VARIOUS CLAY FRACTIONS

Fraction	Average Particle Size, mmu E.S.D.	Specific Surface Area, sq. cm./g.
1	500	107,600
2	268	151,700
3	452	111,100
4	634	93,200
5	820	85,500

PRESENTATION AND DISCUSSION OF EXPERIMENTAL RESULTS

ADSORPTION MEASUREMENTS

The data gathered on all adsorption measurements is shown in Table XIII. The data may be grouped in the following categories: (a) the specific adsorption of citrate ion (x/M) on Fraction 1 kaolinite over a range of pH values, (b) the apparent hydroxyl ion adsorption (y'/M) on Fraction 1 kaolinite over a range of pH values, (c) the variation in (a) incurred by varying both the concentration of sodium chloride and the concentration of sodium citrate, (d) the variation in (b) caused by the same changes, and (e) the variation in x/M and y'/M encountered when the particle size of the kaolinite is varied. Each of these points will be discussed individually.

THE ADSORPTION OF CITRATE IONS

Figure 16 shows the manner in which the citrate ion adsorption changes as the pH is varied. In this case, the amount of sodium citrate placed in the cell was 0.12% based on the ovendry kaolinite. The curve shows several interesting features. In the first place, the presence of sodium chloride apparently has no effect on the adsorption of citrate ions. This suggests that the chloride ion is probably not competing with the citrate ion for adsorption sites on the clay particle. In the second place, the amount adsorbed decreases as the hydroxyl ion content is raised. This suggests that as hydroxyl ion becomes increasingly available for adsorption, it is being adsorbed in preference to the citrate ions.

TABLE XIII

ADSORPTION DATA

Experiment	Fraction	pH	$Na_3C_6H_5O_7$ Added, mg.	NaCl Added, ml. 0.1004N	x/M, mg./g.	Y'/M, meq./g.
1	1	7.5	6.00	0.00	0.36	0.0032
2	1	9.5	6.00	0.00	0.10	0.0129
3	1	10.6	6.00	0.00	0.00	0.0201
4	1	10.9	6.00	0.00	-0.03	0.0206
5	1	11.0	6.00	0.00	-0.05	0.0252
6	1	11.5	6.00	0.00	-0.03	0.0276
7	1	11.8	6.00	0.00	-0.02	0.0334
9	1	9.3	6.00	0.00	0.18	0.0096
10	1	10.4	6.00	0.00	-0.01	0.0174
13	1	8.6	6.00	5.00	0.25	0.0122
14	1	8.6	6.00	10.00	0.22	0.0112
15	1	9.0	6.00	0.00	0.17	0.0088
16	1	9.2	6.00	0.00	0.15	0.0100
17	1	10.3	6.00	0.00	0.01	0.0162
18	1	12.5	6.00	0.00	-0.01	0.044
19	1	10.3	6.00	5.00	0.04	0.0240
20	1	10.2	6.00	10.00	0.05	0.0150
21	1	8.8	6.00	20.00	0.19	0.0226
22	1	7.7	6.00	5.00	0.34	0.0108
23	1	7.9	6.00	10.00	0.25	0.0170

Note: In all experiments, sufficient water was added to adjust the total volume of fluids to 86.0 ml. All experiments except those indicated with the superscript[a] were performed on 5.00 g. kaolinite. The superscript[a] indicates that 3.90 g. kaolinite was used.

TABLE XIII (Continued)

ADSORPTION DATA

Experiment	Fraction	pH	$Na_3C_6H_5O_7$ Added, mg.	NaCl Added, ml. 0.1004N	x/M, mg./g.	Y'/M, meq./g.
24	1	9.9	6.00	5.00	--	0.0172
25	1	11.1	6.00	5.00	--	0.0224
26	1	8.3	6.00	10.00	--	0.0124
27	1	9.5	6.00	10.00	--	0.0158
28	1	9.8	6.00	10.00	--	0.0174
29	1	11.2	6.00	10.00	--	0.0230
30	1	7.4	6.00	20.00	--	0.0110
31	1	10.1	6.00	20.00	--	0.0230
32	1	11.2	6.00	20.00	--	0.0194
33	1	6.6	15.02	0.00	0.71	-0.0006
34	1	8.2	15.02	0.00	0.32	0.0043
35	1	8.6	15.02	0.00	0.22	0.0077
36	1	8.3	15.02	0.00	0.30	0.0055
37	1	8.6	15.02	0.00	0.25	0.0069
38	1	10.1	15.02	0.00	0.02	0.0156
39	1	11.32	15.02	0.00	-0.05	0.0280
40	1	11.87	12.02	0.00	--	0.0306
41	1	12.27	15.02	0.00	-0.02	0.0320
42	1	12.5	15.02	0.00	-0.05	0.044
43	1	12.5	30.0	0.00	-0.02	0.048
44	1	12.2	30.0	0.00	-0.04	0.0348
45	1	11.75	30.0	0.00	0.01	0.0326
46	1	11.19	30.0	0.00	-0.10	0.0242
47	1	10.81	30.0	0.00	-0.00	0.0194
48	1	10.23	30.0	0.00	-0.01	0.0178

Note: In all experiments, sufficient water was added to adjust the total volume of fluids to 86.0 ml. All experiments except those indicated with the superscript[a] were performed on 5.00 g. kaolinite. The superscript[a] indicates that 3.90 g. kaolinite was used.

TABLE XIII(Continued)

ADSORPTION DATA

Experiment	Fraction	pH	$Na_3C_6H_5O_7$ Added, mg.	NaCl Added, ml. 0.1004N	x/M, mg./g.	y'/M, meq./g.
49	1	9.62	30.0	0.00	0.15	0.0132
50	1	9.01	30.0	0.00	0.15	0.0124
51	1	8.29	30.0	0.00	0.48	0.0057
52	1	7.07	30.0	0.00	1.04	--
53	1	9.39	15.02	0.00	0.23	0.0097
54	1	7.27	75.1	0.00	1.00	0.0006
55	1	8.13	75.1	0.00	0.62	0.0054
56	1	9.32	75.1	0.00	0.08	0.0146
57	1	12.30	0.00	0.00	--	0.044
58	1	12.43	75.1	0.00	-0.16	0.042
59	1	11.80	75.1	0.00	0.00	0.0318
60	1	9.45	6.00	20.00	0.12	0.0090
61	1	10.53	75.1	0.00	-0.08	0.0186
63	1	6.46	6.00	0.00	0.65	--
64	1	7.40	6.00	0.00	0.35	--
65	1	9.32	0.00	0.00	--	0.0094
66	1	10.20	0.00	0.00	--	0.0150
67	1	11.19	0.00	0.00	--	0.0266
68	1	11.71	0.00	0.00	--	0.0362
69[a]	2	6.00	6.00	0.00	1.08	--
70[a]	2	7.49	6.00	0.00	0.58	--
71[a]	2	11.11	6.00	0.00	--	0.0297
72	3	6.00	6.00	0.00	0.75	--
73	3	7.60	6.00	0.00	0.31	--
74	3	11.03	6.00	0.00	--	0.0210

Note: In all experiments, sufficient water was added to adjust the total volume of fluids to 86.0 ml. All experiments except those indicated with the superscript[a] were performed on 5.00 g. kaolinite. The superscript[a] indicates that 3.90 g. kaolinite was used.

TABLE XIII (Continued)

ADSORPTION DATA

Experiment	Fraction	pH	$Na_3C_6H_5O_7$ Added, mg.	NaCl Added, ml. 0.1004N	$\frac{x}{M}$, mg./g.	$\frac{Y'}{M}$, meq./g.
75	4	6.13	6.00	0.00	0.61	--
76	4	8.31	6.00	0.00	0.30	--
77	4	11.19	6.00	0.00	--	0.0204
78	5	6.17	6.00	0.00	0.51	--
79	5	8.77	6.00	0.00	0.25	--
80	5	11.24	6.00	0.00	--	0.0190
81[a]	2	7.37	6.00	0.00	0.60	--
82[a]	2	11.68	6.00	0.00	--	0.0423
83[a]	2	10.52	6.00	0.00	--	0.0217
84	3	7.23	6.00	0.00	0.51	--
85	3	11.67	6.00	0.00	--	0.0344
86	3	10.46	6.00	0.00	--	0.0173
87	4	7.72	6.00	0.00	0.31	--
88	4	11.71	6.00	0.00	--	0.0296
89	4	10.32	6.00	0.00	--	0.0158
90	5	8.25	6.00	0.00	0.17	--
91	5	11.72	6.00	0.00	--	0.0288
92	5	10.60	6.00	0.00	--	0.0143

Note: In all experiments, sufficient water was added to adjust the total volume of fluids to 86.0 ml. All experiments except those indicated with the superscript[a] were performed on 5.00 g. kaolinite. The superscript[a] indicates that 3.90 g. kaolinite was used.

(This point will be discussed in greater detail later.) The third feature that the curve exhibits is that no adsorption of citrate ion occurs above a pH of about 10.3. In fact, the citrate ion may be negatively adsorbed to some small degree beyond this pH. This is indicated in Figure 16, although the data are sufficiently imprecise to conclude this as fact.

[Negative adsorption is the result of repulsion from the double layer. In this case, if a citrate ion approaches a particle which has already adsorbed hydroxyl ions, then the negative charge of the particle tends to repel the citrate ion from a zone in the immediate vicinity of the particle. Thus, the average concentration of citrate ions in the region close to the particle is less than the intermicellar concentration of citrate ions. Mathematically, this is expressed by the Boltzmann distributive law, i.e.,

$$\underline{n}_{\underline{d}}^{-} = \underline{n}_{\infty}^{-} e^{-(\underline{V}^{-} \epsilon \ \psi_{\underline{d}}/\underline{KT})}$$

where

$\underline{n}_{\underline{d}}^{-}$ = the average concentration of the anion under consideration at a distance $\underline{d}$ from the particle,

$\underline{n}_{\infty}^{-}$ = the concentration of the anion in the intermicellar solution,

$\underline{V}^{-}$ = the valence of the anion, and

$\psi_{\underline{d}}$ = the difference in potential between that at a distance $\underline{d}$ from the particle and the intermicellar solution.

In regions close to the particle, the potential difference is quite large and the average anionic concentration approaches zero. At regions distant

from the particle, the potential difference is exceedingly small and the exponent approaches zero.]

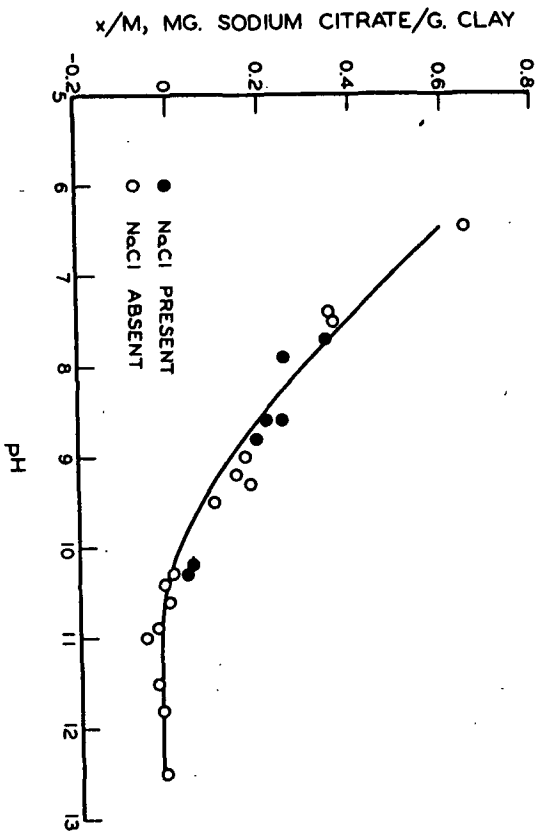

Figure 16. The Effect of Sodium Hydroxide Addition on the Adsorption of Citrate Ions. 0.12% Sodium Citrate (Based on the Clay) at 5.50% Solids

In Figures 17, 18, and 19, the same variables are plotted for different initial concentrations of sodium citrate. It is evident that the scatter of the data increases with increasing sodium citrate concentration and becomes more pronounced when the adsorption is very small. This occurs because of the peculiar nature of the error in these experiments. It can be shown that for a given analytical error in the

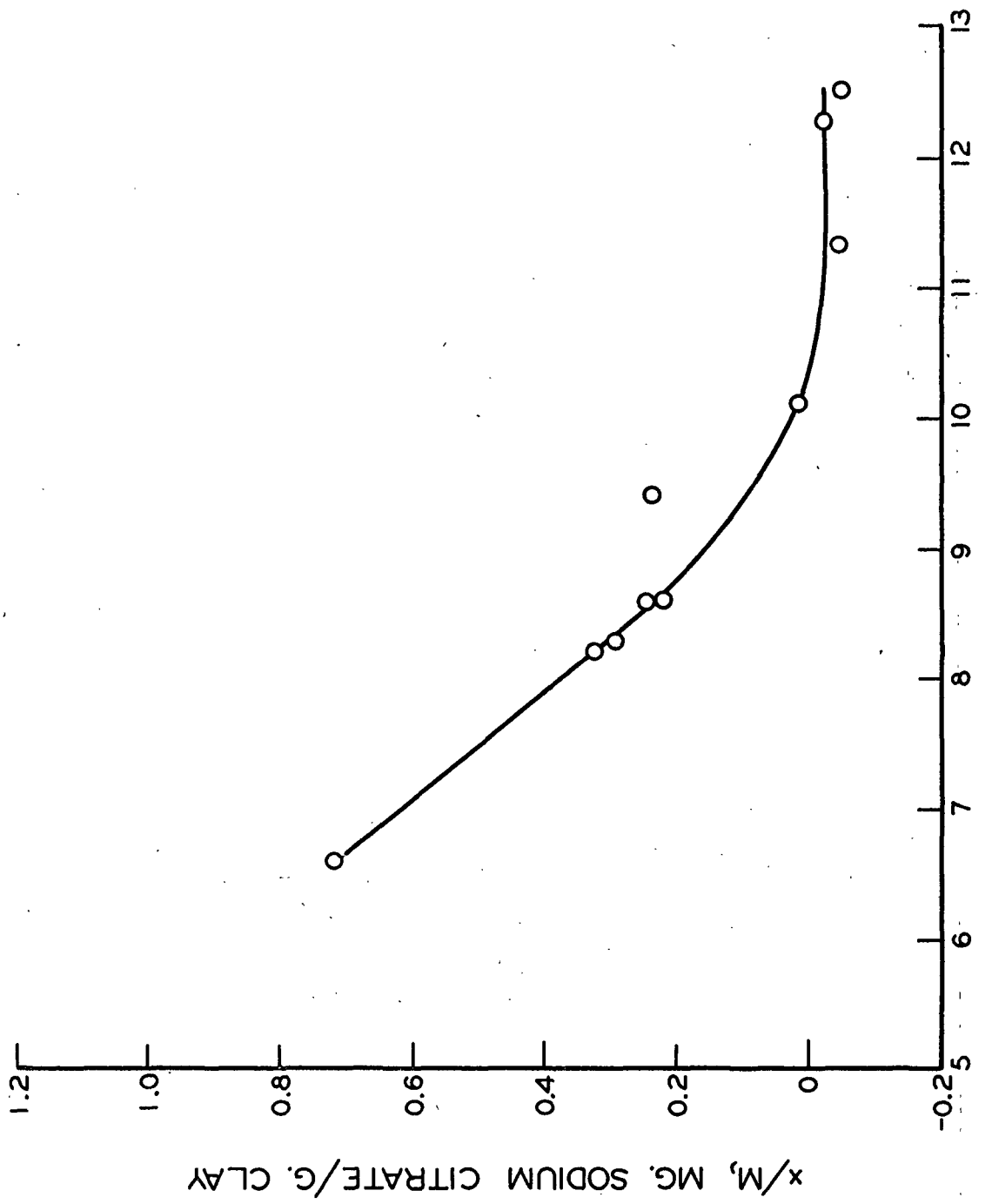

Figure 17. The Effect of Sodium Hydroxide Addition on the Adsorption of Citrate Ions. 0.30% Sodium Citrate (Based on the Clay) at 5.50% Solids

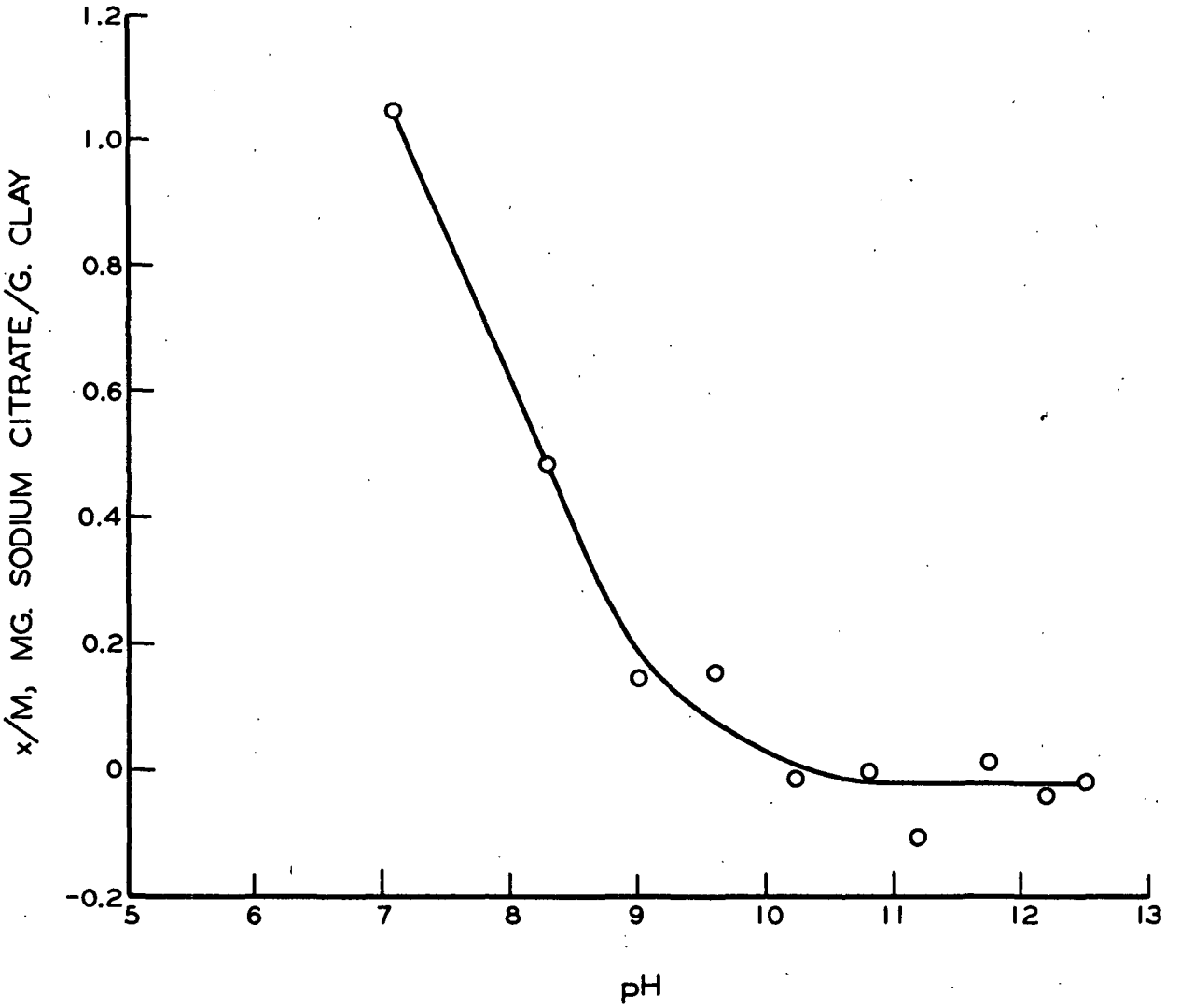

Figure 18. The Effect of Sodium Hydroxide Addition on the Adsorption of Citrate Ions. 0.60% Sodium Citrate (Based on the Clay) at 5.50% Solids.

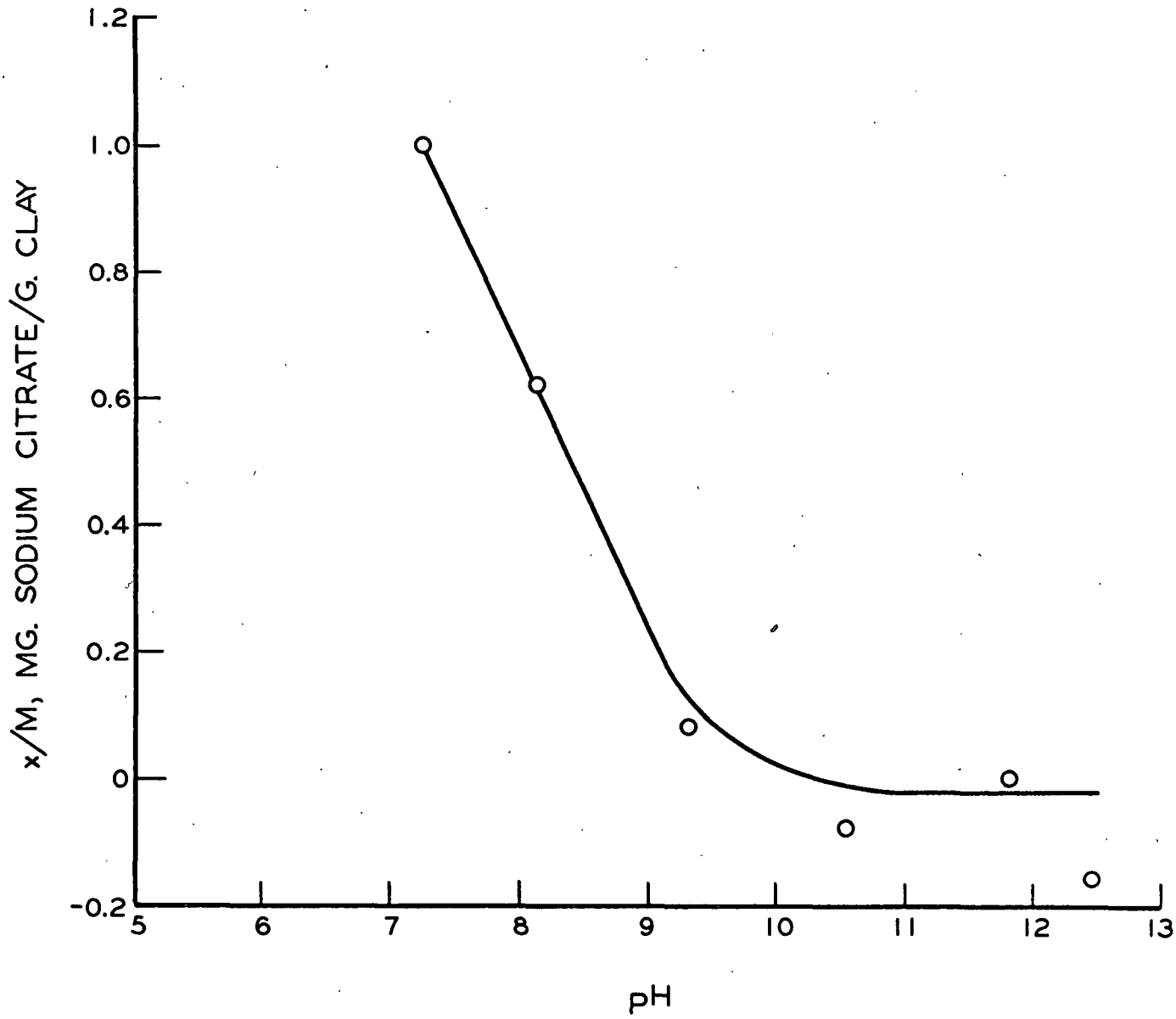

Figure 19. The Effect of Sodium Hydroxide Addition on the Adsorption of Citrate Ions. 1.50% Sodium Citrate (Based on the Clay) at 5.50% Solids.

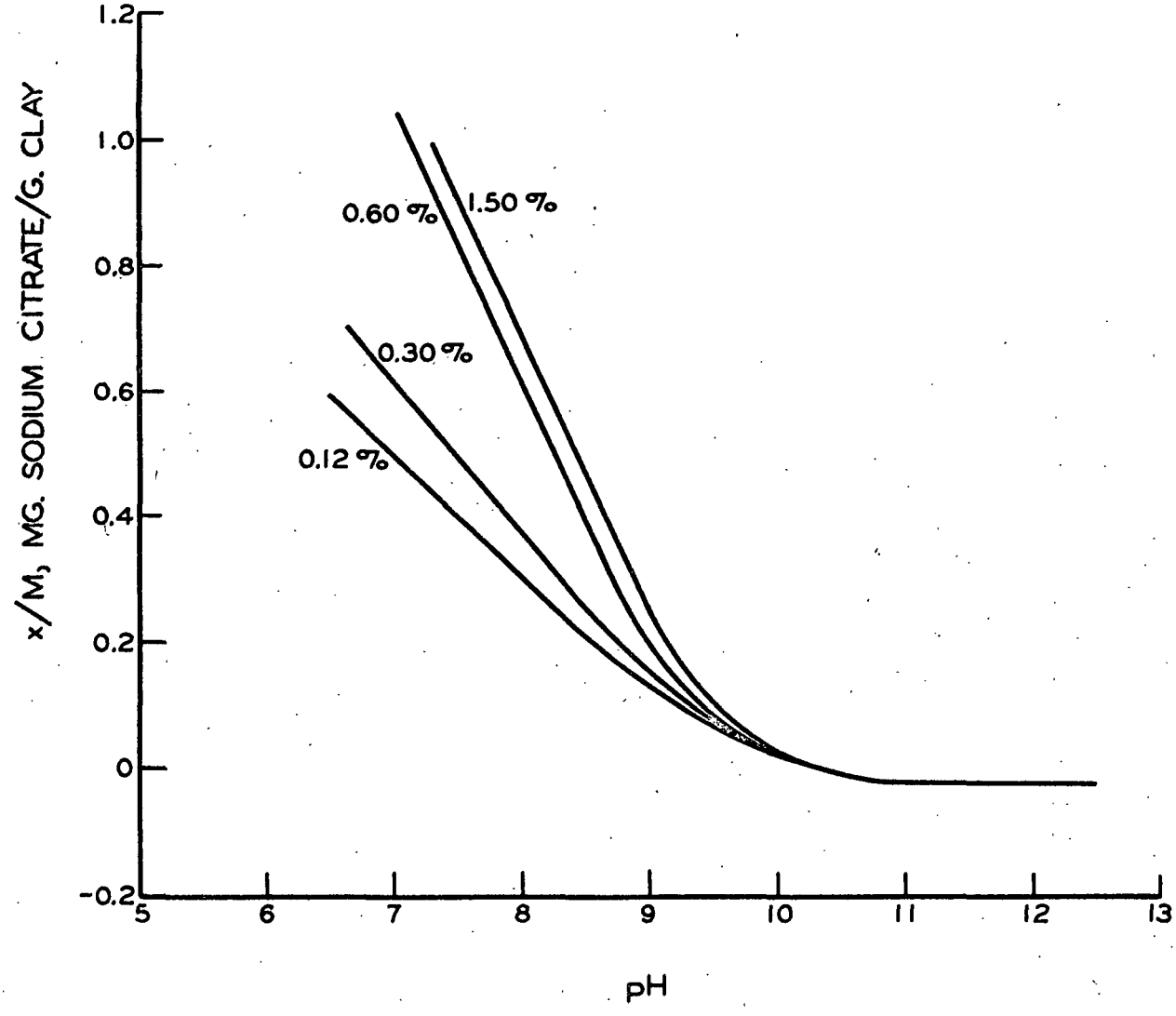

Figure 20. The Adsorption of Citrate Ions at Various Concentrations of Sodium Citrate and Sodium Hydroxide. 5.50% Solids

determination of sodium citrate, the absolute magnitude of the error increases as the adsorption decreases. As the sodium citrate concentration is raised, the error also increases because the calculated results depend upon an essentially constant difference between numbers of increasing magnitude. For example, at 0.12% sodium citrate an analytical error of 2% yields an error in $\underline{x}/\underline{M}$ of 0.012 mg./g. when $\underline{x}/\underline{M}$ is 0.6 mg./g., and an error of 0.024 mg./g. when $\underline{x}/\underline{M}$ is zero. When the sodium citrate content is raised to 1.5%, the same analytical error will yield an error in $\underline{x}/\underline{M}$ of 0.288 mg./g. when $\underline{x}/\underline{M}$ is 0.6 mg./g., and an error of 0.300 mg./g. when no adsorption takes place. Consequently, the left side of each curve should be more precise than the right side. In addition, the data should be more precise for the lower concentrations of sodium citrate.

This analysis provides the basis for drawing the curves in the manner presented. In Figure 16, the curve is fairly well determined by the data points. In Figure 17, this is true for the left side of the curve (where the pH is below 8.8), but the data points generally lie below the curve on the right side. However, there is no reason to believe that less adsorption should take place at 0.30% sodium citrate than at 0.12%. Since the data points do not indicate that the adsorption is greater than that shown in Figure 17, the curve has been constructed to coincide with Figure 16 for pH values greater than 9.5. A similar argument follows for Figures 18 and 19. From these curves, Figure 20 has been constructed.

Figure 20 shows the effect of sodium citrate concentration on the relationship between the adsorption of citrate ion and the pH. For pH values greater than 9, the adsorption is independent of the sodium citrate concentration. Below this pH, it is probable that the hydroxyl ion adsorption is small enough to permit the sodium citrate concentration to have an effect on the adsorption of citrate ion. (This, too, will be discussed in greater detail later.) Figure 20 also indicates that at 1.5% sodium citrate[1], the intermicellar concentration of this salt is great enough so that further increases in concentration will not significantly affect the adsorption of citrate ion[2]. While it may be expected that the 0.6 and 1.5% curves may diverge greatly at lower pH's than those shown in Figure 20, this is physically impossible for this particular system without the addition of another salt. The lowest pH shown in each of the curves is that obtained when the system contains only the purified kaolinite suspension, pure water, and the amount of sodium citrate indicated.

---

1 The reader should recall that this figure (1.5%) is concentration based on the clay and that Figure 20 corresponds to a system containing 5 g. of clay and 86 ml. of water. If a system of higher solids content is to be considered, the concentration of sodium citrate (expressed as a percentage of the clay) at which maximum adsorption would occur would be lower. Examples of this will be cited later.

2 Because of the magnitude of the errors possible in the 1.5% curve, it is not certain that this curve truly differs from the 0.6% curve. The construction was based solely on the best fit of the data.

THE ADSORPTION OF CHLORIDE IONS

The chloride ion adsorption ($\underline{w}/\underline{M}$) was measured on 16 different samples and the results are tabulated in Table XIV. The average of these values indicates a negative adsorption of 0.0011 meq./g. clay. This amount is relatively insignificant compared to the hydroxyl ion adsorption. Because of the possible errors in the determination (which was based on an extremely small difference between two large numbers), the calculation of hydroxyl ion adsorption was made on the assumption that no chloride ion adsorption took place in the alkaline pH range.

Samson (23) has investigated this matter more carefully. He found that the adsorption of chloride ions becomes zero at a pH of about 6, and that for pH's greater than 7.5, the value is constant and negative to the extent of 0.0002-0.0020 meq./g., depending upon the clay sample. Since most of the values were closer to the lower limit, this constitutes a minor correction to the calculation of hydroxyl ion adsorption.

TABLE XIV

CHLORIDE ION ADSORPTION BY KAOLINITE

Expt.	$\underline{w}/\underline{M}$, meq./g.	Expt.	$\underline{w}/\underline{M}$, meq./g.	Expt.	$\underline{w}/\underline{M}$, meq./g.
13	-0.0022	22	-0.0022	27	+0.0074
14	-0.0014	23	-0.0016	28	+0.0012
19	-0.0026	24	-0.0016	29	-0.0002
20	-0.0012	25	-0.0024	30	-0.0040
21	-0.0022	26	+0.0022	31	-0.0032
				32	-0.0030

THE ADSORPTION OF HYDROXYL IONS

Figure 21 shows the manner in which the apparent hydroxyl ion adsorption changes with pH. The data includes all experiments, regardless of sodium citrate content, in which no sodium chloride was added to the system. It is evident that the concentration of sodium citrate has no effect on the apparent hydroxyl ion adsorption.

Figure 22 shows the same information plotted for the cases where sodium chloride was added to the system. The data points show increasing scatter with increasing sodium chloride concentration because this also represents a case where the result depends upon an essentially constant difference between numbers of increasing magnitude. In each case, a curve was constructed which had the general shape of Figure 21 and which best fit the data points.

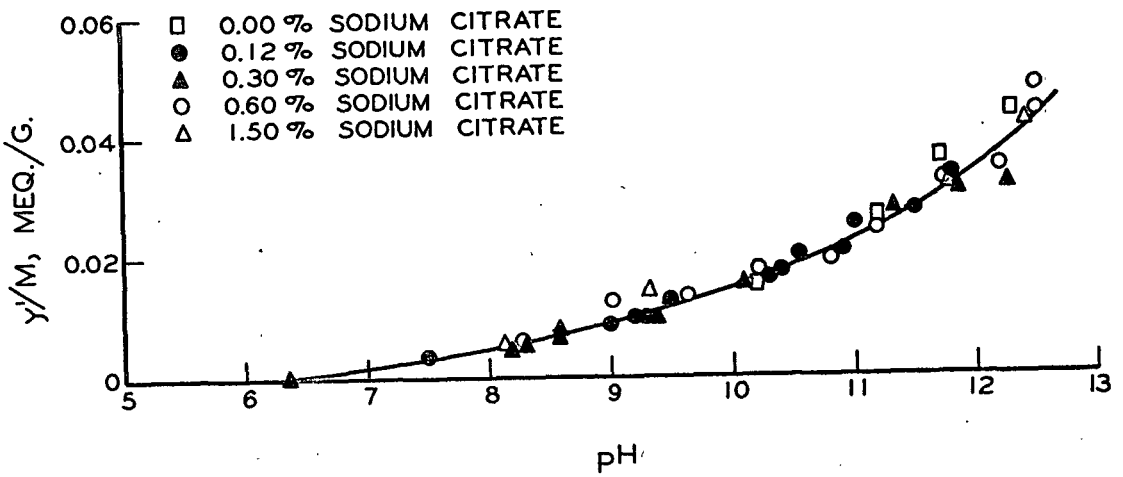

Figure 21. The Effect of pH on the Apparent Hydroxyl Ion Adsorption

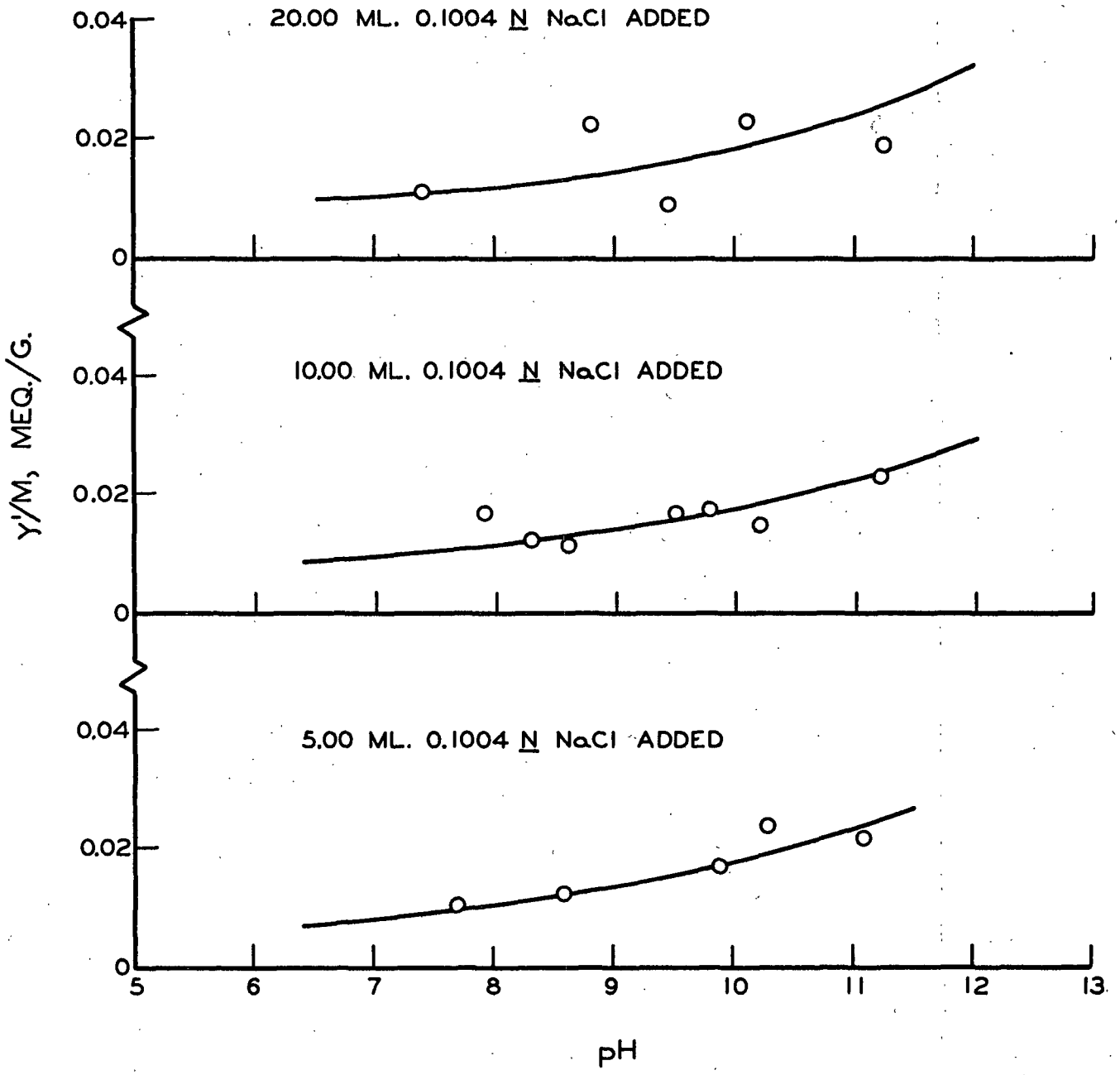

Figure 22. The Effect of Sodium Chloride Additions on the Apparent Hydroxyl Ion Adsorption-pH Relationship

From the smooth curves obtained in Figures 21 and 22, Figure 23 was constructed. At each pH, the data was cross-plotted to obtain $y'/\underline{M}$ as a function of the sodium chloride concentration. Consequently, at a given pH, we have shown the situation where the exchange of sodium counterions for hydrogen counterions is approaching completeness. This makes it possible to estimate the true hydroxyl ion adsorption at that pH.

Figure 23 shows several interesting features. As anticipated, the lower pH values required more sodium chloride to bring about an essentially complete exchange. At a pH of 9, exchange was essentially complete when 10 ml. of 0.1$\underline{N}$ sodium chloride had been added to the system. When sufficient sodium hydroxide had been added to bring the pH to 11, the amount of sodium ion provided by this salt was enough to yield an essentially complete exchange without the addition of sodium chloride. It is interesting to note the profound preference exhibited by kaolinite for a hydrogen counterion to a sodium counterion. On the basis of the two cases cited above, the ratio of sodium ion concentration to hydrogen ion concentration in the intermicellar solution required to bring about an essentially complete exchange was 10^7 and 10^8, respectively. Viewing this in another manner, we can show that sodium ion and hydrogen ion are present to equal extents in the diffuse double layer when the ratio of the concentrations of these ions in the intermicellar solution is about 3×10^4.

The use of the limiting values of $y'/\underline{M}$ obtained in Figure 23 made

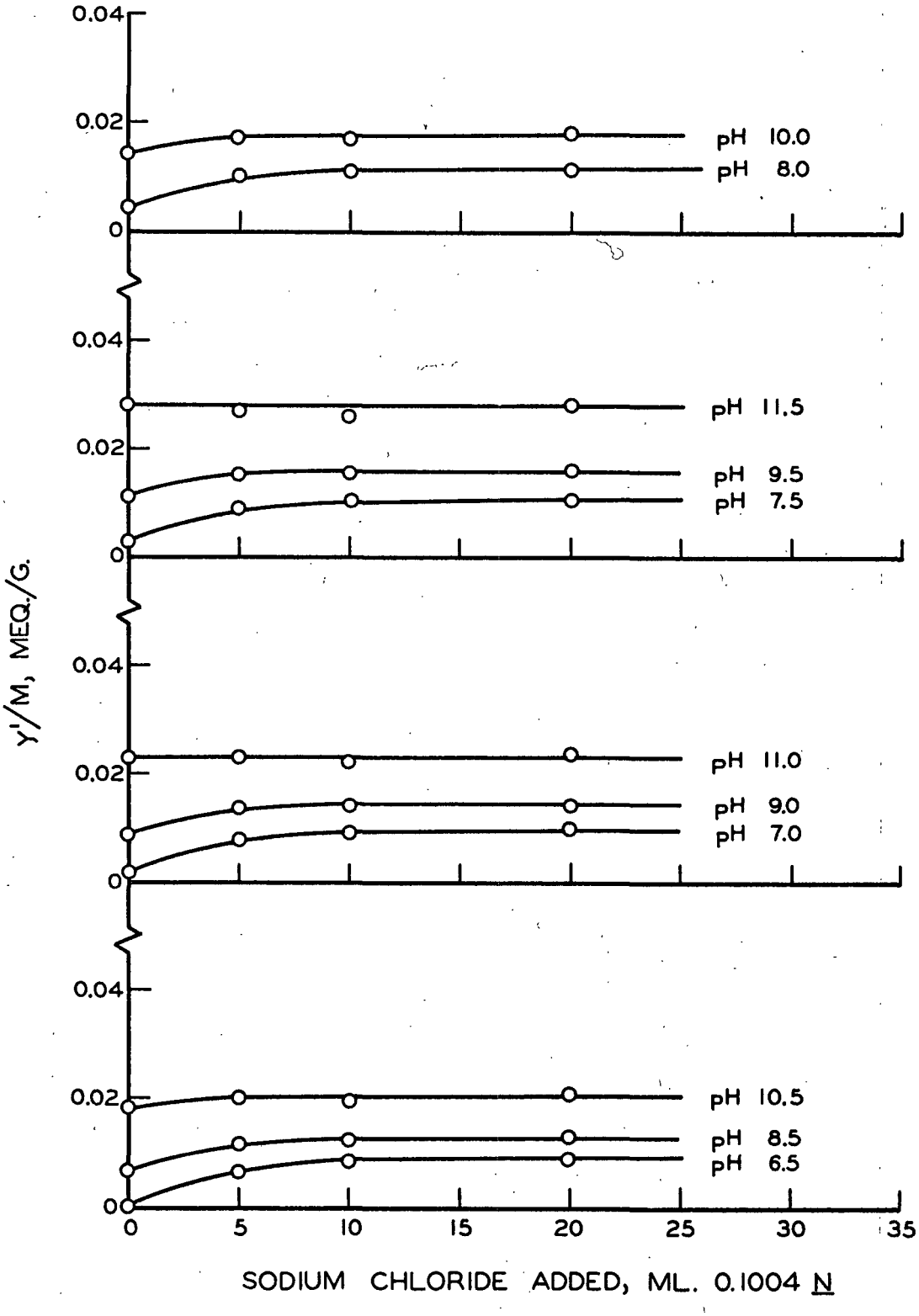

Figure 23. Extrapolation of the Apparent Hydroxyl Ion Adsorption

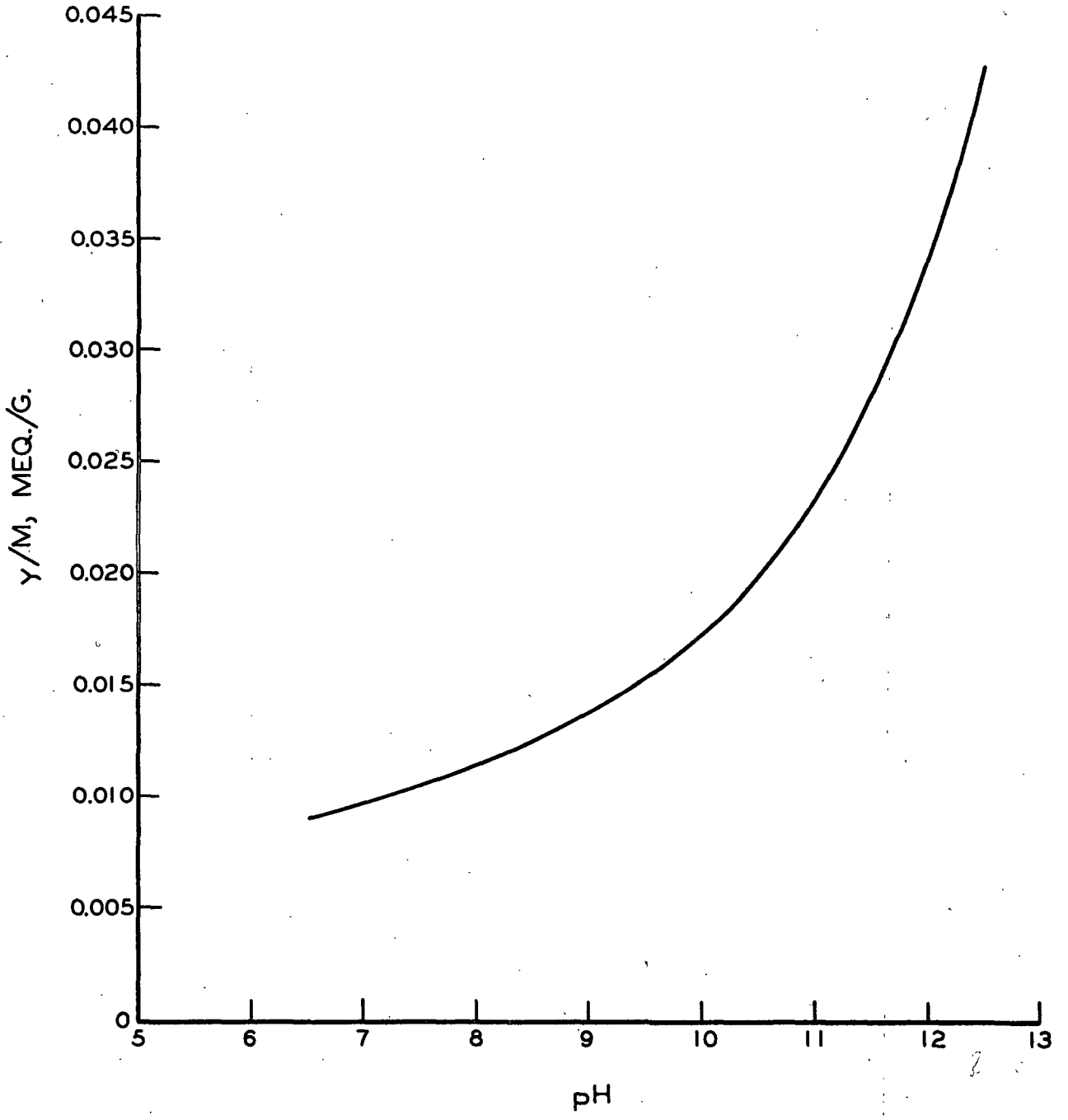

Figure 24. The Relationship Between Hydroxyl Ion Adsorption and pH

it possible to plot the true hydroxyl ion adsorption as a function of pH (Figure 24). For pH values greater than 11.5, the smooth curve of Figure 21 was used to complete the construction. This is possible because, for these high pH values, exchange is essentially complete without the addition of sodium chloride. Figure 24 shows an increasing hydroxyl ion adsorption with increasing pH[1]. It also shows that some hydroxyl ion adsorption occurs even when the system is acidic[2].

THE COMPETITION OF ANIONS FOR ADSORPTION SITES

If we examine Figures 20, 21, and 24 closely, we can learn a good deal about the competition between citrate and hydroxyl ion for adsorption sites. The fact that increasing the sodium citrate concentration did not depress the hydroxyl ion adsorption (Figure 21) gives the first indication that hydroxyl ion is adsorbed in preference to the citrate ion. This is to be expected from the Hofmeister series of anion adsorbability. A better indication of this preference may be demonstrated by comparing the intermicellar concentrations of these ions at a point

---

1 The shape of the curve is misleading because the concentration of hydroxyl ion is plotted logarithmically, expanding the lower portions of the scale. If we were to plot the hydroxyl ion adsorption as a function of the hydroxyl ion concentration expressed linearly (as is the usual practice), the curvature would be reversed.

2 This point has an interesting ramification. If we were to acidify the system with hydrochloric acid, positive chloride ion adsorption would occur (23) by the time the hydroxyl ion ceased to be adsorbed. Consequently, an isoelectric point would not be observed. This may be true for all acids and could possibly explain the reason why an isoelectric point has never been observed for kaolinite.

where both ions are adsorbed in equivalent amounts. At an adsorption of 0.012 meq./g. (pH 8.0 for the hydroxyl ion and 0.6% sodium citrate at pH 7.2 for the citrate ion), the intermicellar concentration of hydroxyl ion is 10^{-6} meq./ml. whereas the intermicellar concentration of sodium citrate is 3×10^{-3} meq./ml. Thus, there must be about 3000 equivalents of citrate ion available for each equivalent of hydroxyl ion available if these ions are to be adsorbed to the same extent. The hydroxyl ion is undoubtedly the preferred anion.

As the concentration of hydroxyl ion decreases, the adsorption of this ion decreases to the extent that enough adsorption sites become available to adsorb a citrate ion in deference to a hydroxyl ion. Consequently, the positive adsorption of citrate ion begins. As the hydroxyl ion concentration is reduced still further, so many sites become available that the concentration of sodium citrate in the intermicellar solution begins to control the magnitude of the citrate ion adsorption. This is indicated by the fanning of the curves in Figure 20.

The chloride ion also competes with the hydroxyl ion for adsorption sites, but this ion lies so far below hydroxyl ion in the Hofmeister series of anion adsorbability that it cannot be adsorbed in the alkaline pH range. It is, however, positively adsorbed at pH's below 6 (23) and exhibits a relationship to pH very similar to that shown for citrate ion in Figure 20. It is conceivable that if the adsorption of many anions were determined as a function of pH, the curves would be aligned along the pH scale in the Hofmeister series of anion adsorbability.

THE SITE OF ANIONIC ADSORPTION

One of the major objections to the use of the Verwey and Overbeek theory as a tool for the explanation of the rheological properties of the kaolinite-water system has been based on the question of charge distribution. The equations have been derived for the case where the charge is uniformly distributed over the face of a flat surface, whereas it is commonly believed that anionic adsorption on kaolinite predominantly occurs at the crystal edges yielding a platelike particle with a charge concentrated in this area. This point was of sufficient importance to merit an investigation of where adsorption takes place on the clay particle.

We may approach this problem by obtaining adsorption data on particles of various sizes. Johnson and Norton (24) have shown that an adaptation of the Müller equation can be successfully applied to kaolinite. In this equation, the dimensions of a disk-shaped particle moving with a random orientation in a force field are related to the dimensions of a spherical particle which will sediment at the same velocity. Thus

$$\underline{r} = (8/3)\,(\underline{a}) \left\{ \frac{1 - (\underline{b}/\underline{a})^2}{\left[\frac{3 - 2(\underline{b}/\underline{a})^2}{1 - (\underline{b}/\underline{a})^2}\right] \frac{1}{2} \left[\frac{\pi}{2} - \arcsin\,(\underline{b}/\underline{a})\right]} \right\} \quad (18)$$

where (see Figure 25)

$\underline{r}$ = the radius of the sperical particle, cm.,

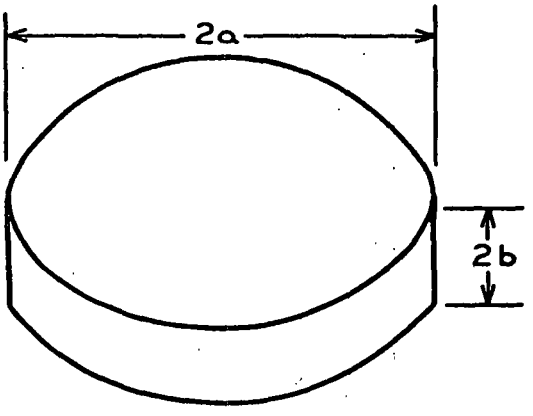

Figure 25. Dimensions of the Circular Disk Described by Equation (18).

$\underline{b}$ = the semithickness of the disk-shaped particle, cm., and

$\underline{a}$ = the semidiameter of the disk-shaped particle, cm.

It should be noted that the fractionation procedure yields particles whose sizes are described in terms of equivalent spherical diameters (or radii) which are, in turn, defined as the diameters (or radii) of spheres which will sediment at the same velocities as the particles under consideration. Thus, the equivalent spherical radius is identical with the term $\underline{r}$ in Equation (18).

Since kaolinite particles are hexagonal plates, the assumption that they are disk-shaped introduces a negligible error. On the basis of this assumption, we may calculate both the surface area and the weight of one particle in terms of its diameter, thickness, and density. Referring to Figure 25, the surface area of the particle is $2\pi\underline{a}^2 + 4\pi\underline{a}\underline{b}$ or $2\pi\underline{a}(\underline{a} + 2\underline{b})$, and the weight of the particle is $2\pi\underline{a}^2\ \underline{b}\ \underline{d}_1$. Thus, we may express the specific surface area by the equation

$$\text{Specific Surface Area} = \frac{2\pi\underline{a}(\underline{a} + 2\underline{b})}{2\pi\underline{a}^2\ \underline{b}\ \underline{d}_1} = \frac{\underline{a} + 2\underline{b}}{\underline{a}\ \underline{b}\ \underline{d}_1} \qquad (19)$$

Since we already know the density of clay (assumed for this calculation to be 2.6 g./cc.) and the equivalent spherical diameter and specific surface area of each fraction (Table XII), we may solve Equations (18) and (19) simultaneously to determine the thickness and diameter of the particles in each fraction. A simplified method for the solution of these equations is shown in Appendix V.

It is also possible to describe each of the two types of areas (edge and face) in terms of the dimensions of the circular disk. Since the face area may be expressed by $2\pi a^2$ and the edge area by $4\pi ab$, it is obvious that the percentage of the total area which consists of face area is given by the equation

$$\% \text{ Face Area} = \frac{100}{1 - 2(b/a)} \qquad (20)$$

Since we already know the average dimensions of the particles in each fraction by the simultaneous solution of Equations (18) and (19), we can now determine, for each fraction, the specific surface areas of both faces and edges. If we couple this knowledge with adsorption measurements on each fraction, it is possible to determine which of these areas is primarily responsible for anionic adsorption phenomena.

For kaolinite, the ratio of particle thickness to particle diameter (b/a) undergoes considerable variation. Johnson and Norton (24) made such measurements on 30 particles and found values of b/a in range 0.06-0.32. This is indeed fortunate, since small changes in this ratio would not

yield sufficiently large changes in the two types of areas to distinguish between adsorption phenomena occurring on one area in preference to the other. For the fractions isolated in this work, the values for this ratio and the particle dimensions are shown in Table XV.

The data presented in Table XV exhibits several important features. The most important of these is the manner in which b/a varies with particle size. As the particles get smaller, b/a increases showing that the particles tend to become chunkier. The writer has examined other sets of data of surface area and particle size, and in all cases this same tendency was evident. This is, after all, to be expected. If the assumption is made that small particles are formed by the fracture of larger particles, it is probable that the smallest particles would become more thick-set since this shape represents a condition of greater mechanical stability. However, it is improbable that the value of b/a will become much greater than about 0.5 because the bonding in the direction of the basal cleavage plane (primary valence bonding) has a considerably higher energy than bonding in a direction perpendicular to this plane (hydrogen bonding). It would seem that the shape of a particle is governed by the number and type of bonds in each direction and by the mechanical stability of the particle as a whole.

A second feature evident in the data of Table XV is the manner in which the particle dimensions vary with particle size. As the particles get smaller, their thickness decreases, but to a far lesser extent than the decrease in diameter. This shows that essentially all

TABLE XV

DIMENSIONS OF THE VARIOUS CLAY FRACTIONS

Fraction	1	2	3	4	5
Average particle size, mmu E.S.D.	500	268	452	634	820
Total surface area, sq. cm./g.	107,600	151,700	111,100	93,200	85,500
Thickness-to-diameter ratio, b/a	0.274	0.418	0.304	0.237	0.183
Average particle thickness, 2b, mmu	111	93	111	122	122
Average particle diameter, 2a, mmu	404	223	365	513	669
Face area, sq. cm./g.	69,500	82,700	69,100	63,200	62,600
Edge area, sq. cm./g.	38,100	69,000	42,000	30,000	22,900
Face area, % of total area	64.6	54.5	62.2	67.8	73.2

fracture has occurred perpendicular to the basal cleavage plane and tends to substantiate the argument that mechanical stability is of importance in determining the particle shape. It may also show that so many hydrogen bonds have been formed perpendicular to the basal cleavage plane that fracture in this plane requires more energy than fracture perpendicular to this plane--in spite of the fact that the perpendicular fracture breaks primary valence bonds.

The third feature indicated in Table XV is the relatively large change in the types of areas exhibited by each of the fractions. The change is sufficient to provide a good indicator of where adsorption takes place.

The data showing the variation in adsorption obtained on the various fractions is presented in Experiments 69-92 in Table XIII. The adsorption data were plotted as a function of pH for each of the fractions, and from the resulting smooth curves, values of x/M and y/M[1] were obtained at several pH values. This was done so that the adsorption data for the various fractions could be compared at a definite pH. The results are shown in Table XVI.

Using the data in Tables XV and XVI, we may plot the ionic adsorption as a function of the surface area of the sample. This is done in Figures 26-9. At a specified set of conditions, three curves are possible: (a) the adsorption as a function of the edge area, (b) the adsorption as a

[1] Although the data gives y'/M, the chosen pH values were sufficiently high that y'/M was essentially equal to y/M.

function of the face area, and (c) the adsorption as a function of the total area. In every case, the adsorption as a function of edge area yielded a curve having a constantly decreasing slope, whereas the relationship between adsorption and face area exhibited a curve of constantly increasing slope. However, the relationship between adsorption and total area is linear, and the line relating the two variables passes through the origin. It may be reasonably argued that a straight line can be constructed through the data points for both edge area and face area. If this is done, the lines of best fit would show a finite adsorption when no edge area is present and no adsorption when a finite amount of face area is present. The indication is that adsorption is occurring uniformly over the total surface of the particle.

TABLE XVI

THE EFFECT OF PARTICLE SIZE ON THE ADSORPTION OF CITRATE IONS AND HYDROXYL IONS

Fraction	2	3	4	5
$\underline{x}/\underline{M}$ at pH 6.50, mg./g.	0.818	0.601	0.520	0.441
$\underline{x}/\underline{M}$ at pH 7.50, mg./g.	0.571	0.417	0.359	0.297
$\underline{y}/\underline{M}$ at pH 11.00, meq./g.	0.0278	0.0209	0.0187	0.0167
$\underline{y}/\underline{M}$ at pH 11.50, meq./g.	0.0372	0.0289	0.0248	0.0231

This point is vividly demonstrated in Figure 30. In this case, the adsorption per unit surface area is plotted as a function of the particle size. Since adsorption is a surface phenomenon, the adsorption per unit area should be independent of particle size if the appropriate area is

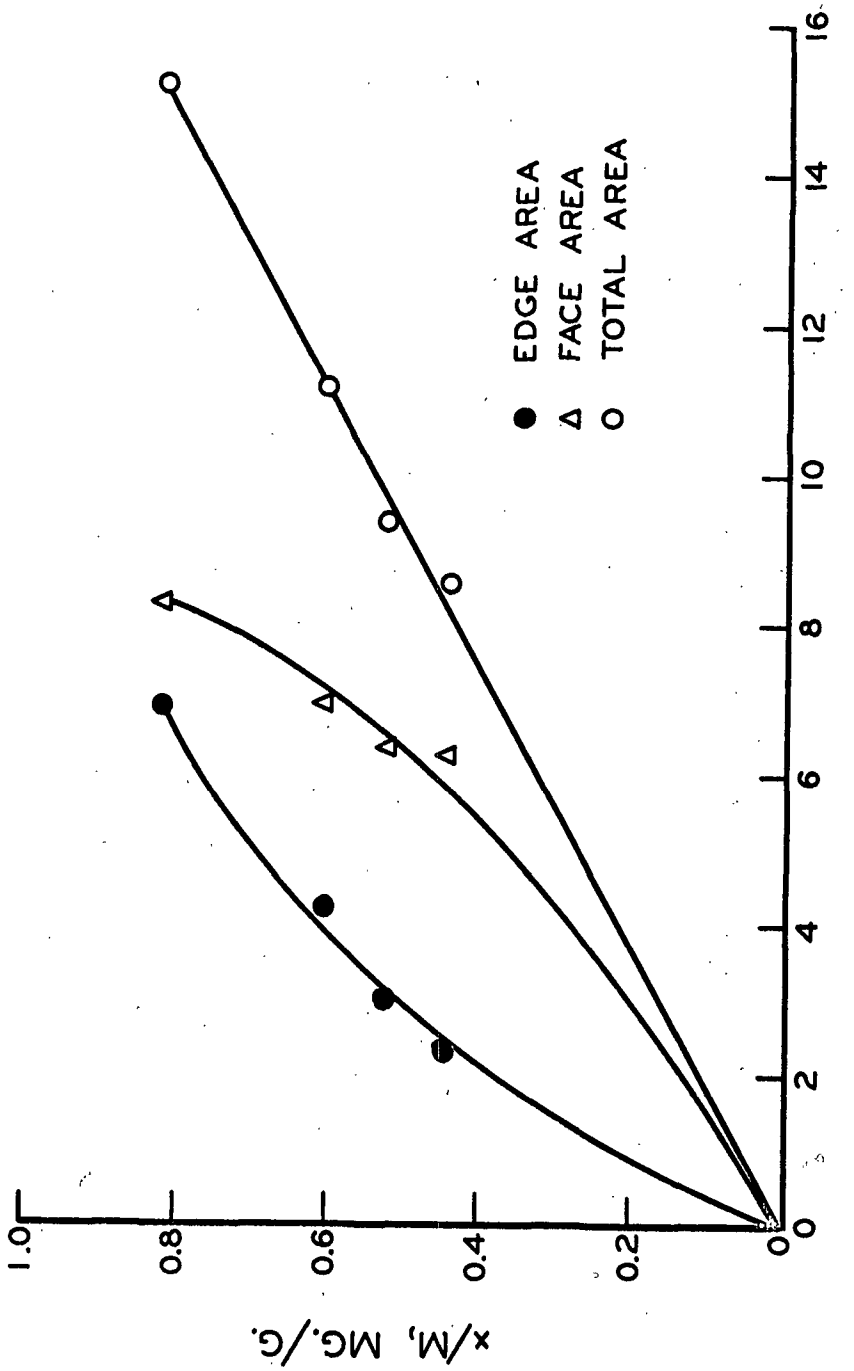

Figure 26. The Effect of Surface Area on the Citrate Ion Adsorption at pH 6.50

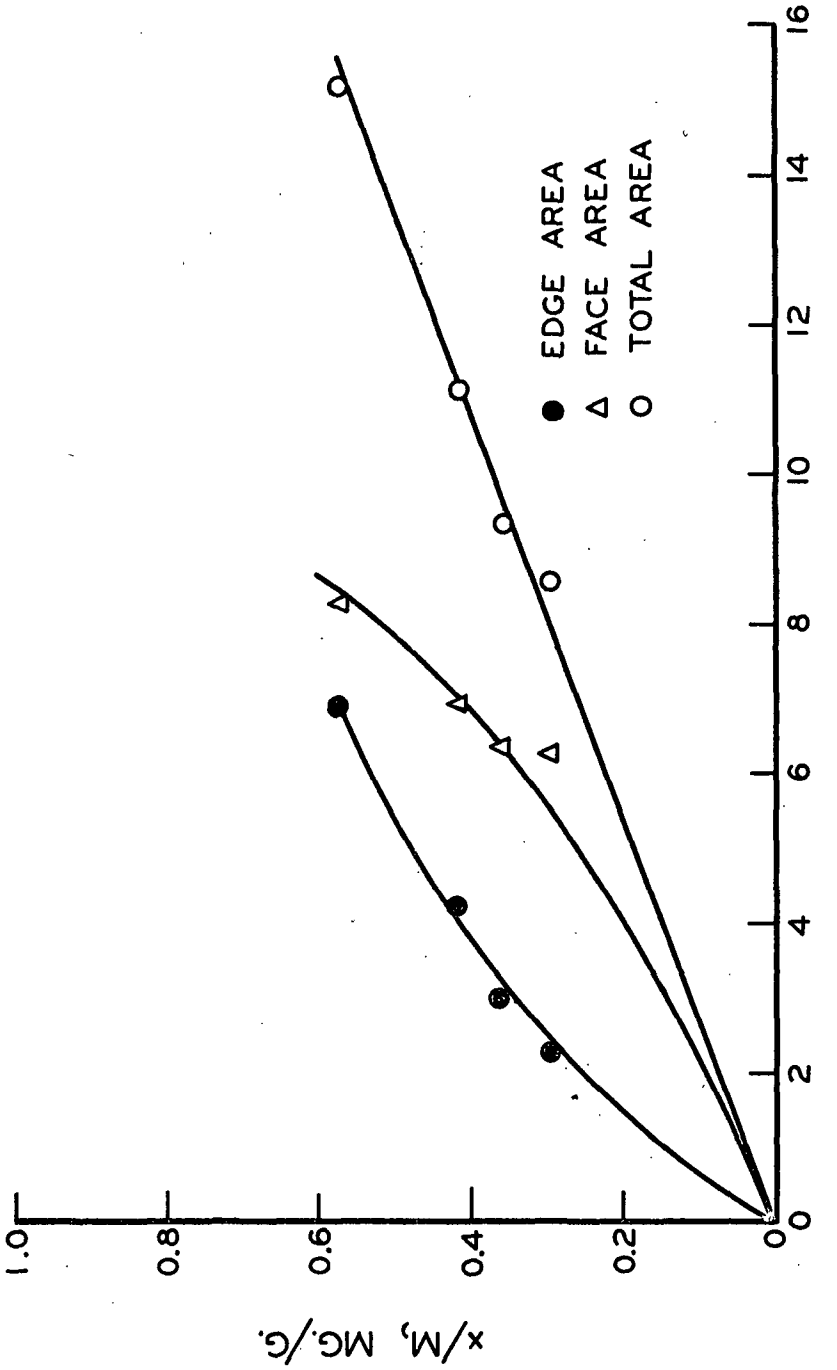

Figure 27. The Effect of Surface Area on the Citrate Ion Adsorption at pH 7.50

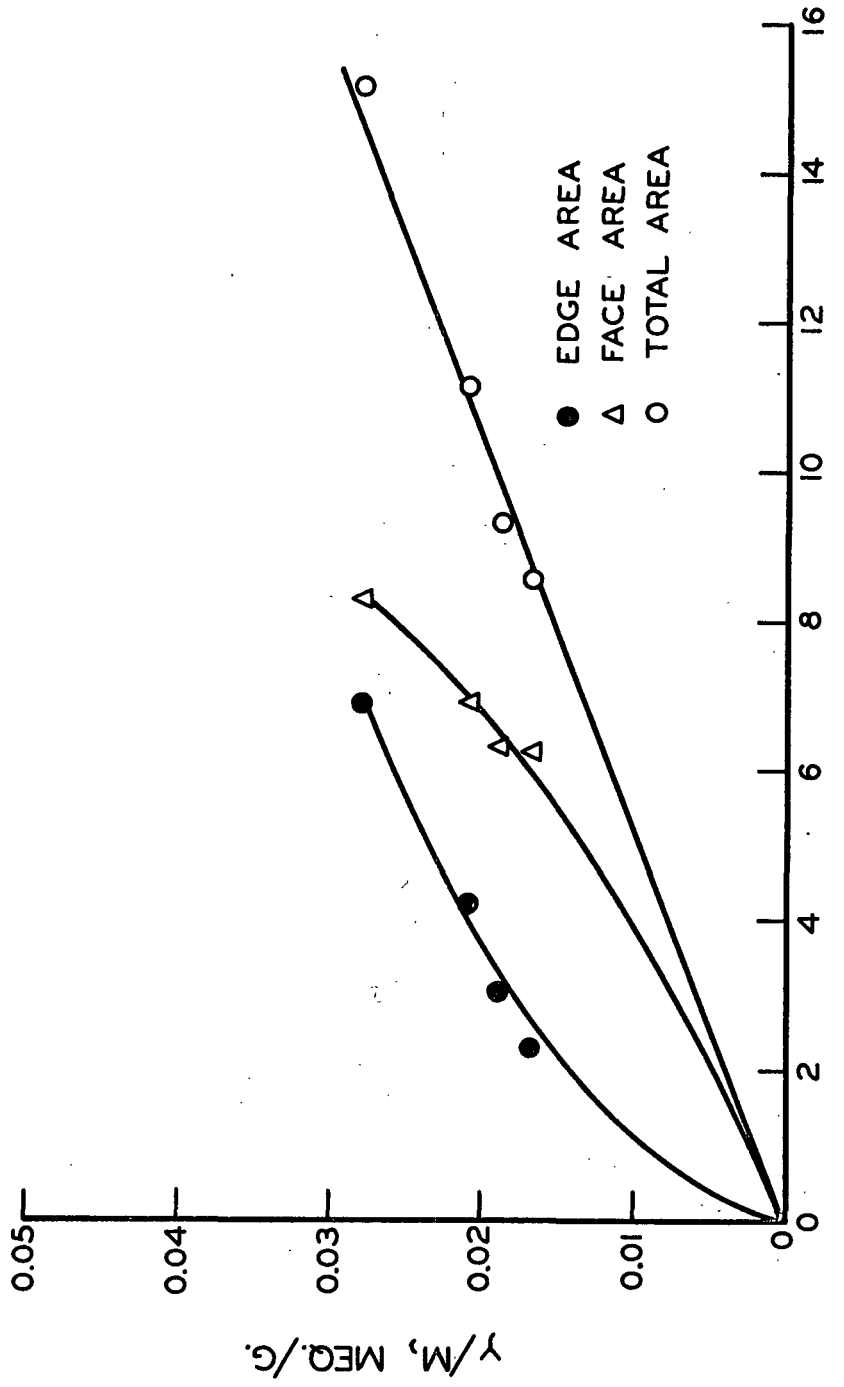

Figure 28. The Effect of Surface Area on the Hydroxyl Ion Adsorption at pH 11.00

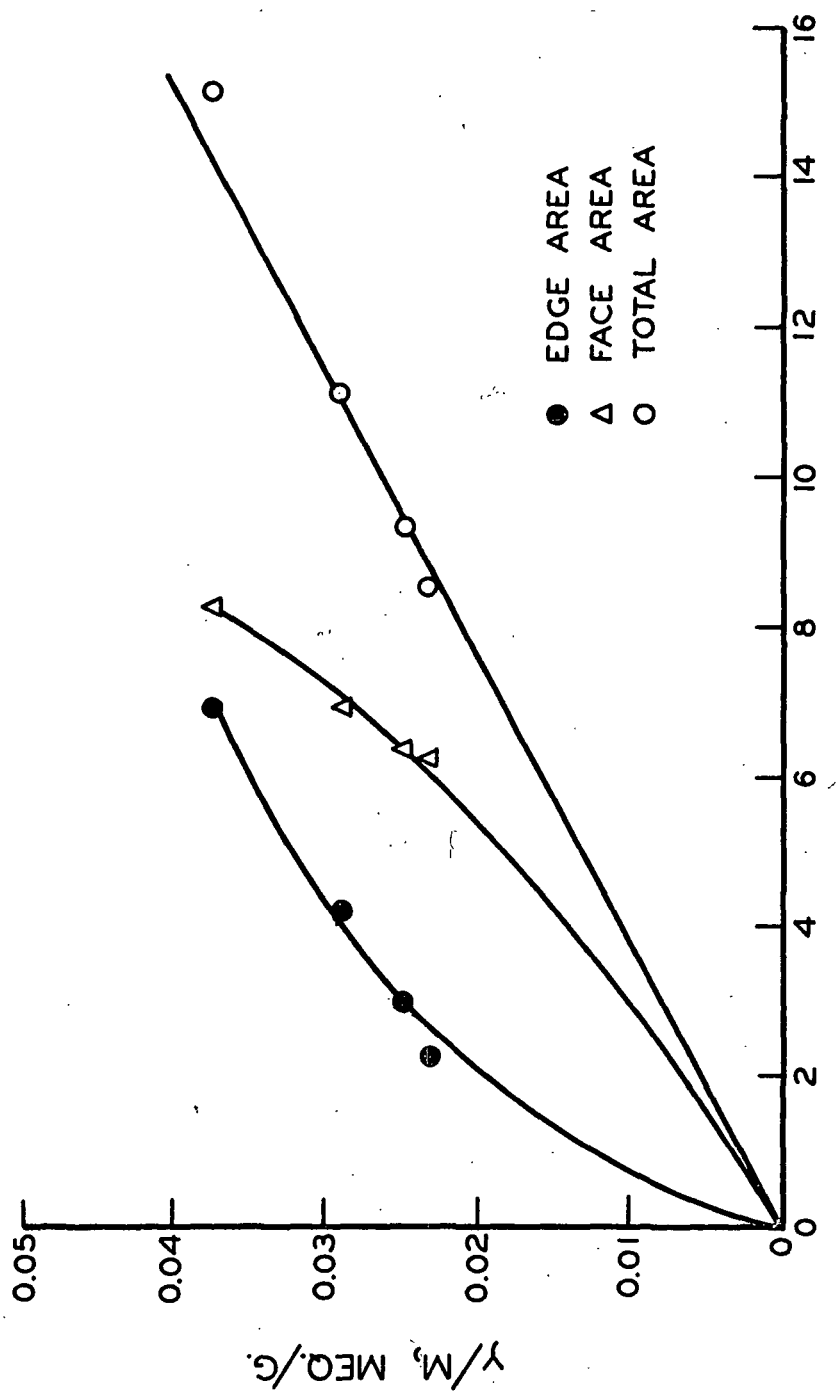

Figure 29. The Effect of Surface Area on the Hydroxyl Ion Adsorption at pH 11.50

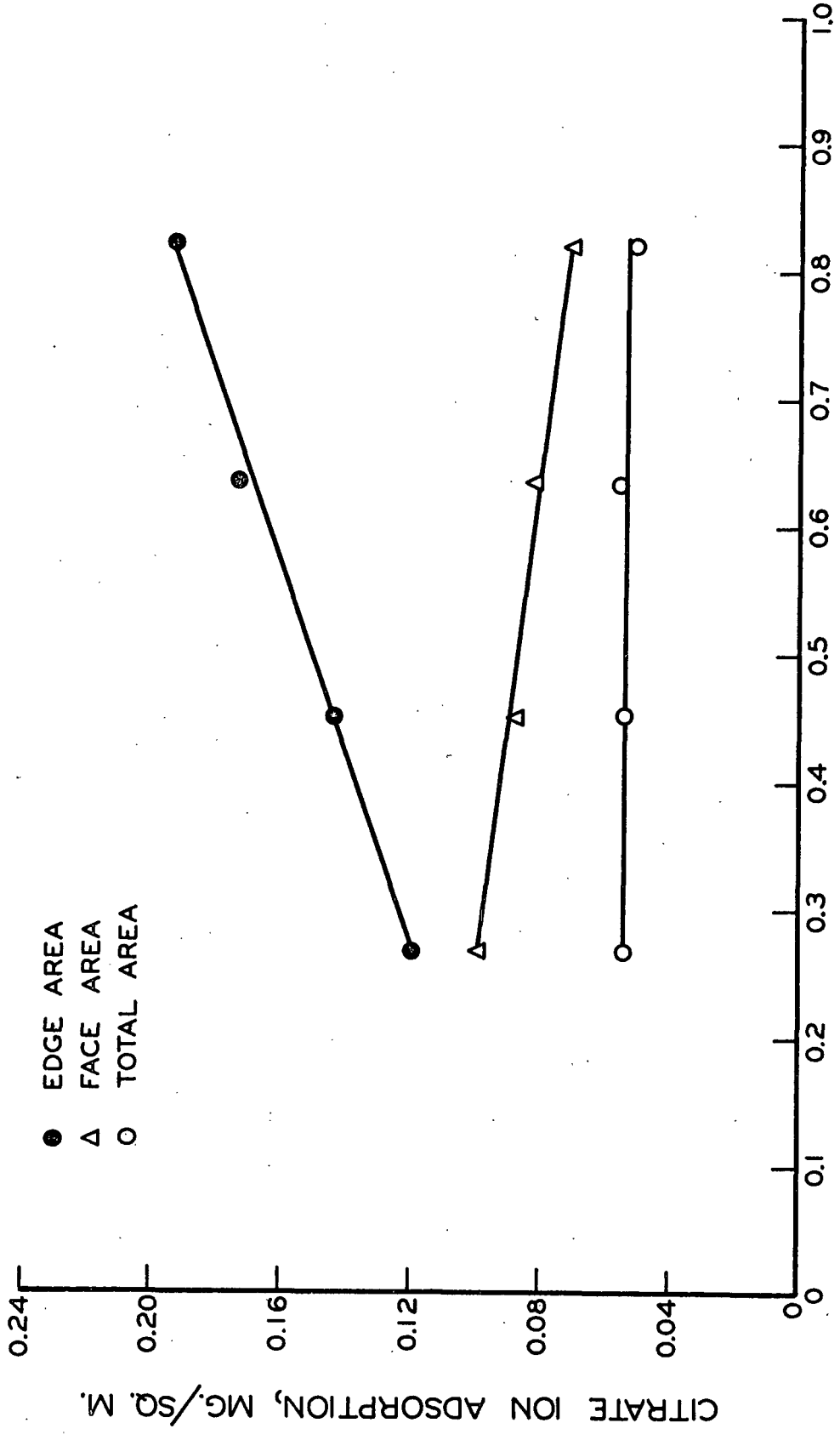

Figure 30. The Adsorption per Unit Area of Citrate Ions at pH 6.50 vs. Particle Size

considered. The adsorption per unit edge area is not independent of particle size; therefore, adsorption cannot be occurring solely on this surface. The adsorption per unit face area is also dependent upon particle size and, consequently, adsorption cannot be occurring solely on this surface. However, the adsorption per unit total area is independent of particle size; therefore the charge is probably uniformly distributed over the entire surface of the particle.

Although the data in Figure 30 have been plotted for a specific pH and for citrate ion adsorption, similar graphs will be obtained at other pH's for both citrate and hydroxyl ion adsorption. Therefore, the conclusion is not limited to one pH and one type of ionic adsorption, but is rather general. The reader should note that a slight preference for adsorption to occur on one type of area rather than the other will not be detected by this method of analysis. However, gross preferences become readily evident.

POTENTIAL ENERGY CURVES

DETERMINATION OF THE VARIABLES IN THE POTENTIAL ENERGY EQUATIONS

The determination of the magnitude of the variables used in the potential energy equations has been discussed to some degree in the PRESENTATION OF THE PROBLEM. At this time, the matter will be considered more thoroughly, particularly the methods used to obtain the numbers actually substituted in the equations. All calculations of potential energy were derived from the adsorption data on Fraction 1 kaolinite.

Of the various fractions isolated, this fraction is most representative of commercially available kaolin.

The numbers substituted for the variable n in Equations (5), (8), and (10) were obtained from the data on the sodium ion analyses. This made it possible to plot the intermicellar concentration of sodium ions as a function of pH for each of the various additions of sodium citrate[1]. One of the graphs obtained is shown in Figure 31[2]. From the smooth curve, values of the sodium ion concentration at definite pH intervals were obtained. These values were then converted to sodium ion concentrations expressed in terms of ions per cubic centimeter of intermicellar solution, and the numbers thus obtained were substituted directly into the equations. In all experimental cases except that cited in the footnote, the contribution of the hydrogen ion concentration to n was negligible.

The value of σ substituted in Equation (10) was obtained in the following manner. From the smooth curves in Figure 20, values of the

---

1 The data obtained in the experiments where sodium chloride was added were not used in the graphs because we wish to show only the effect of additions of sodium citrate and sodium hydroxide on the potential energy functions at this time. The effect of sodium chloride additions will be considered later.

2 The reader will note that the ordinate in Figure 31 is logarithmic. For the case where no sodium citrate was added, a linear co-ordinate system was used for the lower portions of the curve. This made it possible to include the point where no sodium ions were added to the system. In this case, n was determined from the hydrogen ion concentration at pH 5.50. The hydroxyl ion adsorption used in the calculations for this special case was obtained by the extrapolation of Figure 24 to pH 5.50.

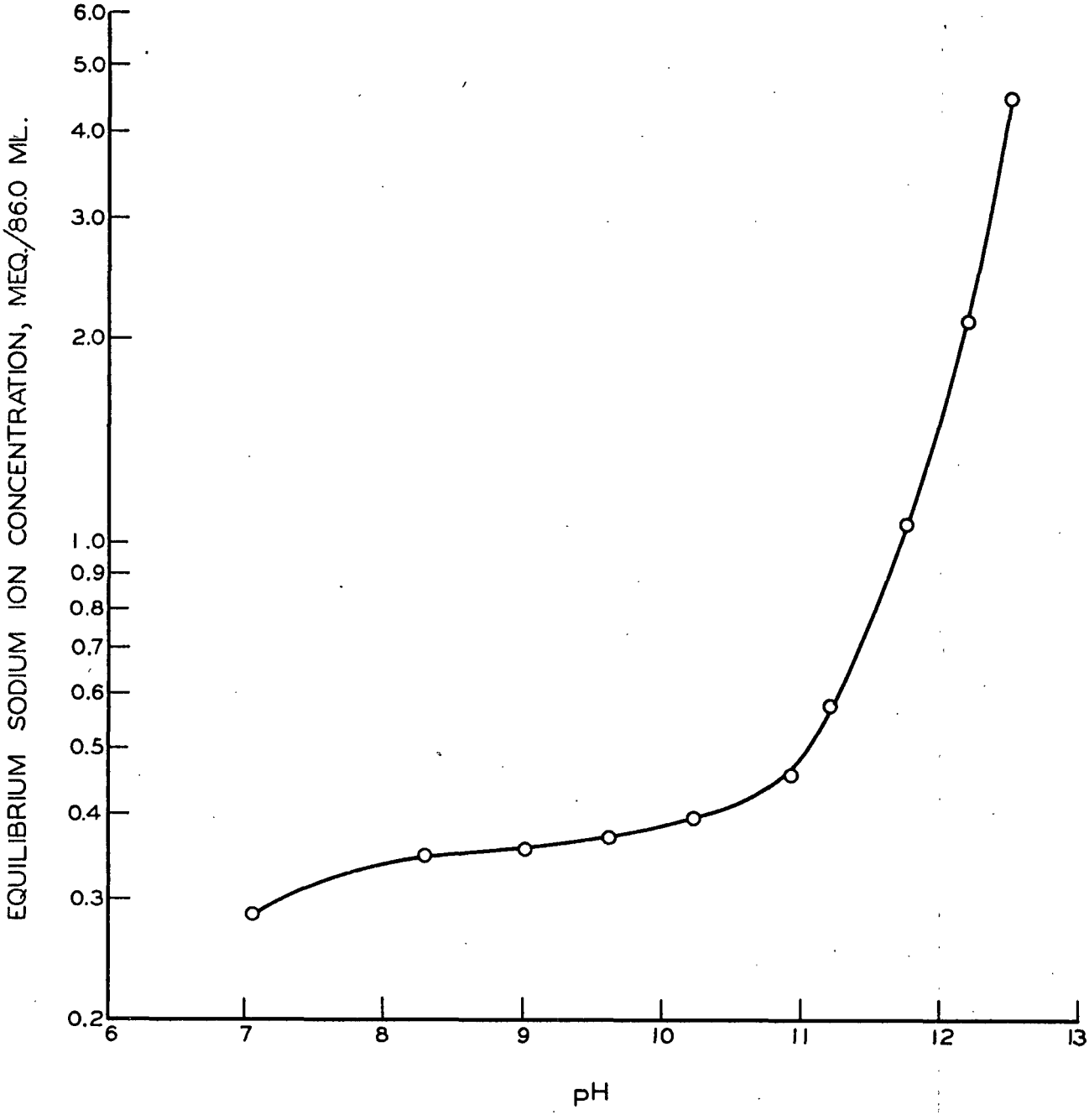

Figure 31. The Equilibrium Sodium Ion Content of the Intermicellar Solution During the Addition of Sodium Hydroxide. 0.60% Sodium Citrate (Based on the Clay) at 5.81% Solids.

citrate ion adsorption were read at the same pH's used in tabulating the values of n. Those numbers were converted to milliequivalents per gram and added to the numbers obtained in Figure 24 (hydroxyl ion adsorption) at the corresponding pH values. The total adsorption expressed in milliequivalents per gram was then converted to electrostatic units per square centimeter by multiplying by the appropriate Avogadro number and the electronic charge and dividing by the specific surface area for Fraction 1 kaolinite.

From these two variables (n and σ), all the terms in Equations (4) and (5) may be calculated except A and d. The calculation of these two terms will be considered in the succeeding sections. A sample calculation of the potential energies from the raw data is given in Appendix VI.

THE EFFECT OF pH ON THE REPULSIVE POTENTIAL ENERGY

In this section we will consider the changes in the repulsive potential energy wrought by additions of sodium citrate and sodium hydroxide in various combinations. The calculations of V_R have been made in the manner previously described.

Let us first consider the addition of sodium hydroxide to a hydrogen-saturated kaolinite suspension. The first problem which must be considered concerns the value of d to be used in calculating V_R from Equation (5). This problem has been the source of some confusion in previous attempts to quantitatively apply the Verwey and Overbeek theory to kaolinite-water systems because values of d were chosen which corresponded

to the average distance between particles at a given solids content. The question is not one of how great the average separation of the particles may be, but rather how close two particles can approach each other before they encounter a repulsive force great enough to keep them apart. As we shall see, this distance is considerably less than the average distance between two particles in a dilute suspension.

We may estimate the value of $\underline{d}$ by using one known fact concerning the dispersion of kaolinite suspensions with sodium hydroxide; namely, the addition of sodium hydroxide to a kaolinite suspension yields a minimum viscosity of the suspension at a pH of 11. If the gross changes in viscosity of a kaolinite suspension are to be predicted by the Verwey and Overbeek theory, then there must be some value of $\underline{d}$ for which the repulsive potential energy exhibits a maximum at pH 11 when only sodium hydroxide is added to the kaolinite suspension. Indeed there is such a value (3.0×10^{-7} cm.), and the dependence of $\underline{V_R}$ on pH at this value of $\underline{d}$ is shown in Figure 32[1]. The mere fact that there exists a value of $\underline{d}$ for which $\underline{V_R}$ is a maximum at pH 11 tends to indicate that the Verwey and Overbeek theory can be quantitatively applied to the kaolinite-water system because there is nothing implicit in Equation (5) which dictates that the change exhibited by $\underline{V_R}$ as sodium hydroxide is added to the system must go through a maximum. The fact that a maximum does appear results from the specific changes in $\underline{n}$ and σ accompanying the addition

[1] The effect of $\underline{d}$ on the repulsive potential energy is shown in Figure 41 and is discussed at greater length on pages 116-18.

of sodium hydroxide. Depending upon the manner in which these two terms could conceivably change with the addition of sodium hydroxide, almost any shape curve of V_R vs. pH is possible.

When both sodium citrate and sodium hydroxide are added to a hydrogen-saturated kaolinite suspension, the change in V_R accompanying the pH change is somewhat different from that shown in Figure 32. Figure 33 shows the case where 0.12% sodium citrate (based on the ovendry clay) was added to the system and followed by the addition of various amounts of sodium hydroxide. Figures 34, 35, and 36 show the same situation for 0.30, 0.60, and 1.50%, respectively. In each case, the lowest pH shown is that obtained by the addition of only sodium citrate in the amount specified.

If Figure 33 is compared with Figure 32, it is evident that the most significant change has occurred in the pH range 7.5-10.5. In this area, the addition of sodium citrate has yielded a higher repulsive potential energy than was obtainable with the use of sodium hydroxide alone. However, Figure 33 still retains the gross features of Figure 32 indicating that the addition of 0.12% sodium citrate is insufficient to mask the effect of caustic addition.

If the amount of sodium citrate is increased to 0.30% or 0.60% (Figures 34 and 35), the repulsive potential energy stays relatively independent of pH below pH 11. In this range, the addition of sodium hydroxide has essentially no effect on the value of V_R obtained by the addition of sodium citrate. The maximum value of V_R is virtually the same

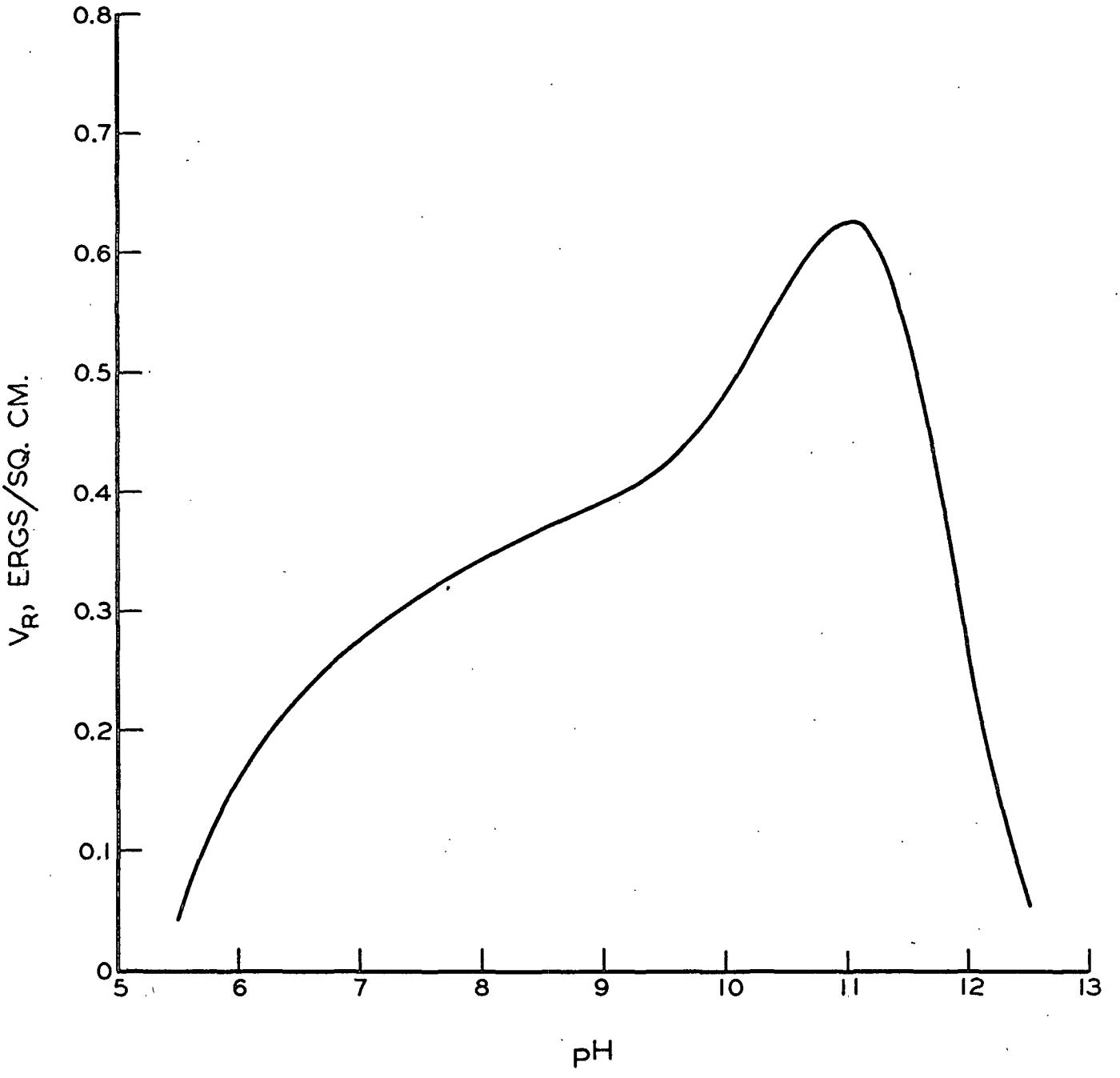

Figure 32. The Effect of pH on the Repulsive Potential Energy
0.00% Sodium Citrate Based on the Clay

$\underline{d} = 3.0 \times 10^{-7}$ cm.

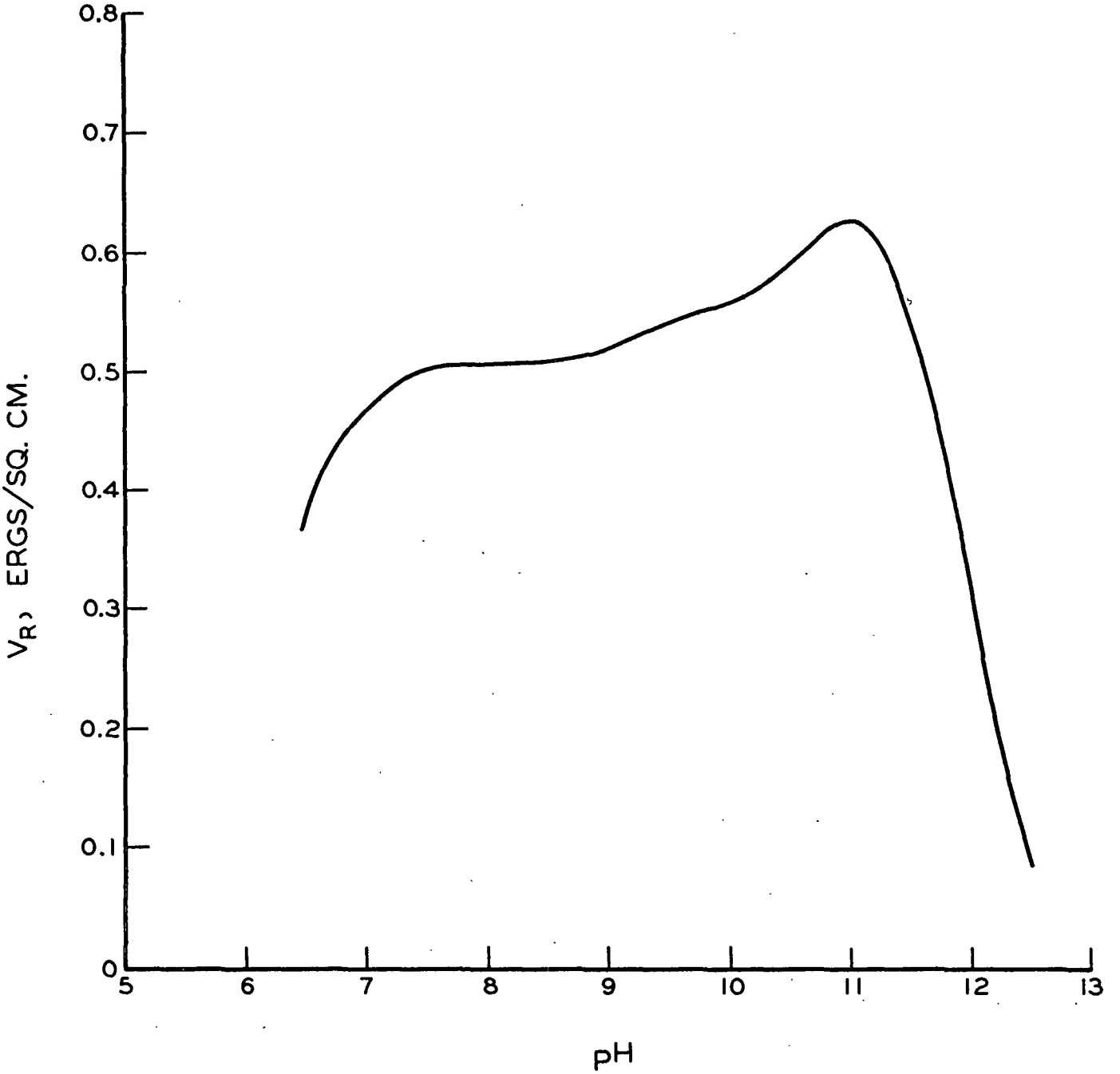

Figure 33. The Effect of pH on the Repulsive Potential Energy 0.12% Sodium Citrate Based on the Clay

$\underline{d} = 3.0 \times 10^{-7}$ cm.

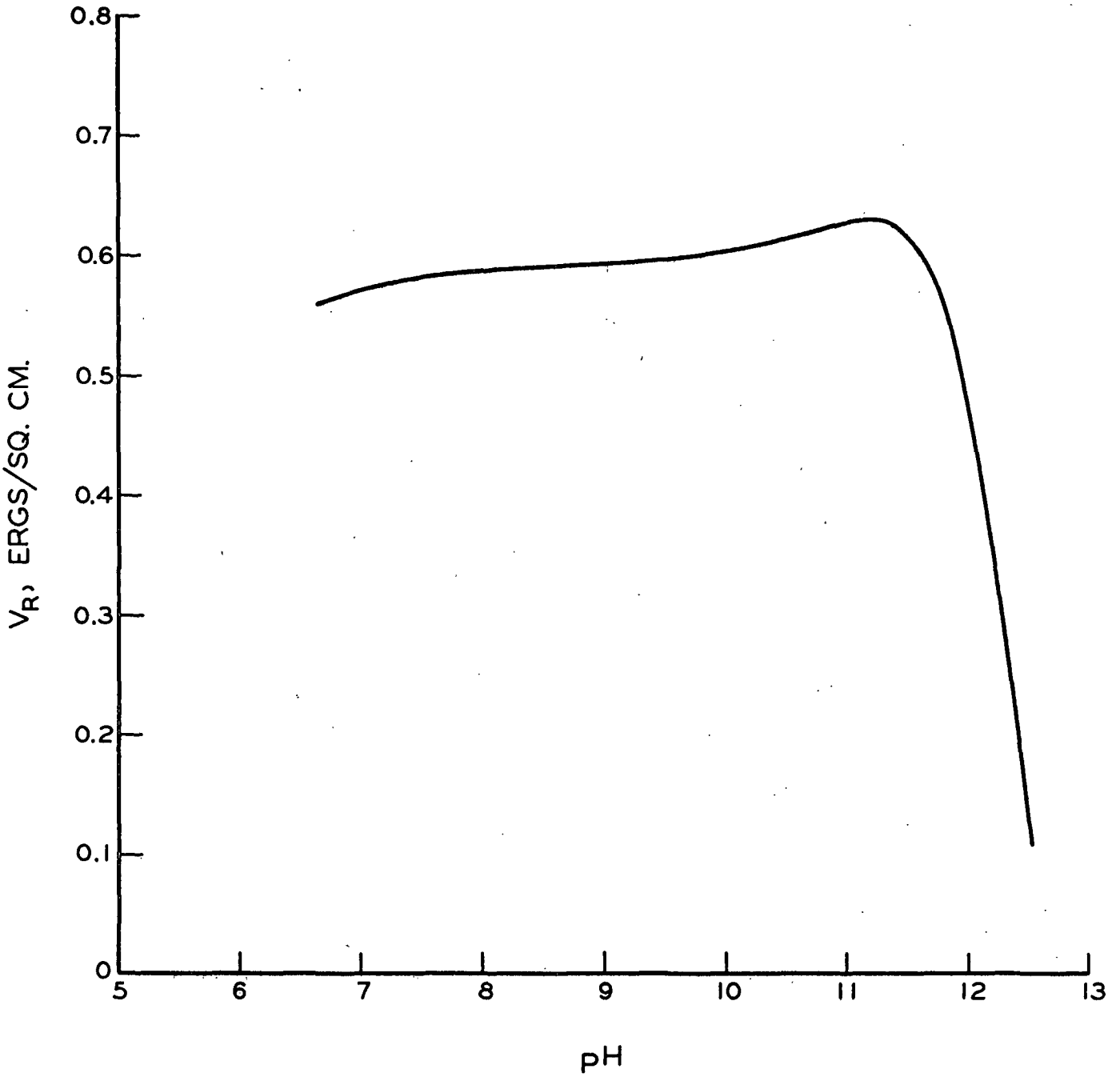

Figure 34. The Effect of pH on the Repulsive Potential Energy 0.30% Sodium Citrate Based on the Clay

$\underline{d} = 3.0 \times 10^{-7}$ cm.

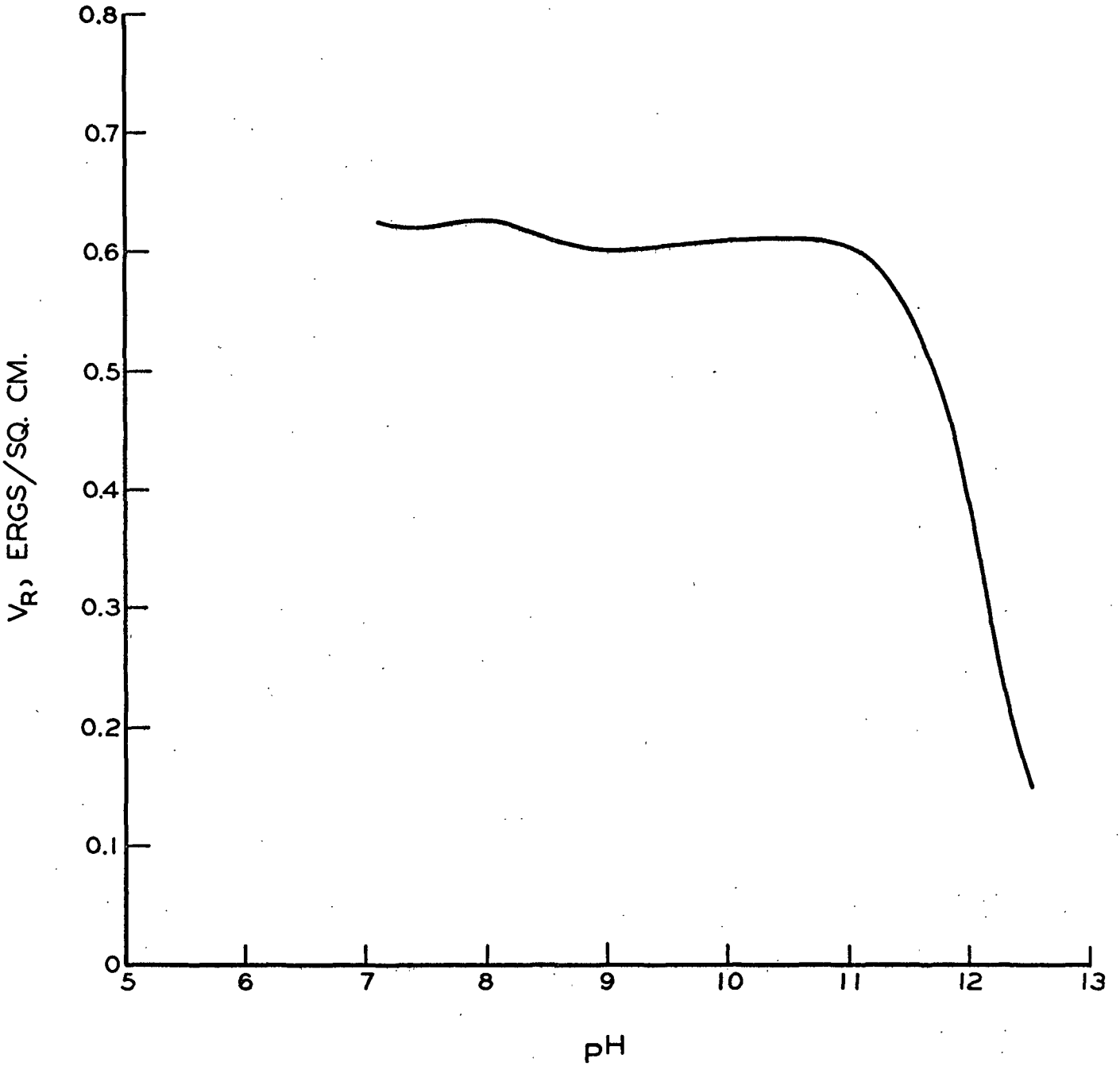

Figure 35. The Effect of pH on the Repulsive Potential Energy 0.60% Sodium Citrate Based on the Clay

$\underline{d} = 3.0 \times 10^{-7}$ cm.

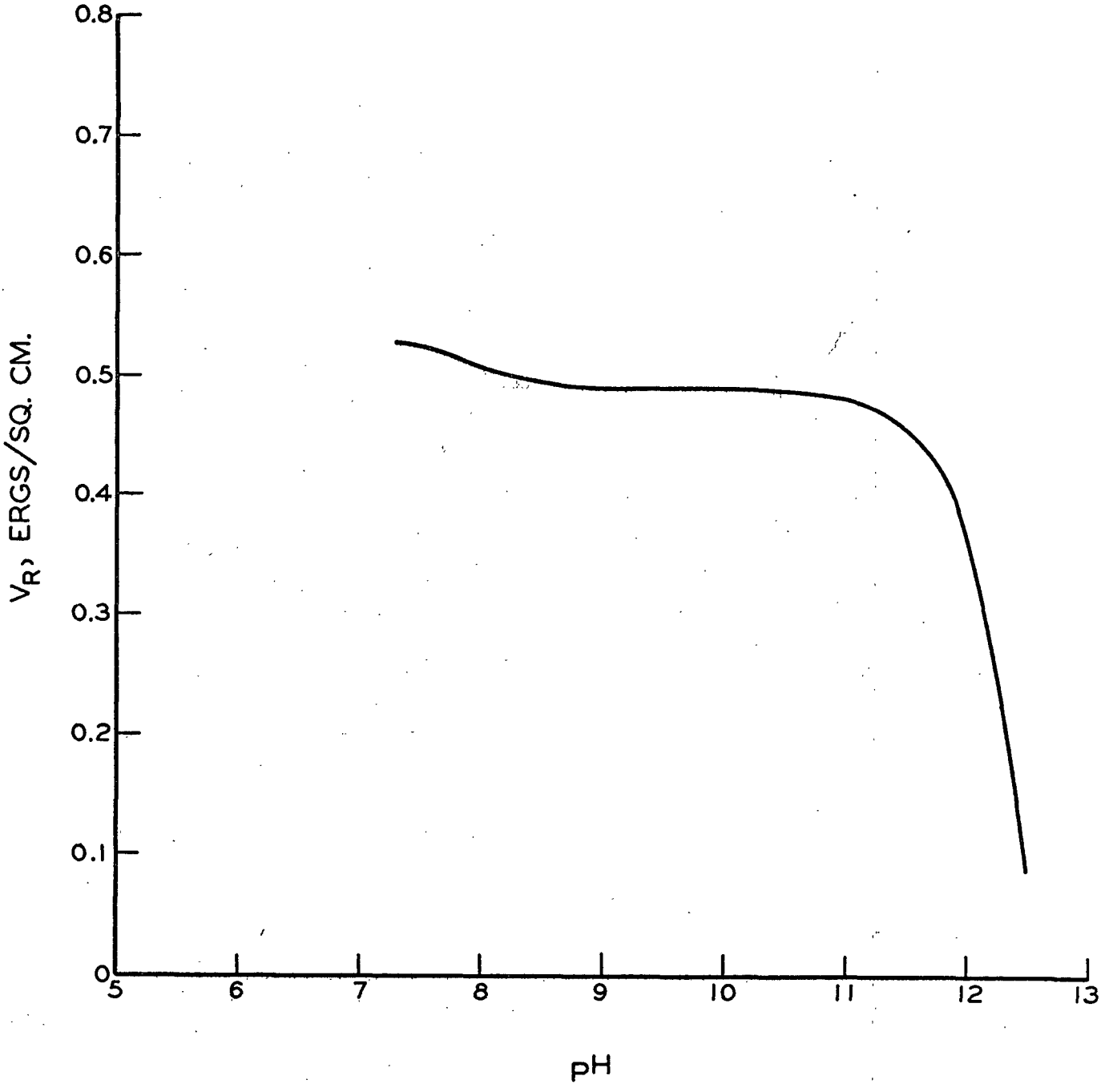

Figure 36. The Effect of pH on the Repulsive Potential Energy 1.50% Sodium Citrate Based on the Clay

$\underline{d} = 3.0 \times 10^{-7}$ cm.

as that obtained when only sodium hydroxide is added to the kaolinite suspension. Thus, we might expect a kaolinite suspension dispersed only with sodium citrate to exhibit its minimum viscosity at a pH of about 7, whereas a system dispersed only with sodium hydroxide would exhibit its minimum viscosity at a pH of 11. This is in agreement with common experience.

At 1.5% sodium citrate (Figure 36), the addition of sodium hydroxide continously decreases the repulsive potential energy. Furthermore, the maximum value of V_R is less than that obtained at the lower sodium citrate concentrations indicating that further additions of sodium citrate will tend to flocculate the suspension. This too is usually observed.

THE DISPERSING AGENT REQUIREMENT

We may compare the dispersing action of sodium citrate and sodium hydroxide in a more conventional manner by plotting V_R as a function of the amount of dispersing agent added. This is done in Figure 37. The data for the sodium hydroxide curve was obtained by plotting the amount of sodium hydroxide actually added in the experiments at 0% sodium citrate as a function of the equilibrium pH of the intermicellar solution. Using the values of pH thus obtained at any amount of sodium hydroxide added, the corresponding values of V_R were read from Figure 32. The sodium citrate curve was computed from the points at the extreme left of Figures 33-36. These points represent the cases where no sodium hydroxide was added to the system.

The most interesting feature of Figure 37 is the sharper drop in V_R obtained for excesses of sodium hydroxide compared to excesses of sodium citrate. This is related to the commonly observed phenomenon that the use of sodium hydroxide as a dispersing agent invariably exhibits a sharper minimum in the viscosity-per cent dispersing agent curve than any other dispersing agent.

It is extremely important to point out that Figure 37 represents the case for a suspension containing only 5.50% solids. Nevertheless, at higher solids contents, the same relationship between the two curves exists. The major difference between Figure 37 and a similar graph computed at a higher solids content occurs in the scale of the abscissa. For instance, if the scale of the abscissa in Figure 37 were expanded fourfold (i.e., 0.8% in Figure 37 is now 0.2%), the curves would be roughly equivalent to that which theoretically would be obtained at 50% solids. This is also related to two commonly observed phenomena: (1) The minimum in the viscosity-% dispersing agent relationship becomes sharper as the solids content is increased, and (2) the amount of dispersing agent required for minimum viscosity at 50% solids is in the neighborhood of 0.1-0.2% based on the clay rather than the 0.4-1.0% indicated by Figure 37. It is most unfortunate that the dispersing agent requirement is commonly expressed as a per cent based on the clay. Expressed in this manner, the dispersing agent requirement changes with the solids content of the system. If the amount of dispersing agent were expressed as an <u>initial</u> concentration in the intermicellar solution (e.g., equivalents dispersing agent per liter of fluids added

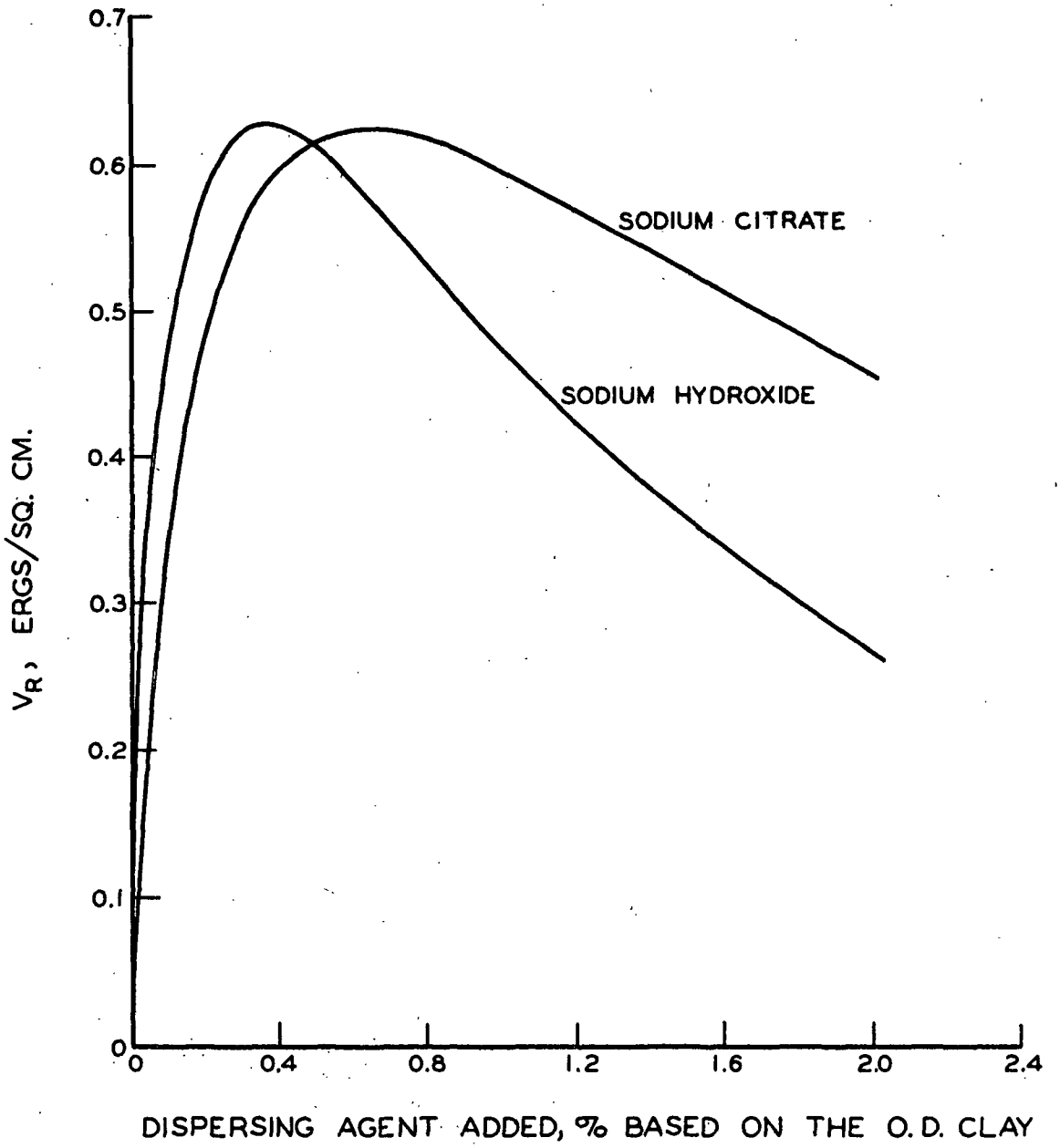

Figure 37. Repulsive Potential Energy vs. Per Cent Dispersing Agent at 5.50% Solids

$\underline{d} = 3.0 \times 10^{-7}$ cm.

to the dry clay), then a plot of V_R vs. concentration of dispersing agent would be almost independent of solids content. It would, of course, be completely independent of solids content if the amount of dispersing agent were expressed as the equilibrium concentration in the intermicellar solution.

THE EFFECT OF NEUTRAL SALTS

If we know the manner in which the addition of any ion changes the adsorption characteristics of the clay, it is then possible to calculate the manner in which V_R will change with the addition of this ion. This provides us with a powerful tool because we may now hypothetically add any salt to a kaolinite suspension and determine the concurrent changes in V_R--providing a reasonable estimate in the changes in adsorption accompanying the addition of this salt can be made. In this section, the effect of the hypothetical addition of sodium chloride on V_R will be considered for a few special cases. The assumption is made that the addition of sodium chloride to a kaolinite suspension does not change the intermicellar pH. Consequently, the hydroxyl ion adsorption is independent of the amount of sodium chloride added.

Figure 38 shows the effect of sodium chloride additions to a dispersed clay. In this case, sufficient sodium hydroxide was hypothetically added to a hydrogen saturated kaolinite suspension to obtain a pH of 11.0. At this point sodium chloride was hypothetically added to the system in the amounts[1] shown in Figure 38. The accompanying

[1] Since chloride ion is not adsorbed by the clay, the equilibrium intermicellar concentration of this salt is the same as the initial concentration of this salt in the fluids added to the dry clay.

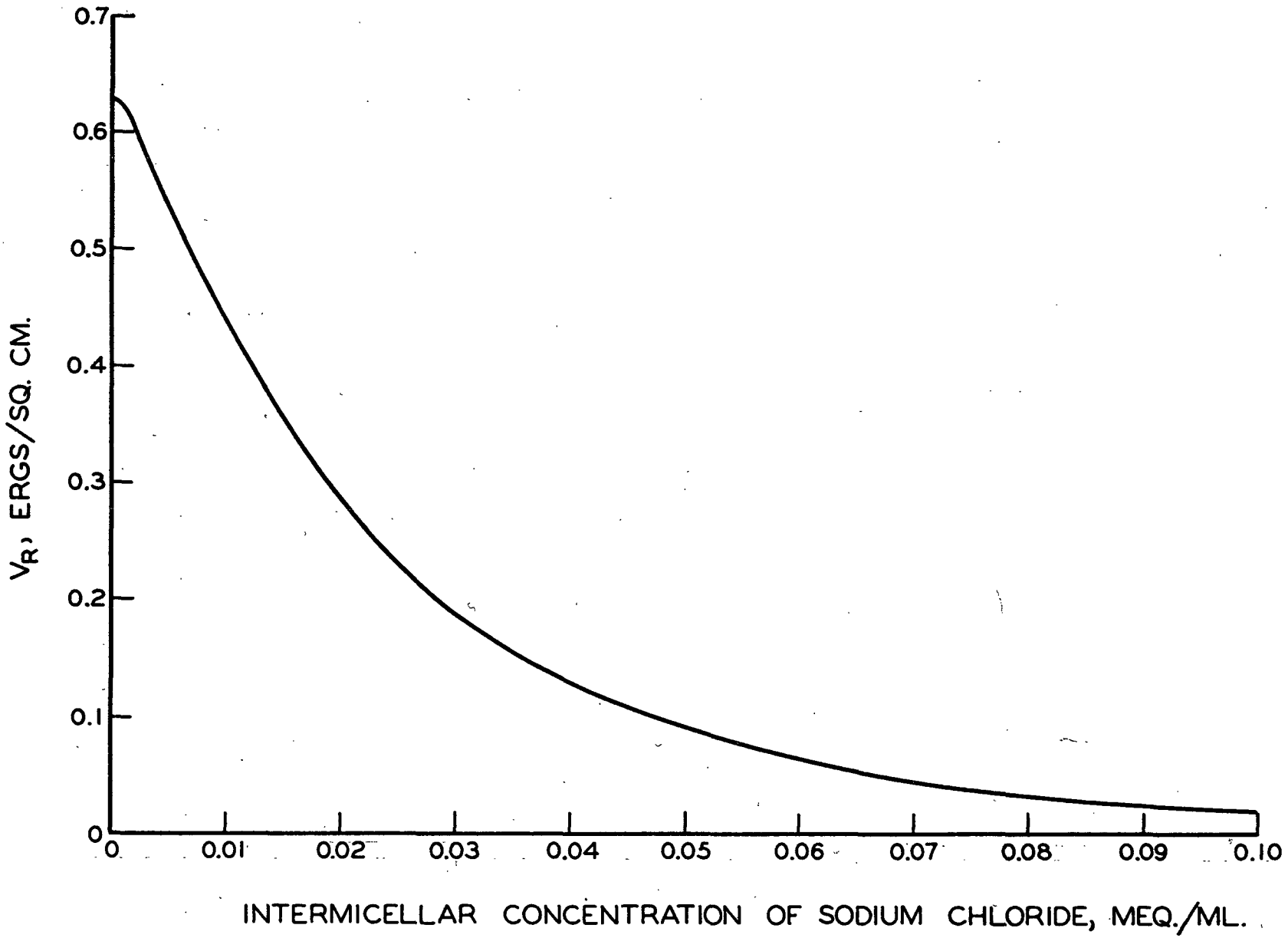

Figure 38. The Effect of Sodium Chloride Additions on the Repulsive Potential Energy
Initial Conditions: Suspension Dispersed with Sodium Hydroxide to a pH of 11.00
$\underline{d} = 3.0 \times 10^{-7}$ cm.

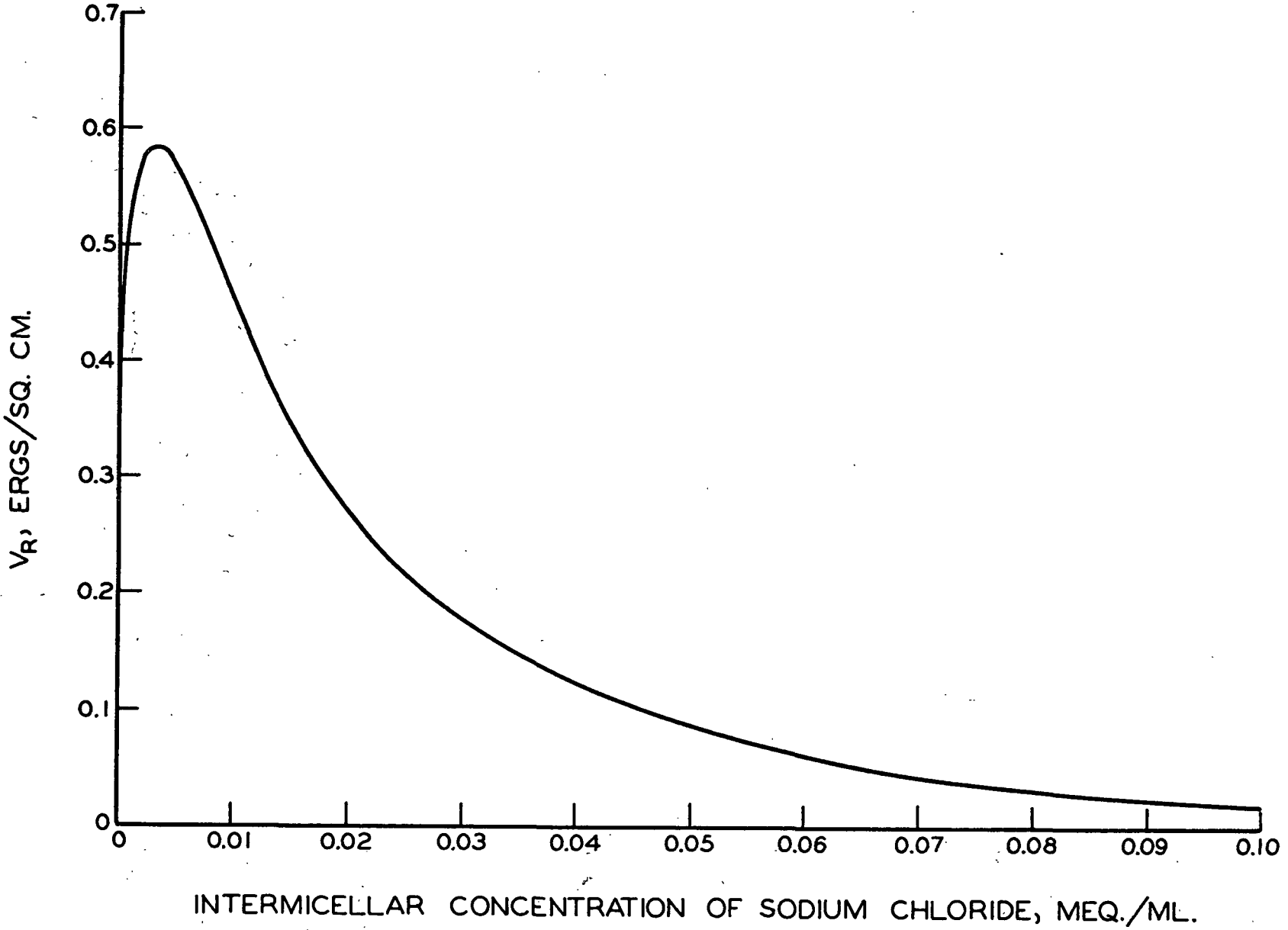

Figure 39. The Effect of Sodium Chloride Additions on the Repulsive Potential Energy
Initial Conditions: Suspension Partially Dispersed with Sodium Hydroxide to a pH of 8.00
$\underline{d} = 3.0 \times 10^{-7}$ cm.

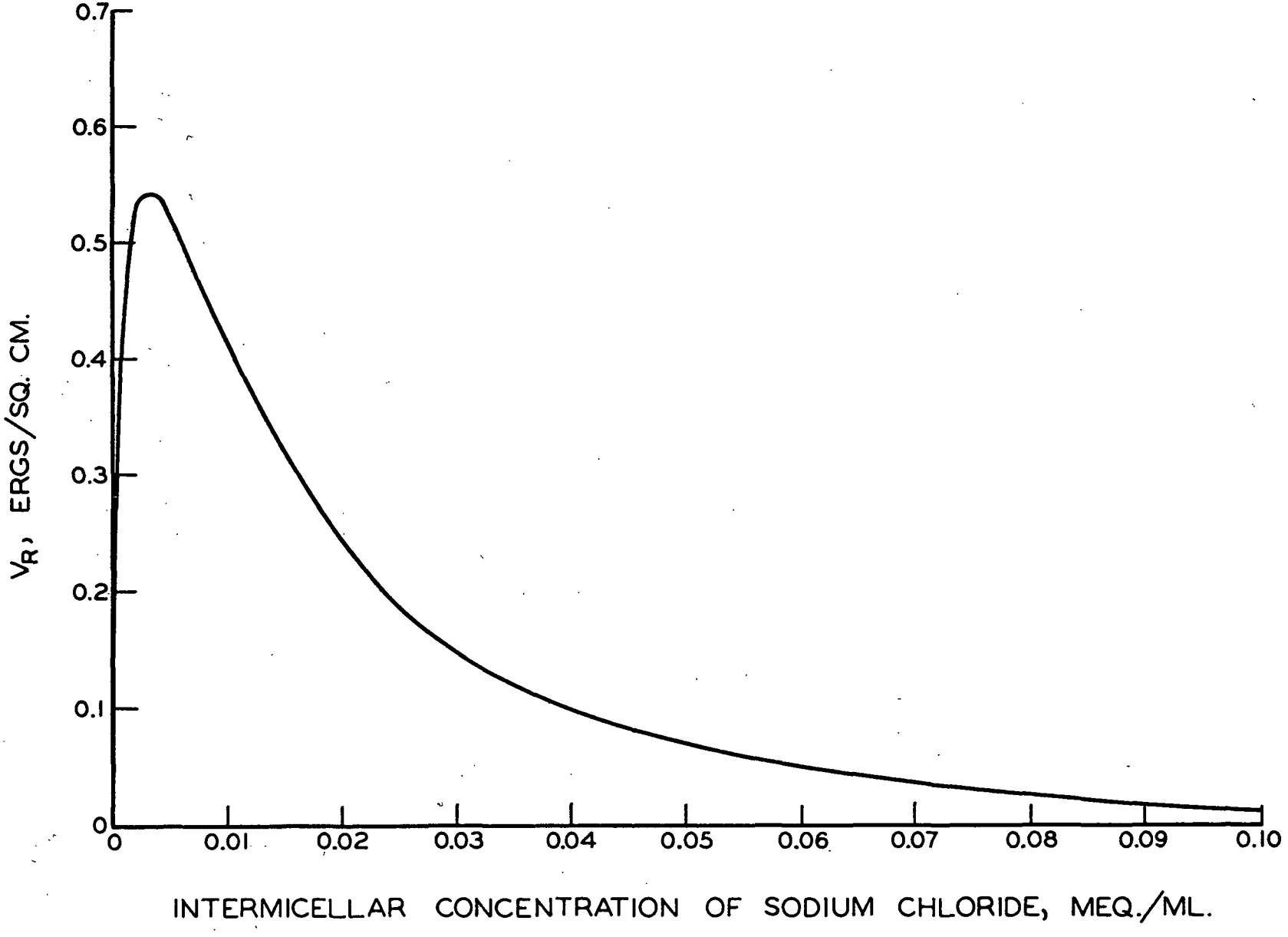

Figure 40. The Effect of Sodium Chloride Additions on the Repulsive Potential Energy
Initial Condition: Hydrogen-Saturated Kaolinite Suspension
$\underline{d} = 3.0 \times 10^{-7}$ cm.

change in V_R proceeds in the expected manner since it is well known that the addition of such salts to dispersed clay slurries tends to flocculate the suspension.

A different situation arises when the initial condition of the clay suspension is either partially dispersed or completely flocculated. Figure 39 considers the case where a hydrogen-saturated clay suspension has been brought to a pH of 8.0 with sodium hydroxide and then subjected to various additions of sodium chloride. Figure 40 considers the direct addition of sodium chloride to a hydrogen-saturated kaolinite suspension. Again, the assumption that the pH remains constant throughout the addition of sodium chloride is invoked.[1] From the curves obtained, one would expect the viscosity of the clay suspension to be reduced by the addition of appropriate amounts of sodium chloride. Indeed such a phenomenon has been observed (25).

Figures 39 and 40 show some interesting aspects concerning the possibility of deflocculating kaolinite suspensions with sodium chloride. First of all, it is readily apparent that the optimum concentration of

[1] The writer has noticed that the addition of sodium chloride to kaolinite suspensions does indeed lower the pH to some degree, although a quantitative study of this matter has not been made. However, the general tendency has been an insignificant depression of the pH above an initial pH of 10 (about 0.1 units) and an appreciable depression at initial pH values below this—particularly when the initial pH is about 7. This is to be expected since the addition of sodium chloride at the lower pH's essentially accomplishes a partial exchange of sodium ions for hydrogen ions in the diffuse part of the double layer. Any small amounts of hydrogen ion thus released to the intermicellar solution could cause an appreciable depression of the pH when the initial pH is near the neutral point. The total effect would be a lowering of the peak values of V_R in Figures 39 and 40.

sodium chloride is quite critical. In addition, the optimum concentration of this salt is quite small and may account for the fact that the possibility of using a neutral salt as a dispersing agent has been overlooked. For example, the optimum amount of sodium chloride for a system containing 70% solids is about 0.0075% based on the dry clay.

It is improbable that a neutral salt will disperse a hydrogen-saturated kaolinite suspension as well as sodium hydroxide, although the maximum values of V_R in Figures 38 and 40 would appear to make this situation approachable. The difficulty arises because of the assumption that the addition of sodium chloride does not alter the intermicellar pH. If the pH were lowered, the maximum value of V_R would be lowered. The nature of the counterion may be of even greater importance. When a kaolinite suspension is dispersed to its optimum condition with sodium hydroxide, essentially all the counterions are sodium ions. However, the addition of sodium chloride to a hydrogen-saturated kaolinite suspension yields, at the optimum concentration of this salt, a system which still maintains a great number of hydrogen ions as counterions. Since it is frequently observed in colloidal phenomena that hydrogen ion has a coagulation power roughly equivalent to a trivalent or tetravalent cation, the maximum value of V_R in Figure 40 is greater than that which would be obtained if this fact were taken into consideration. Nevertheless, the general shape of the curve would be retained and the addition of the neutral salt would tend to deflocculate the suspension to some degree.

THE TOTAL POTENTIAL ENERGY ($V_R + V_A$)

In the previous sections, the effect of a variety of conditions on the repulsive potential energy has been described in terms of a fixed value of d. Comparisons of the various effects at a constant value of d are valid because the attractive potential energy (V_A) at a given value of d is constant. Thus, if the ordinates in Figures 32-40 were total potential energy rather than repulsive potential energy, the net effect would be a lowering of all parts of the curves by a fixed amount.

The attractive potential energy was determined by the use of Equation (4). This equation is applicable because the distances under consideration are far less than the particle thickness. Whereas the particle thickness is about 100 mmu (Table XV), the values of d which are of importance range from 1 to 30 mmu. Consequently, the application of Equation (4) in lieu of Equation (1) introduces an error of only 2% under the most disadvantageous condition.

It is now possible to calculate the total potential energy under a given set of conditions if we can make a reasonable estimate of the value of A in Equation (4) applicable to the kaolinite-water system. We may do this by using the same assumption that was used for the calculation of the appropriate values of d for the repulsive potential energy curves, i.e., that the addition of sodium hydroxide to a kaolinite suspension yields a minimum viscosity at a pH of 11. It has already been shown that at a value of d equal to 3.0×10^{-7} cm., a maximum value of V_R is obtained at a pH of 11 when only sodium hydroxide is added to

the clay suspension. If we accept the above assumption, not only must V_R exhibit a maximum at pH 11 for one value of d, but the largest value of $V_R + V_A$ as a function of d must occur at pH 11. This immediately sets limits on the possible values of A.

Let us pursue this matter further. In Figure 41, the changes in V_R accompanying the addition of sodium hydroxide to the kaolinite suspension are shown for several values of d. It is immediately obvious that the values of V_R for $d = 2.0 \times 10^{-7}$ cm. and $d = 1.0 \times 10^{-7}$ cm. are much greater than V_R for $d = 3.0 \times 10^{-7}$ cm., particularly at pH values above 11. If $V_R + V_A$ is to be a maximum at pH 11 for all values of d, the value of A must be such that $V_R + V_A$ for pH 11.5 and $d = 2.0 \times 10^{-7}$ cm. and for pH 12.0 and $d = 1.0 \times 10^{-7}$ cm. is less than $V_R + V_A$ at pH 11.0 and $d = 3.0 \times 10^{-7}$ cm. This places a lower limit on A of 2×10^{-12} ergs. Furthermore, $V_R + V_A$ at pH 11.0 and $d = 3.0 \times 10^{-7}$ cm. must be positive. This places an upper limit on A of 8×10^{-12} ergs. If we also consider the fact that $V_R + V_A$ at pH 11.0 and $d = 3.0 \times 10^{-7}$ cm. must be greater than $V_R - V_A$ for any combination of pH below 11.0 and d greater than 3.0×10^{-7} cm., we obtain a most probable value of A equal to 4×10^{-12} ergs. In Figure 42, the change in total potential energy accompanying the addition of sodium hydroxide to the kaolinite suspension is shown for the same values of d used in Figure 41. It is obvious that a value of A equal to 4×10^{-12} ergs meets all the above limitations and yields a maximum value of $V_R + V_A$ at a pH of 11. It is interesting to note that the value of A thus determined lies between the value of A

cited by Verwey and Overbeek (26) as the most plausible value for colloidal phenomena ($\underline{A} = 2 \times 10^{-12}$ ergs) and that experimentally determined by Overbeek and Sparnaay (27) for glass and quartz plates ($\underline{A} = 3 \times 10^{-11}$ ergs).

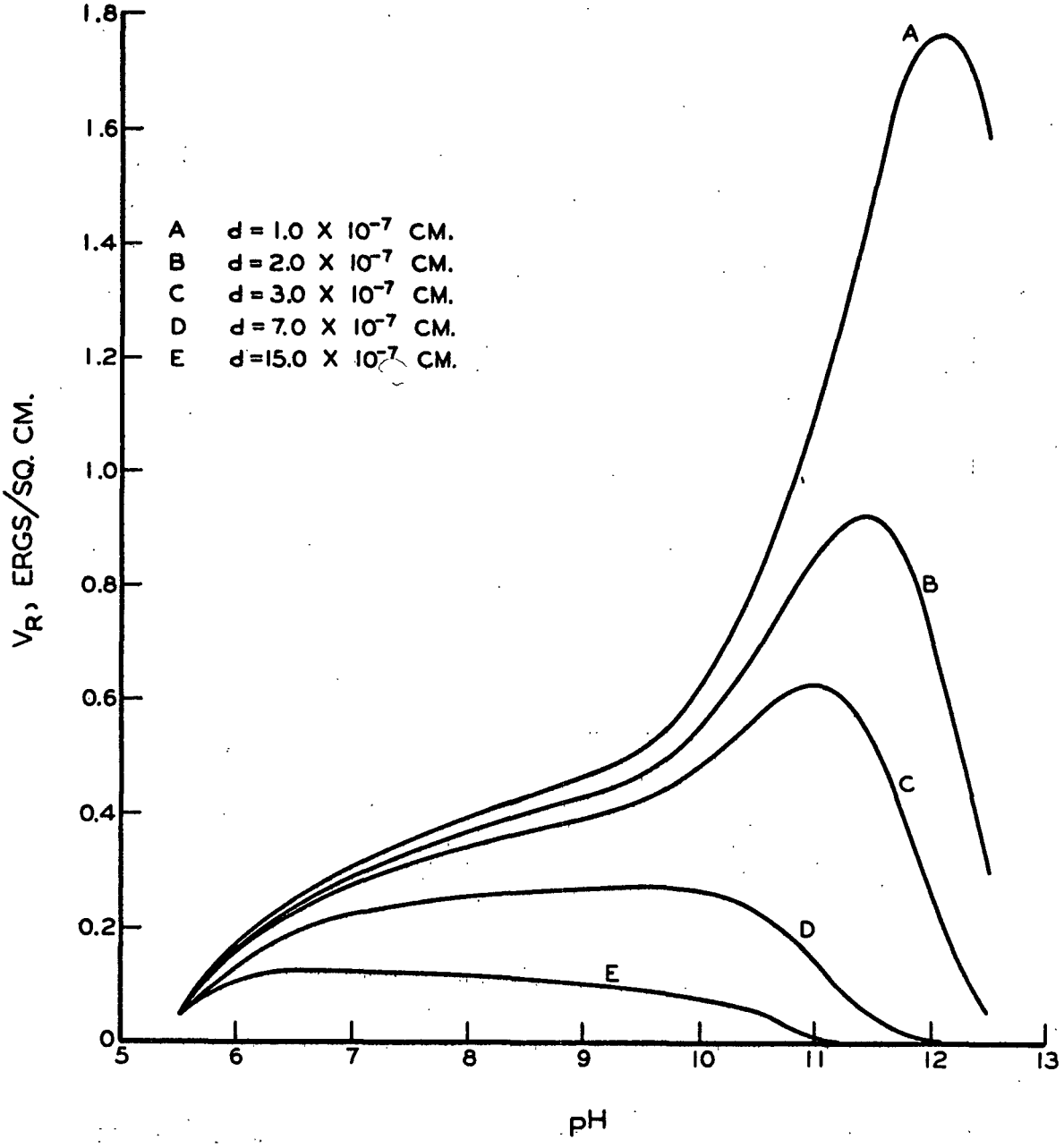

Figure 41. The Relationship Between pH and Repulsive Potential Energy During the Addition of Sodium Hydroxide to a Hydrogen-Saturated Kaolinite Suspension

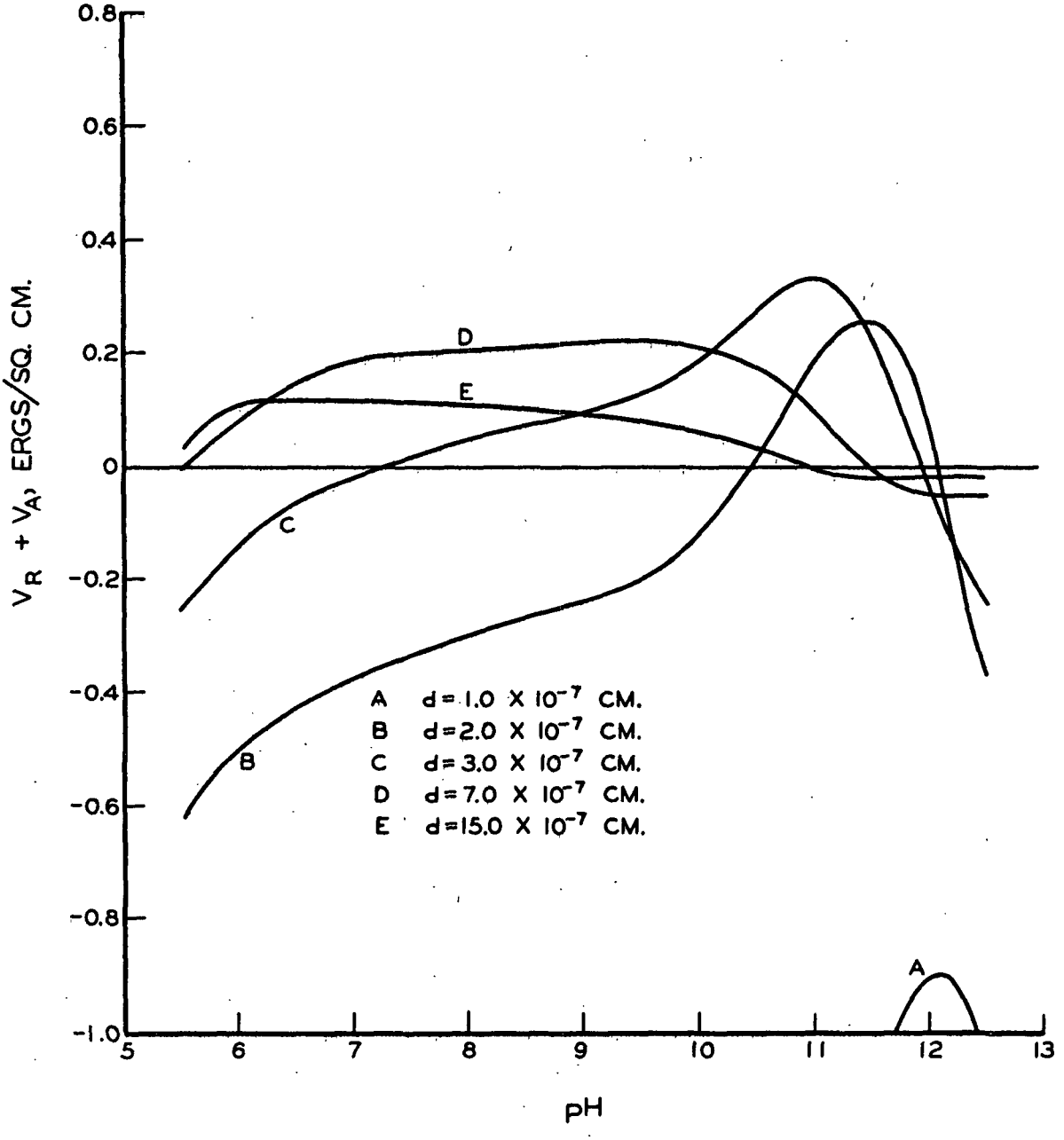

Figure 42. The Relationship Between pH and Total Potential Energy During the Addition of Sodium Hydroxide to a Hydrogen-Saturated Kaolinite Suspension

$\underline{A} = 4.0 \times 10^{-12}$ ergs

THE MECHANISM OF THE DEFLOCCULATION OF AQUEOUS KAOLINITE SUSPENSIONS

THE APPROACH OF TWO PARTICLES

Let us now consider the changes in total potential energy that occur as two particles approach each other. We may begin by attaching a greater physical significance to the potential energy functions. The repulsive potential energy is the amount of work required to bring a flat plate, one square centimeter in area, from an infinite distance to a distance of 2d centimeters from another flat plate, also one square centimeter in area. Expressed on the same basis, the attractive potential energy is the amount of work which can be performed by the Van der Waals-London attractive forces in bringing two plates separated by an infinite distance up to a distance 2d centimeters apart. Thus, the total potential energy at some value of d is the amount of work which must be done on the system to bring two plates from an infinite distance of separation to a distance of separation equal to twice the given value of d. If the total potential energy is negative at a given value of d and is not positive at values of d greater than the given value, then the two plates will spontaneously arrive at the specified distance of separation. If, however, the total potential energy is positive at a given value of d, then some work must be performed on the plates to bring them to a distance 2d apart.

With these points in mind, let us turn to a specific example showing the total potential energy at various distances of separation

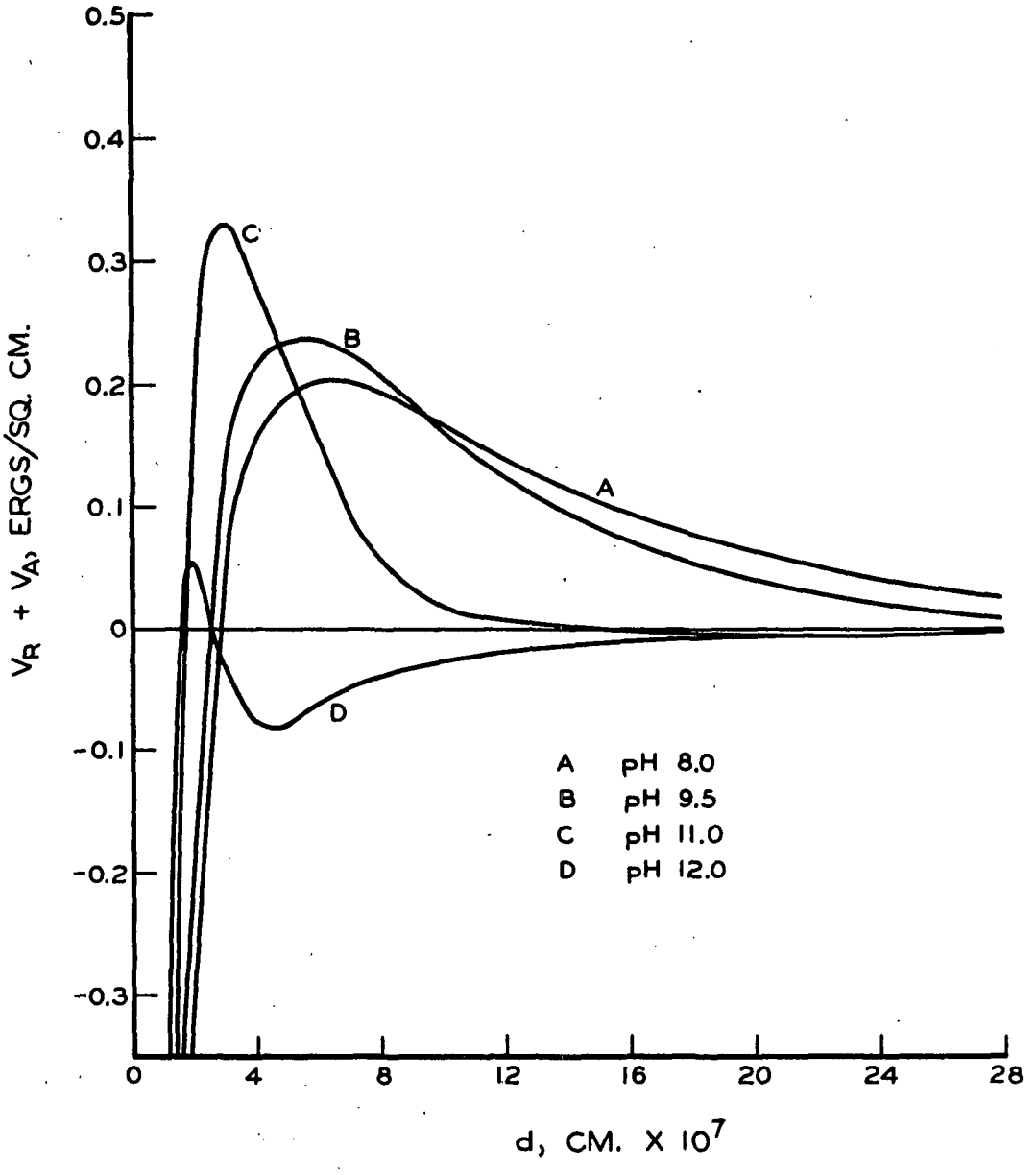

Figure 43. The Total Potential Energy at Various Distances Between Plates (2d) During the Addition of Sodium Hydroxide to a Hydrogen-Saturated Kaolinite Suspension

$\underline{A} = 4.0 \times 10^{-12}$ ergs

of the clay particles. Figure 43 shows this variation at several pH values for the case where only sodium hydroxide is added to a hydrogen-saturated kaolinite suspension. We note that the maximum value of $\underline{V}_R$ + $\underline{V}_A$ at a pH of 11.0 is greater than the maxima obtained at all other pH values. This condition results because it has been imposed by the choice of $\underline{A}$ which validated the assumption that maximum dispersion occurs at this pH. However, the magnitude of this maximum would seem to indicate that dispersion at a pH of 11.0 is not much better than dispersion at a pH of 9.5 and 8.0. While the argument still applies that the $\underline{V}_R$ component at these lower pH's (9.5 and 8.0) may be high because an appreciable number of hydrogen ions remain as counterions (see page 115), it is conceivable that the difference in viscous behavior of a suspension at pH 8.0 and pH 11.0 may be due, in part, to the manner in which the work load changes with distance of separation at each of these two pH's.

Let us cite a concrete example from Figure 43. If two particles were brought from infinity to a distance of 12×10^{-7} cm. apart ($\underline{2d}$), it would require 0.20 ergs/sq. cm. of surface to accomplish this feat when the pH of the system is 8.0. If, however, the pH of the system were 11.0, the work requirement would be 0.33 ergs/sq. cm. of surface to bring the two particles from an infinite distance of separation to a distance of 6×10^{-7} cm. apart. But suppose the particles had, in some manner, arrived at a distance of separation of 30×10^{-7} cm. ($\underline{d} = 15 \times 10^{-7}$ cm.). Then, at pH 8.0, the additional work required to bring the particles to a distance of separation of 12×10^{-7} cm. would be 0.20 -

0.11 or 0.09 ergs/sq. cm., whereas a pH of 11.0 would still require the expenditure of 0.33 ergs/sq. cm. to move the particles from 30 x 10^{-7} cm. apart to 6 x 10^{-7} cm. apart.

The reader may well ask how the particles could arrive at a separation of 30 x 10^{-7} cm. Apparently this would require some work to be performed when the system is at a pH of 8.0, whereas the particles would spontaneously arrive at this point under a pH of 11.0. However, when the solids content is high (and particularly when the average particle size is small), the average distance of separation of the particles is not much greater than 30 x 10^{-7} cm. Thus, any small motion of one particle relative to another would force some pair of particles to such distances of separation. If there is any truth to this argument, then we might expect the viscosity-pH relationship for sodium hydroxide-dispersed slurries to exhibit a much sharper minimum for higher solids contents than for lower solids contents.

In spite of this argument, it is probable that for all but the highest solids contents (above about 50% solids), the height of the potential energy barrier will govern the electrical contribution to the viscosity of a kaolinite suspension. With this point in mind, the effect of the addition of sodium hydroxide on the viscosity of a clay suspension may be better illustrated by a plot of the maximum value of $\underline{V}_R + \underline{V}_A$ as a function of pH rather than $\underline{V}_R$ vs. pH for a given value of $\underline{d}$, as is shown in Figure 32. Such a plot should have a more valid relationship to viscosity because it is evident in Figure 43 that the

maximum height of the barrier does not always occur at the same value of d. In Figure 44, the maximum height of the potential energy barrier is plotted as a function of pH for the case where sodium hydroxide is added to a hydrogen-saturated kaolinite suspension. From a comparison of Figures 44 and 32, it is evident that the shapes of the curves are very similar. The major difference between the two figures is the scale of the ordinate. Consequently, a comparison of the effect of a number of variables on the repulsive potential energy at $d = 3.0 \times 10^{-7}$ cm. is, after all, indicative of the effect these variables will have on the height of the potential energy barrier if all values of d are considered.

Figure 45 shows the variation in total potential energy encountered when only sodium citrate is added to the clay slurry in the amounts indicated. The largest barrier is obtained with 0.60% sodium citrate based on the clay--a fact which was previously inferred by Figure 37. The most notable feature of Figure 45 is the relatively small changes in both the height and shape of the barrier incurred by the changes in sodium citrate concentration. Again, the reader should be cautioned that the indicated percentages of dispersing agent apply only to a system of 5.50% solids. If the solids content were changed, the magnitude of these figures would also change.

THE DOUBLE LAYER PHENOMENA ACCOMPANYING FLOCCULATION AND DEFLOCCULATION

The Interaction Effect

Before these phenomena can be discussed in an intelligible manner,

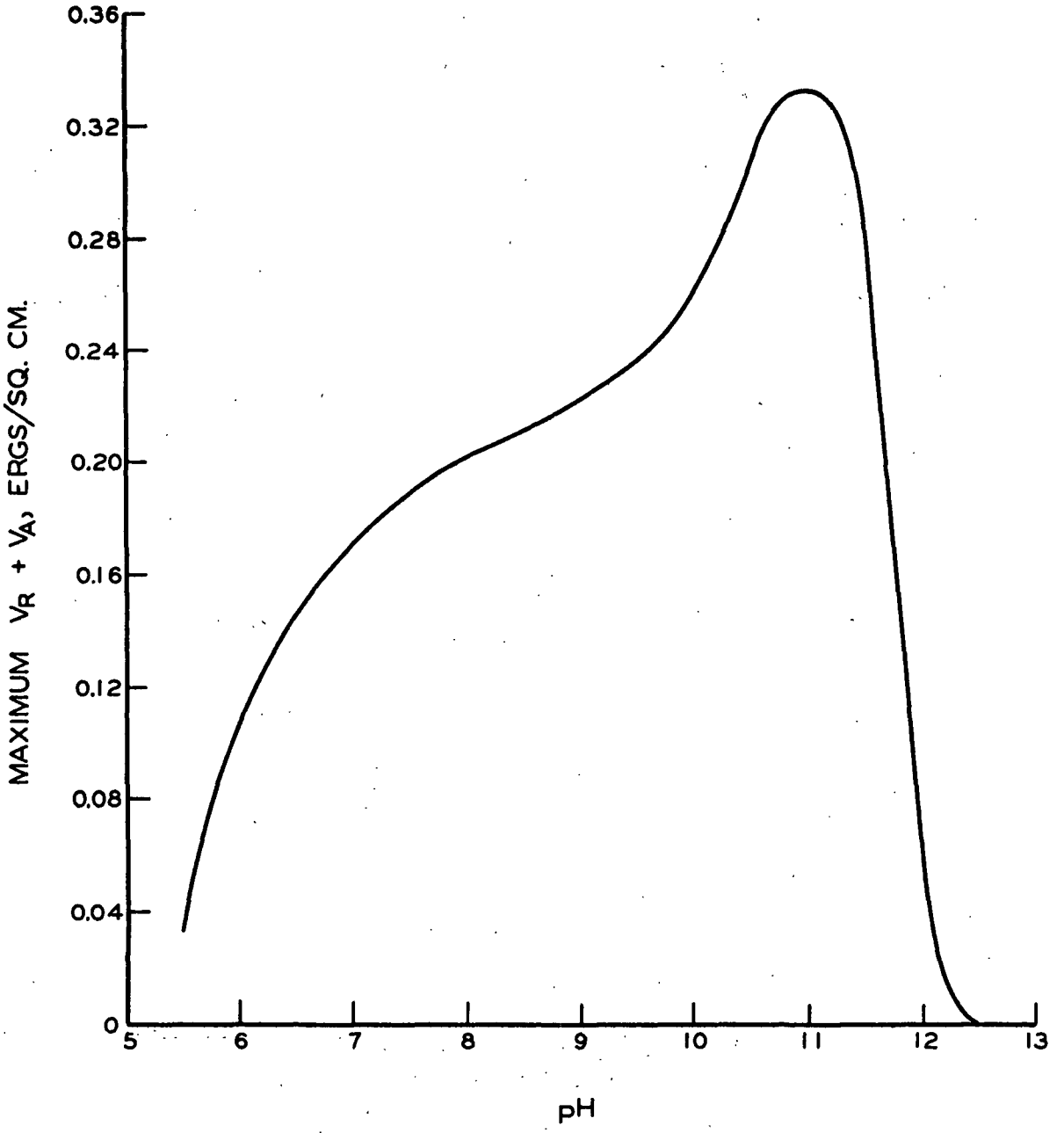

Figure 44. The Maximum Height of the Potential Energy Barrier as a Function of pH During the Addition of Sodium Hydroxide to a Hydrogen-Saturated Kaolinite Suspension

$\underline{A} = 4.0 \times 10^{-12}$ ergs

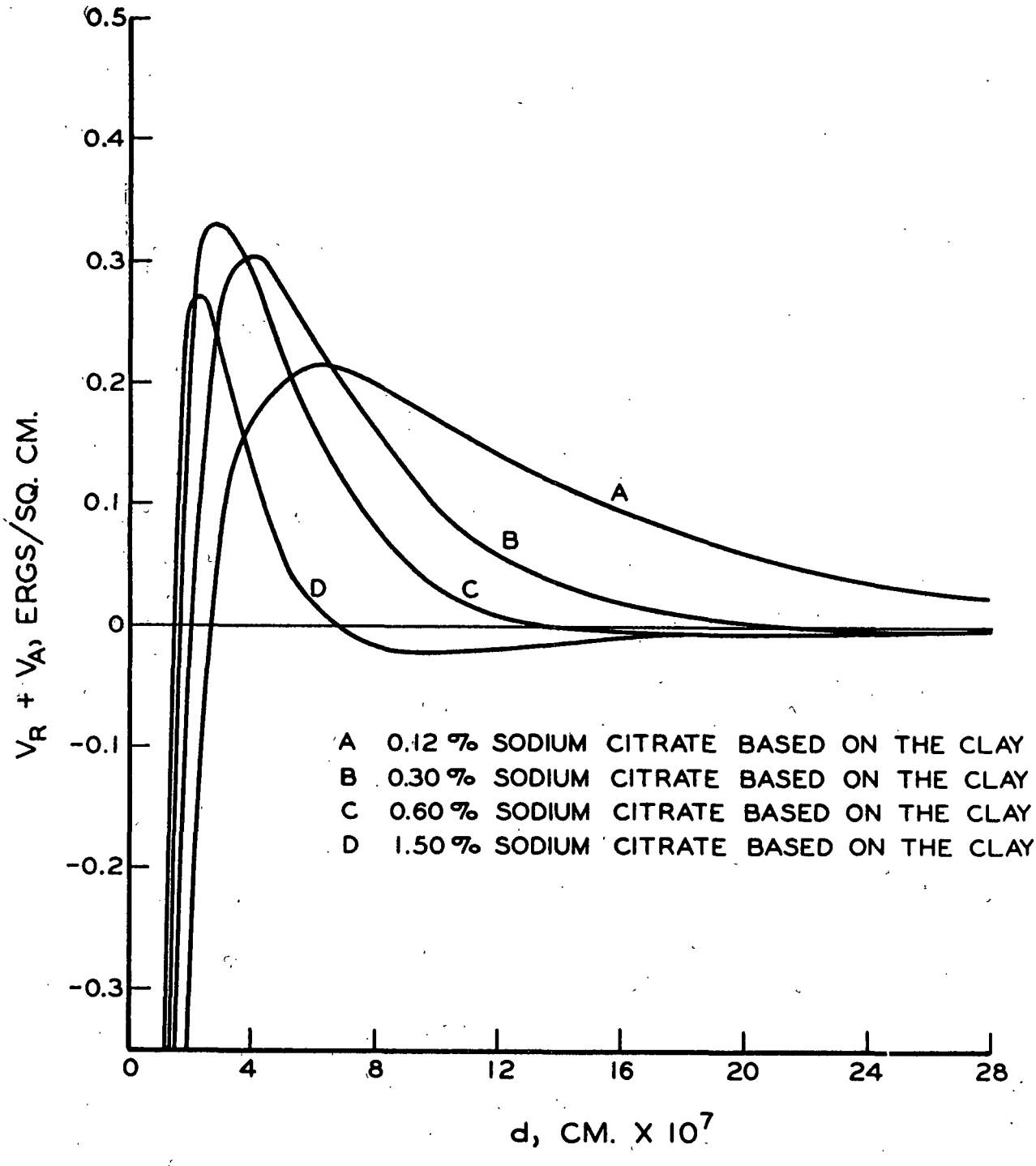

Figure 45. The Total Potential Energy at Various Distances Between Plates (2d) During the Addition of Sodium Citrate to a Hydrogen-Saturated Kaolinite Suspension at 5.50% Solids

$\underline{A} = 4.0 \times 10^{-12}$ ergs

some fundamental principles must be asserted. The most important principle of all is the fundamental cause of the repulsion between particles. As Verwey and Overbeek have clearly shown, it is the interaction of the diffuse part of two double layers which gives rise to a repulsion between the surfaces bearing the double layers. The importance of this point cannot be overstated. Upon this principle rests the entire theory of Verwey and Overbeek concerning the stability of lyophobic colloids.

The degree to which two diffuse double layers interact may be expressed by the dimensionless quantity Xd. This parameter is derived from the only two variables which could describe the interaction, namely, the distance of separation of the surfaces bearing the double layers (2d) and the reciprocal of the effective thickness of the individual double layers if they had not interacted (X). The effect of the degree of interaction on the repulsive potential energy is described by the term 1 - tanh Xd in Equation (5). Consequently, we may view this term as the contribution of interaction to the repulsive potential energy. It is the nature of this hyperbolic expression that it can only assume values between one and zero for positive values of Xd. When the interaction is small (i.e., Xd is large by virtue of a consideration of either large distances between the surfaces or relatively nondiffuse double layers), the repulsive potential energy approaches zero.

The Effects of Total Charge and Potential Difference

The combined effects of the total charge and the potential difference between the surface of the particle and the intermicellar solution on the repulsive potential energy are expressed by the dimensionless quantity γ^2 in Equation (5), since the only way in which these interdependent variables enter into Equation (5) is through Equations (10), (7), and (6). An inspection of Equation (6) shows that the term γ^2 can only assume values between zero and one for positive values of Z.

The Distribution Effect

The third factor which controls the repulsive potential energy at a given value of d is related to the distribution of counter charges within the diffuse part of the double layer and is expressed by the ratio n/X in Equation (5). We may view this term as the planar density of counter charges at some characteristic distance from the particle surface. It is evident from Equation (8) that this ratio is proportional to the square root of n. Consequently, any increase in n resulting from the addition of any salt to the system tends to enlarge the repulsive potential energy as a result of this effect. However, the concurrent effects of the salt addition may have a more severe effect on both the potential difference between the surface of the particle and the intermicellar solution and the degree of interaction at a given value of d.

The Interplay of the Various Effects at Constant d for Sodium Chloride Additions

It is instructive to follow the changes in these various quantities accompanying the addition of some salt to a kaolinite suspension. As a first example, let us consider the changes in the repulsive potential energy at $d = 3.0 \times 10^{-7}$ cm. for the case where sodium chloride is added to a hydrogen-saturated kaolinite suspension at pH 5.50 (Figure 40). In Figure 46, the changes in the various quantities which constitute the repulsive potential energy are shown as a function of the amount of sodium chloride added. An examination of Figures 40 and 46 shows that although the interaction ($1 - \tanh Xd$) and potential difference (γ^2) tend to depress the repulsive potential energy, the extremely rapid change in the charge distribution[1] accounts for the rise in the repulsive potential energy in the range of sodium chloride concentrations of 0.000-0.003 meq./ml. Beyond this point, the decrease in the potential difference and the interaction outweigh the increase in the repulsive potential energy attributable to the changes in charge distribution. Consequently, the total effect is one of decreasing V_R with increasing additions of sodium chloride.

One of the striking features of Figure 46 is the relatively small change occuring in γ^2. This shows that the hydroxyl ion adsorption at a pH value as low as 5.50 is still great enough to yield values of

[1] The constants 32 KT are included in the curve showing the changes in n/X so that the product of the three curves at any given value of the abscissa is equal to the repulsive potential energy in ergs/sq. cm. at that value of the abscissa. This is also true for Figure 47.

γ^2 very close to unity. The depression of γ^2 with the addition of sodium chloride is not caused by a change in the total charge of the particle (σ is assumed constant throughout the addition of sodium chloride), but reflects the changes in the potential difference between the surface of the particle and the intermicellar solution resulting from the increase in the chemical potential of the intermicellar solution. In other words, the addition of sodium chloride raises the reference level for ψ_0. This is expressed by the inverse relationship between n and Z in Equation (10).

With these points in mind, it is possible to depict the changes in the double layer accompanying the addition of sodium chloride. First of all, the addition of this salt depresses the double layer, i.e., X increases according to Equation (8). This depression of the double layer affects the repulsive potential energy in two ways: (1) It concentrates the charge of the diffuse layer (n/X increases), and (2) it lessens the interaction at a given value of d (Xd increases and $1 - \tanh Xd$ decreases). At the same time, the addition of this salt raises the reference level for ψ_0. The net effect of these changes is an initial rise in V_R due to a rise in the distribution function more rapid than the depression of the interaction and potential functions, and a subsequent decay in V_R caused by a fall in the interaction and potential functions more rapid than the rise in the distribution function.

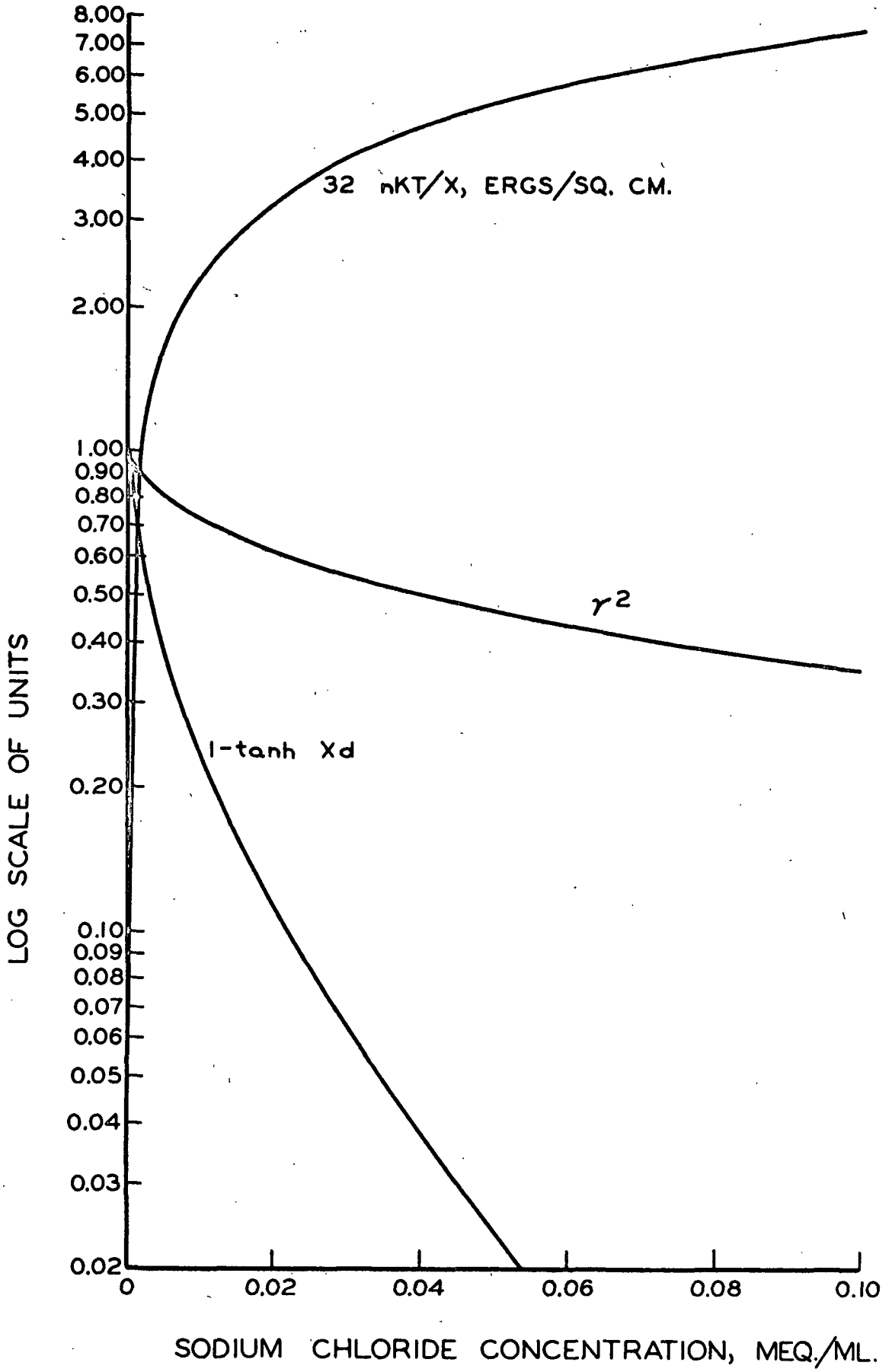

Figure 46. The Components of the Repulsive Potential Energy for the Addition of Sodium Chloride to a Hydrogen-Saturated Kaolinite Suspension

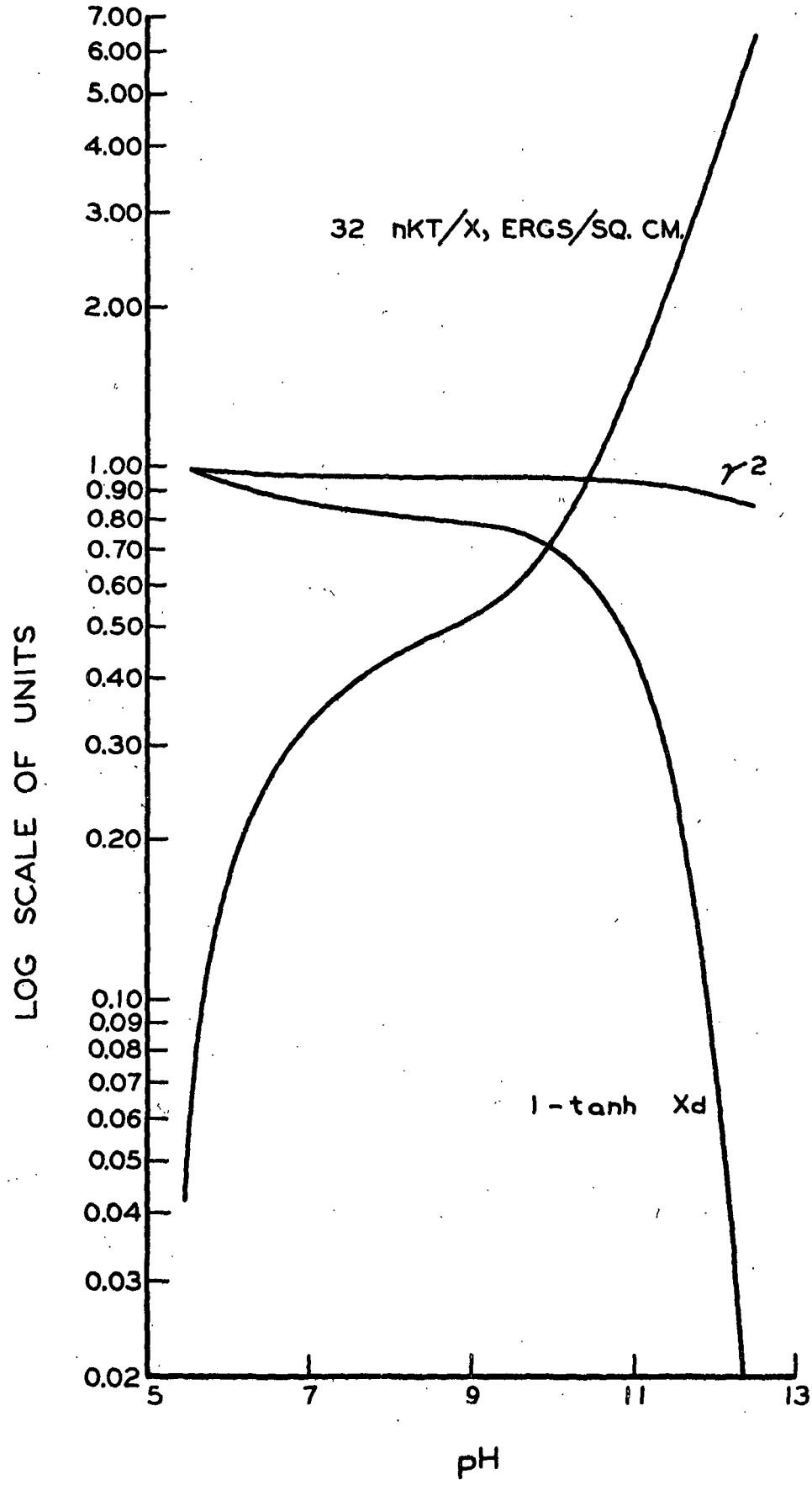

Figure 47. The Components of the Repulsive Potential Energy for the Addition of Sodium Hydroxide to a Hydrogen-Saturated Kaolinite Suspension

The Interplay of the Various Effects at Constant d for Sodium Hydroxide Additions

A somewhat different situation prevails when we consider the addition of a salt which contains an adsorbable anion. In Figure 47, the components of V_R are plotted as a function of pH for the case where only sodium hydroxide is added to a hydrogen-saturated kaolinite suspension. The actual changes in V_R occurring under these conditions are shown in Figure 32. If we compare these two figures, it is possible to show the phenomena which govern the changes in V_R at $d = 3.0 \times 10^{-7}$ cm. as sodium hydroxide is added to the system.

In the pH range 5.5-7.0, the rather rapid increase in V_R is attributable to the rapid depression of the double layer which, in turn, concentrates the charge of the diffuse layer. This is shown by the steep rise of the expression $32\ nKT/X$. However, the thickness of the double layer is of such a magnitude that although interaction rapidly decreases, it exerts, by means of the hyperbolic expression $1 - \tanh Xd$, only a small depressing effect on V_R.

In the pH range 7.0-9.5, the rise in the term $32\ nKT/X$ proceeds at a decreased rate. This occurs because small additions of sodium hydroxide cause large changes in pH in this range. The situation is quite similar to the titration of a weak acid with a strong base. Again the concurrent effect of interaction is small ($1 - \tanh Xd$ decreases only slightly) and the net effect is a slow rise in V_R in this range which is attributable almost entirely to the changes in charge distribution.

From a pH of 9.5 to 11.0, the distribution function again rises steeply and accounts for the rapid rise of V_R in this range. At pH's beyond 11.0, the addition of sodium hydroxide not only appreciably decreases the interaction at $d = 3.0 \times 10^{-7}$ cm., but also profoundly alters the effect of the interaction on the repulsive potential energy. As a result, $1 - \tanh Xd$ decreases far more rapidly than $32\ nKT/X$ increases with the net effect that the repulsive potential energy drops off sharply.

One of the most interesting features of Figure 47 is the magnitude and constancy of γ^2. This term stays relatively constant because the increase in total charge caused by greater hydroxyl ion adsorption at higher pH's (Figure 24) almost exactly compensates for the rise in the reference potential for ψ_o. The fact that the magnitude of γ^2 is very near the maximum possible value (1.0) indicates that any additional adsorption would yield only a very small increase in the repulsive potential energy. Since it is apparent that the combined effects of total charge and potential play a minor role in the addition of neutral salts (Figure 46) and an insignificant role in the addition of sodium hydroxide, it would seem these effects have little relationship to flocculation and dispersion of kaolinite suspensions. However, there is one case in which these effects could possibly play a major role.

The Effects of Acid Addition

Let us consider a hypothetical addition of an acid to a kaolinite-water suspension. Although this would increase the distribution function

in a manner somewhat similar to Figure 47 the γ^2 term would now decrease much more rapidly because of a twofold effect: (a) the total charge would decrease because of the decrease in hydroxyl ion adsorption accompanying the addition of the acid (Figure 24), and (b) the potential difference between the surface of the particle and the intermicellar solution would decrease because the potential of the intermicellar solution would increase with increasing acid addition. Even if the acid anions were adsorbed, it can be shown that this would tend to impede the decay of γ^2 only slightly.

The General Pattern of Dispersing Agent Action

Let us now broaden the discussion of the double layer phenomena from one value of d to all values of d, and from the repulsive potential energy to the total potential energy. When this is done, a distinct pattern for the mechanism of dispersing agent action emerges. Although this discussion will be limited to the double layer phenomena accompanying the addition of sodium hydroxide to a kaolinite suspension, it can be shown that an almost identical pattern prevails for the addition of sodium citrate. In fact, the same general pattern will persist for any dispersing agent which functions through the adsorption of its anion.

The first point which must be recognized is that the combined contribution of total charge and potential between the surface of the particle and the intermicellar solution to both the repulsive potential energy and the total potential energy remains essentially constant throughout the addition of the dispersing agent. This is shown by the

constancy of the γ^2 term in Figure 47.[1] Since the slight variations in these effects constitute only a minor correction to the over-all picture, it is possible to neglect their influence altogether.

The most important effect of the initial additions of dispersing agents is the depression of the diffuse part of the double layer. In so doing, the charge in this diffuse layer is concentrated in a smaller volume and at a distance closer to the particle bearing the double layer. The result is that the interaction of the diffuse layers of two particles—which is responsible for the repulsion between the particles—is reduced at large distances of separation. This is shown in Figure 43. At $d = 28 \times 10^{-7}$ cm., the total potential energy is greater at the lower pH values. However, at some lesser distance of separation, the value of V_R alone will be greater after the addition of the dispersing agent than before because the diffuse charge is now more concentrated. This is mathematically expressed by the fact that n/X must rise as dispersing agent is added, whereas there will always be some value of d for which the expression $1 - \tanh Xd$ will, after the addition of the dispersing agent, be at least equal to this same expression before the addition of the dispersing agent. Consequently, the product of these two terms—which is essentially V_R—will always be greater at some small value of d after the addition of dispersing agent than at a large value of d before the dispersing agent has been added.

[1] The same situation prevails for the addition of sodium citrate. If the abscissa were comparable (the logarithm of the sodium citrate concentration), the resulting γ^2 curve would be virtually undistinguishable from that obtained in Figure 47.

As the dispersing agent is added in increasing amounts, the advantageous effect of the diffuse layer depression is overridden by another circumstance. Since the center of charge of the diffuse layer comes closer to the particle surface as the collapse is continued, the particles themselves must come closer and closer together before any appreciable interaction can occur. Eventually, the proximity of the center of charge to the particle surface is such that the attractive forces are appreciable when the particles are close enough to permit their diffuse layers to interact. Even though the repulsive potential energy would be quite large when the diffuse layers did interact, the attractive potential energy at values of $\underline{d}$ in the range $0\text{-}3.0 \times 10^{-7}$ cm. rises more rapidly than the repulsive potential energy. This is demonstrated by the curve for pH 12.0 in Figure 43. It is apparent from Figure 41 that $\underline{V}_R$ at pH 12.0 and $\underline{d} = 1.0 \times 10^{-7}$ cm. is quite large, but $\underline{V}_A$ at this value of $\underline{d}$ is such that $\underline{V}_R + \underline{V}_A$ at these conditions is quite small (Figure 42). Figure 43 does not show the curve for pH 12.5, but at this pH, $\underline{V}_R + \underline{V}_A$ is negative for all values of $\underline{d}$. This represents the case where so much dispersing agent had been added and the diffuse layer was so depressed that attractive forces predominated before any substantial interaction could occur.

This entire picture points to one inescapable fact: That the dispersion of kaolinite suspensions at solids contents greater than about 75% is, in terms of the Verwey and Overbeek theory, an impossibility. At solids contents above this value, the average distance between particles decreases sharply and approaches the distance of separation at which the

potential energy barrier exists. The limitation, then, is imposed by the value of $\underline{A}$ in Equation (4)--a constant characteristic of the mineral itself. Because the magnitude of γ^2 is, for sodium hydroxide, very near its limiting value of 1.0, a new dispersing agent can offer little or no improvement in the total potential energy. Since the terms $\underline{n}$ and $\underline{X}$ are implicit in each other, we can do no more to cause $\underline{n}/\underline{X}$ to rise without lowering the value of $\underline{d}$ at which interaction will occur than can be done with sodium hydroxide. The only possibility is to change the attractive potential energy at small values of $\underline{d}$, and this can only be done by changing $\underline{A}$.

GENERAL SUMMARY

The material presented in this paper may be summarized as follows:

1. A general method for measuring the adsorption of various anions on kaolinite has been presented. Using this method, the adsorption of citrate ions and hydroxyl ions on kaolinite has been described over the alkaline pH range. Previous measurements of the chloride ion adsorption in the alkaline pH range have been essentially substantiated.
2. The competition of the various anions for adsorption sites on the kaolinite particle has been discussed. The preference kaolinite exhibits for the adsorption of hydroxyl ions in deference to other anions has been amply demonstrated.
3. It has been shown that the adsorption of citrate ions and hydroxyl ions does not occur primarily on the edges or faces of the kaolinite crystal, but probably occurs rather uniformly over the entire surface of the clay particle.
4. A mathematical analysis of the efficiency of separation of a monodisperse fraction of kaolinite has been presented. Using this method, it is possible to obtain the profile of an isolated fraction or to calculate the number of siphonings required to achieve a desired separation. The method is generally applicable to any fractionation by sedimentation, and is particularly useful in determining the errors in isolating a monodisperse fraction where the upper boundary is less than twice the lower boundary.

5. The applicability of the Verwey and Overbeek theory to the stability of kaolinite-water systems has been tested. Through the use of the adsorption measurements, all quantities pertinent to the theory have been calculated for a great variety of circumstances. It has been shown, with no overt contradictions, that this theory will explain a great deal of the viscous behaviour of aqueous kaolinite suspensions.

6. A mechanism for the flocculation and deflocculation of aqueous kaolinite suspensions has been formulated. In essence, the mechanism is based upon three circumstances which control the repulsion between two particles. These are:

    1. The extent to which the diffuse parts of the double layers of the particles interact,

    2. The total charge of the particles and the potential existing between the surface of the particles and the intermicellar solution, and

    3. The distribution of charges in the diffuse part of each double layer.

    In most cases, the second circumstance is of minor importance. An aqueous kaolinite suspension deflocculates as dispersing agent is added because the addition of the dispersing agent concentrates the charge of the diffuse part of the double layer. In addition to this effect, the presence of the dispersing agent also brings the center of the diffuse layer charge closer to the surface of the particle. When an excess of dispersing agent is added, the center of the diffuse layer charge lies so close to the particle that attractive forces between the particles are greater than the repulsive forces which could arise from the interaction of the diffuse layers. As a result, the suspension flocculates.

LITERATURE CITED

1. Thompson, H. S. In Grim's Clay Mineralogy. p. 128. New York, McGraw-Hill, 1953.

2. McAuliffe, C. D., Hall, M. S., Dean, L. A., and Hendricks, S. B., Soil Sci. Soc. Am. Proc. 12:119-23(1947).

3. Dickman, S. R., and Bray, R. H. In Grim op. cit. p. 156.

4. Buswell, A. M., and Dudenbostel, B. F., J. Am. Chem. Soc. 63, no. 10:2544-59(Oct. 6, 1941).

5. Johnson, A. L., and Norton, F. H., J. Am. Ceram. Soc. 24, no. 6: 189-203(June, 1941).

6. Asdell, B. K., Paper Mill News 70, no. 22:82-96(May 31, 1947).

7. Asdell, B. K., Paper Mill News 71, no. 26:36-42, 82(June 26, 1948).

8. Kingery, W. D., J. Am. Ceram. Soc. 34, no. 8:242-4(Aug. 1951).

9. Verwey, E. J. W., and Overbeek, J. T. G. Theory of the stability of lyophobic colloids. New York, Elsevier Publishing Company, 1948. 205 p.

10. Verwey, E. J. W., and Overbeek, J. T. G. op. cit. p. 98-105.

11. Verwey, E. J. W., and Overbeek, J. T. G. op. cit. p. 97.

12. Verwey, E. J. W., and Overbeek, J. T. G. op. cit. p. 24, 83.

13. Hasted, J. B., Ritson, D. M., and Collie, C. H. In Robinson and Stokes' Electrolyte solutions. p. 19. London, Butterworths Scientific Publications, 1955.

14. Verwey, E. J. W., and Overbeek, J. T. G. op. cit. p. 30-2.

15. Davis, L. E. Donnan equilibria and suspension effects in colloidal clay systems. Doctor's Dissertation. p. 12-13. Berkeley, Cal., University of California, 1941.

16. Donnan, F. G., Chem. Rev. 1, no. 1:73-90(April, 1924).

17. Low, P. F., Soil Science 77, no. 1:29-41(Jan. 1954).

18. Van Slyke, D. D., and Folch, J. J., J. Biol. Chem. 136, no. 1: 509-41(1940).

19. Van Slyke, D. D., Plazin, J., and Weisiger, J. R., J. Biol. Chem. 191:299-304(1951).

20. Van Slyke, D. D., Steele, R., and Plazin, J., J. Biol. Chem. 192, no. 2:769-805(1951).

21. Hemstock, G. A., and Swanson, J. W., Tappi 39, no. 1:35-9(Jan. 1956).

22. Jenny, H., Nielsen, T. R., Coleman, N. T., and Williams, D. E., Science 112:164-7(Aug. 11, 1950).

23. Samson, H. R. The deflocculation of kaolinite suspensions. Doctor's Dissertation. p. 17, 49, 93. London, University of London, 1953.

24. Norton, F. H., and Johnson, A. L., J. Am. Ceram. Soc. 27:77-80(1944).

25. Samson, H. R. op. cit. p. 91.

26. Verwey, E. J. W., and Overbeek, J. T. G. op. cit. p. 110.

27. Overbeek, J. T. G., and Sparnaay, M. J., J. Colloid Sci. 7:343-5 (1952).

APPENDIX I

THE DISSOCIATION OF CITRIC ACID

All calculations in this paper have been based on the assumption that all citrate ions are present in the trivalent form. If any other forms of this anion were present, an error would be imparted in two of the calculated quantities: (a) the surface charge density (σ) because the adsorption of a bivalent citrate ion, for instance, would endow the particle with two electronic charges rather than three, and (b) the hydroxyl ion adsorption because the number of sodium ions associated with an adsorbed citrate ion would be less than three if the adsorbed ion were not trivalent. However, the assumption introduces only a negligible error over the range of pH values considered.

This may be shown by the following calculation. The dissociation constants for citric acid are

$K_1 = 8.4 \times 10^{-4}$ for the first hydrogen,

$K_2 = 1.8 \times 10^{-5}$ for the second hydrogen, and

$K_3 = 4.0 \times 10^{-6}$ for the third hydrogen.

From the definition of these constants, it can be shown that the ratio of trivalent citrate ions to bivalent citrate ions is given by the expression $K_3/(H^+)$ where (H^+) is the hydrogen ion concentration. Furthermore, the ratio of trivalent citrate ions to monovalent citrate ions is equal to $K_2 K_3/(H^+)^2$; and the ratio of trivalent citrate ions to undissociated citric acid is $K_1 K_2 K_3/(H^+)^3$. On the basis of these expressions,

it can be shown that at a pH of 6.50 (the lowest pH obtained in the experiments with sodium citrate), 92.5% of the citrate ions are present in the trivalent form, 7.5% are present in the bivalent form, and essentially none are present as either monovalent citrate ions or undissociated citric acid. The average valence of the ions in such a mixture is 2.925. Thus, an error of no more than 2.5% would be introduced into each of the calculations. If a pH of 7.50 is considered, the average valence is calculated to be 2.993. This obviously injects a negligible error.

APPENDIX II

METHOD FOR THE DETERMINATION OF SODIUM IN SOLUTIONS CONTAINING SODIUM CHLORIDE, SODIUM CITRATE, AND SODIUM HYDROXIDE

Approximately 30-33 ml. of Amberlite IRA-401 anion-exchange resin were placed in a 50-ml. buret. Chloride-free 2N sodium hydroxide was passed through the column until the effluent gave a negative chloride test with acidified silver nitrate solution. During this regeneration, the column was backwashed several times to expand the resin. After regeneration, the column was washed with purified water until the effluent was both neutral and chloride-free.

A sample containing less than 1.0 meq. of sodium ion was pipetted into the column. The remaining space in the buret was then completely filled with purified water. A 125-ml. flask was placed under the buret to collect the effluent. The stopcock was opened and the flow rate was adjusted to 7-10 ml./min. This was determined by starting the stopwatch when the meniscus passed the zero mark on the buret and noting the buret reading after one minute had expired. When the liquid level reached the resin bed, the buret was immediately filled with purified water without disturbing the stopcock setting. This washing procedure was carried out a second time and the column was shut off after the sample and two washes had passed through. About 4-6 drops of phenolphthalein were added to the effluent and the sample was then immediately titrated with standardized 0.1N sulfuric acid contained in either a ten-milliliter buret or a two-milliliter microburet. The amount of acid consumed is equivalent to the amount of sodium present in the sample.

The column was regenerated after two milliequivalents of sodium ion had been passed through. The regeneration procedure was identical to that used in the initial preparation of the column.

APPENDIX III

SAMPLE CALCULATION OF THE CITRATE ION ADSORPTION AND THE APPARENT HYDROXYL ION ADSORPTION

The following calculation is based on the information in Table VI (page 40). The density of water is 0.998 g./ml. and the equivalent weight of sodium citrate is 86.0 mg./meq.

1. Weight of ovendry clay

   Cells 6 and 9 $0.1356 \times 36.8 = 4.99$ g.

2. Total fluid volume

   Cells 6 and 9 $50.0 + 1.0 + 1.0 + 2.0 + 0.864(36.8/0.998)$

   $= 85.9$ ml.

3. Sodium citrate found

   Cell 6 $(1435 \times 85.9)/(12{,}850 \times 2.00) = 4.80$ mg.

   Cell 9 $(1444 \times 85.9)/(12{,}850 \times 2.00) = 4.83$ mg.

4. Citrate ion adsorption ($\underline{x}/\underline{M}$)

   Cell 6 $(2.998 \times 2.00 - 4.80)/4.99 = 0.240$ mg./g.

   Cell 9 $(2.998 \times 2.00 - 4.83)/4.99 = 0.234$ mg./g.

5. Initial sodium ion content of the system

   Cells 6 and 9 $0.1004(1.00) + 0.1000(1.00) + 2.00(2.998/86.0)$

   $= 0.270$ meq.

6. Sodium ions associated with adsorbed sodium citrate

   Cell 6 $0.24(4.99)/86.0 = 0.014$ meq.

   Cell 9 $0.23(4.99)/86.0 = 0.014$ meq.

7. Sodium ions found

Cell 6 $0.0638(85.9/25.0) = 0.219$ meq.

Cell 9 $0.0639(85.9/25.0) = 0.219$ meq.

8. Apparent hydroxyl ion adsorption ($\underline{y}'/\underline{M}$)

Cell 6 $(0.270 - 0.219 - 0.014)/4.99 = 0.0074$ meq./g.

Cell 9 $(0.270 - 0.219 - 0.014)/4.99 = 0.0074$ meq./g.

APPENDIX IV

DERIVATION OF THE EQUIVALENT RADIUS OF CENTRIFUGATION AND THE AVERAGE DISTANCE OF TRAVEL OF A PARTICLE UNDER A VARYING FORCE FIELD

According to Stokes's law, the instantaneous velocity ($\underline{V}'$) of a particle moving in a viscous medium is related to the instantaneous acceleration ($\underline{G}'$) on the particle by the equation

$$\underline{V}' = \frac{2\,(d_1 - d_2)\,\underline{G}'\,r^2}{9\eta} \qquad (21)$$

Since we chose to view the situation as a sedimentation under a constant force field, we may describe the average velocity of the particle in the siphoning zone ($\underline{V}_o$) in terms of a constant acceleration ($\underline{G}$) for this zone. Thus

$$\underline{V}_o = \frac{2\,(d_1 - d_2)\,\underline{G}\,r^2}{9\eta} \qquad (22)$$

We will now define the equivalent radius of centrifugation $\underline{R}'$ as that distance for which

$$\underline{G} = \underline{R}'\,\omega^2 \qquad (23)$$

Combining Equations (22) and (23), we obtain

$$\underline{V}_o = \frac{2\,(d_1 - d_2)\,\underline{R}'\,\omega^2\,r^2}{9\eta} \qquad (24)$$

and since $\omega = 2\pi N$, Equation (24) may be written as

$$\underline{V}_o = \frac{8\pi^2 (\underline{d}_1 - \underline{d}_2)\, \underline{R}'\, \underline{N}^2\, \underline{r}^2}{9\eta} \qquad (25)$$

However, the average velocity of the particle in the siphoning zone may be described by the boundary conditions. Thus

$$\underline{V}_o = \frac{\underline{R}_2 - \underline{R}_1}{\underline{t}} \qquad (26)$$

Substituting this value of $\underline{V}_o$ in Equation (25) and rearranging, we obtain

$$\underline{t} = \frac{9\eta}{8\pi^2 (\underline{d}_1 - \underline{d}_2)\, \underline{N}^2\, \underline{r}^2} \cdot \frac{\underline{R}_2 - \underline{R}_1}{\underline{R}'} \qquad (27)$$

In Equation (15) (page 47) we found that

$$\underline{t} = \frac{9\eta \ln (\underline{R}_2/\underline{R}_1)}{8\pi^2 (\underline{d}_1 - \underline{d}_2)\, \underline{N}^2\, \underline{r}^2} \qquad (15)$$

Comparing Equation (15) with Equation (27), it is obvious that

$$\underline{R}' = \frac{\underline{R}_2 - \underline{R}_1}{\ln (\underline{R}_2/\underline{R}_1)} \qquad (16)$$

which is the logarithmic mean radius of centrifugation.

By using the concept of an equivalent centrifuging radius, we inject a minimal error into the viewing of the centrifugation procedure as a sedimentation in a constant force field. We now assume that the velocity of a particular particle in the siphoning zone is independent of the

distance of that particle from the axis of rotation of the centrifuge. Consequently, we may describe the distance of travel of a particular particle (S) by the equation

$$S = \frac{8\pi^2 (d_1 - d_2) R' N^2 r^2 t}{9\eta} \qquad (28)$$

Under the conditions employed, Equation (28) reduces to

$$S = 1.88 \times 10^4 N^2 r^2 t \qquad (17)$$

where S and r are expressed in centimeters, N in revolutions per second, and t in seconds.

APPENDIX V

SIMPLIFIED METHOD FOR THE SOLUTION OF THE MÜLLER AND RELATED EQUATIONS

Equation (18) (page 84) may be written in the form

$$\underline{r} = (\underline{k})\ (\underline{a}) \qquad (29)$$

where $\underline{k}$ is a function of $\underline{b}/\underline{a}$ and is equal to the expression contained in the braces of Equation (18) multiplied by 8/3. The relationship between $\underline{k}$ and $\underline{b}/\underline{a}$ is shown in Figure 48.

Figure 49 shows the relationship between the specific surface area and $\underline{b}/\underline{a}$ for several values of the equivalent spherical radius of the particle ($\underline{r}$). These curves were derived from a combination of Equations (19) and (29) assuming a density for the kaolinite of 2.6 g./cc. Figure 50 is a plot of Equation (20) and shows the per cent face area as a function of $\underline{b}/\underline{a}$. As in Figure 48, the actual size of the particle is immaterial.

These figures were used in the following manner. From a knowledge of the specific surface area (obtained by nitrogen adsorption measurements) and the equivalent spherical radius of the particle (obtained by the fractionation procedure), the value of $\underline{b}/\underline{a}$ may be read from Figure 49. Using this value of $\underline{b}/\underline{a}$, the per cent face area is read directly from Figure 50. The semidiameter and semithickness of the disk-shaped particle are obtained by using the value of $\underline{b}/\underline{a}$ to determine $\underline{k}$ (Figure 48) and by calculating ($\underline{a}$) from the appropriate values of $\underline{r}$ and $\underline{k}$ in Equation (29). The value of $\underline{b}$ is obviously equal to ($\underline{b}/\underline{a}$) ($\underline{a}$).

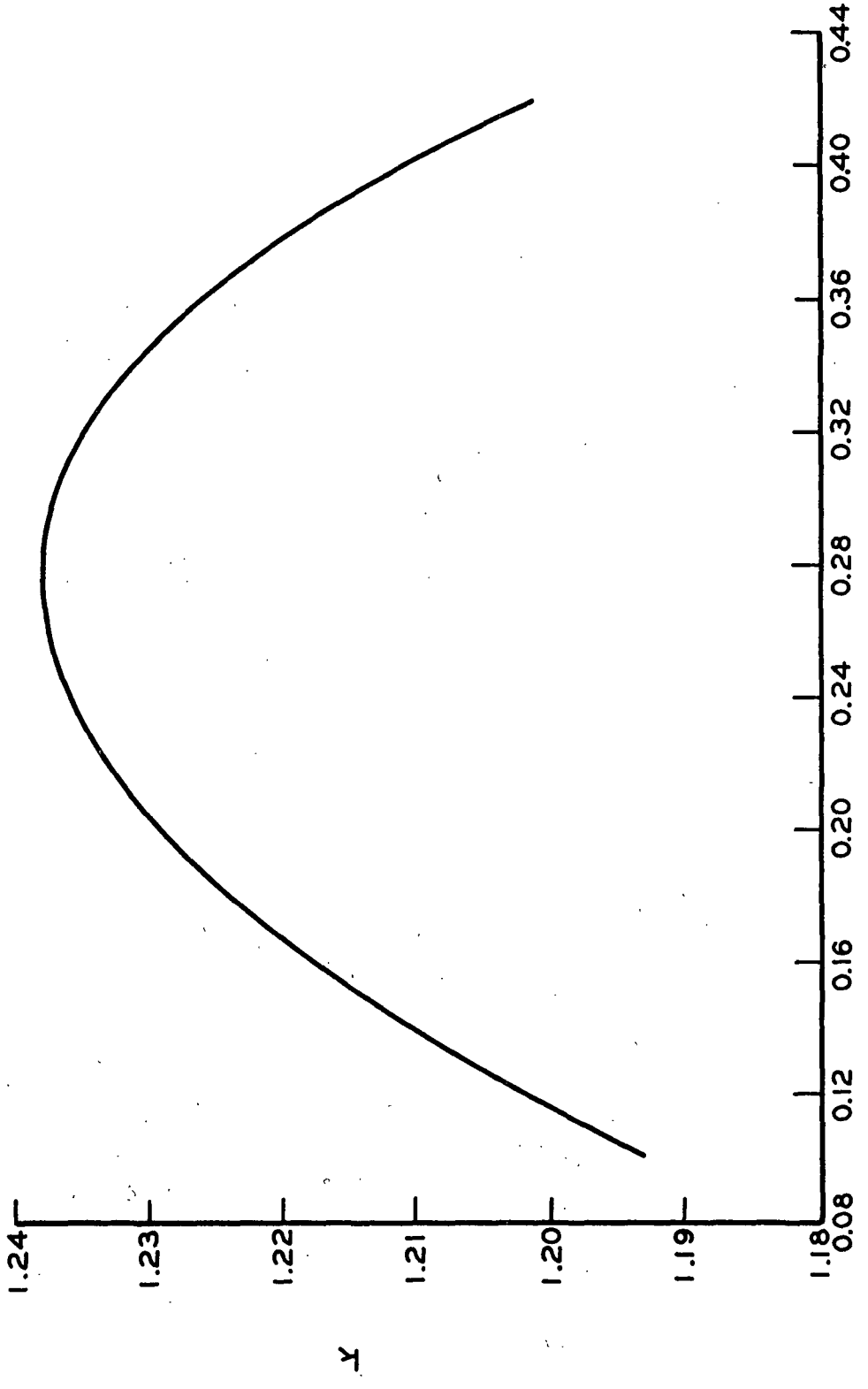

Figure 48. A Portion of the Miller Equation

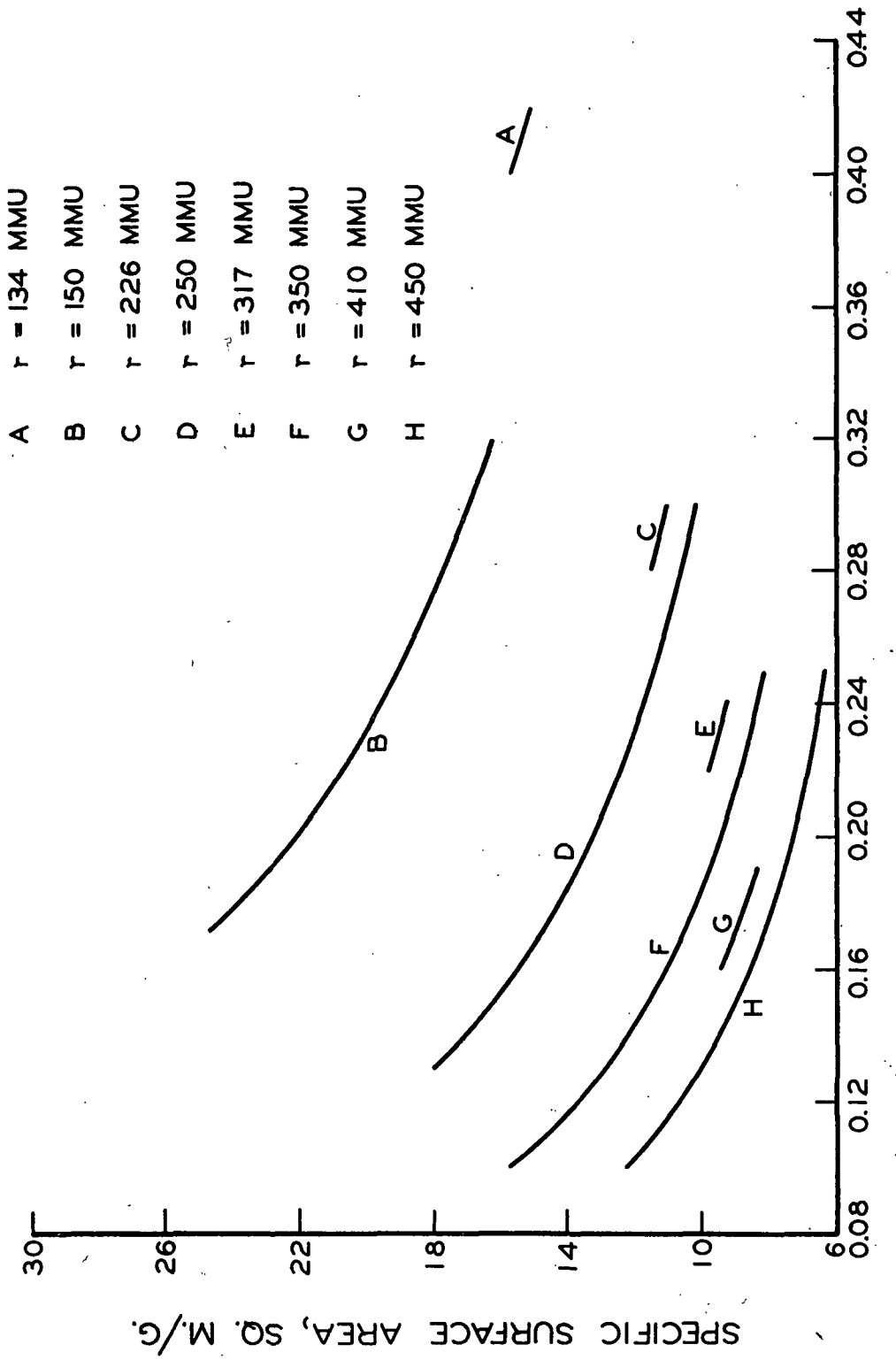

Figure 49. The Ralationship Between the Specific Surface Area, Thickness-to-Diameter Ratio, and Equivalent Spherical Radius for Kaolinite Particles

$\underline{d}_1$ = 2.6 g./cc.

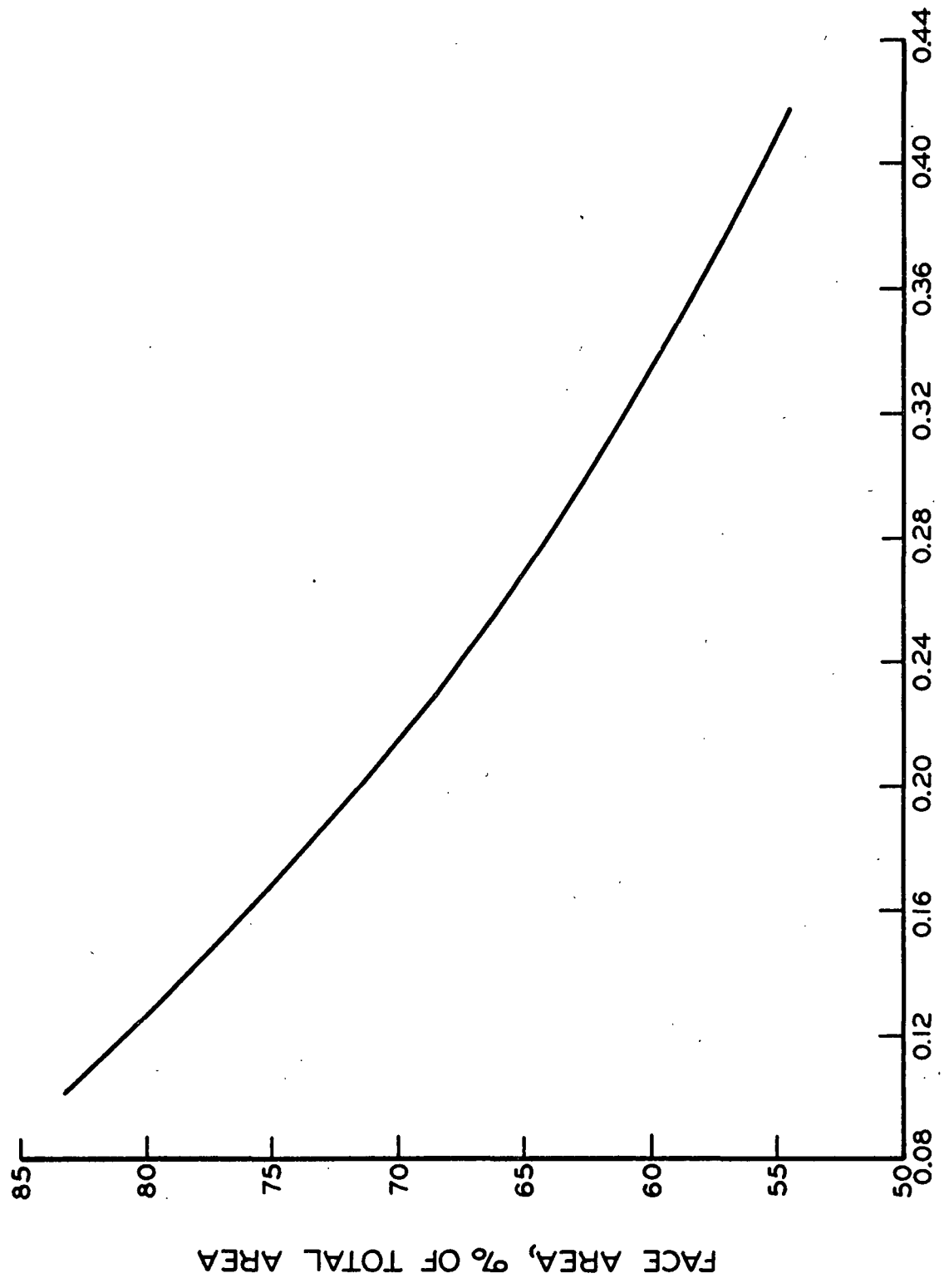

Figure 50. The Relationship Between the Face Area and the Thickness-to-Diameter Ratio for a Disk-Shaped Particle

APPENDIX VI

SAMPLE CALCULATION OF THE POTENTIAL ENERGY FUNCTIONS

This sample shows the calculation of the total potential energy $(\underline{V}_R + \underline{V}_A)$ at the following conditions:

$\underline{d} = 3.0 \times 10^{-7}$ cm.

pH = 9.00

Sodium citrate added = 0.60% based on the clay

The following constants are used in the calculation:

$\pi = 3.14$

$\underline{D} = 78.9$

$\underline{K} = 1.380 \times 10^{-16}$ ergs/°K./ion

$\underline{T} = 296$ °K.

$\epsilon = 4.80 \times 10^{-10}$ e.s.u./ion

$\underline{a}' = 1.076 \times 10^{-5}$ sq. cm./g. (the specific surface area for fraction 1 kaolinite)

$\underline{N}_o = 6.02 \times 10^{20}$ ions/meq. (the Avogadro number)

$\underline{m} = 86.0$ mg./meq. (the equivalent weight of sodium citrate)

1. The calculation of σ

$\underline{x}/\underline{M} = 0.167$ mg./g. (Figure 20)

$\underline{y}/\underline{M} = 0.0139$ meq./g. (Figure 24)

$$\sigma = \frac{\underline{N}_o \epsilon}{\underline{a}'} \left[\frac{\underline{x}/\underline{M}}{\underline{m}} + \underline{y}/\underline{M} \right] \qquad (30)$$

$$= \frac{(6.02 \times 10^{20})(4.80 \times 10^{-10})}{1.076 \times 10^{5}} \left[\frac{0.167}{86.0} + 0.0139\right]$$

$$= 4.26 \times 10^{4} \text{ e.s.u./sq. cm.}$$

2. The calculation of $\underline{n}$

The sodium ion content on the intermicellar solution is 0.360 meq. in 86.0 ml. (Figure 31). The hydrogen ion contribution to $\underline{n}$ is negligible.

$$\underline{n} = 0.360\ \underline{N}_o/86.0 = (0.360)(6.02 \times 10^{20})/86.0$$

$$= 2.52 \times 10^{18} \text{ ions/ml.}$$

3. The calculation of γ^2

The parameter $\underline{P}$ is introduced and defined as

$$\underline{P} = \sigma \sqrt{\pi/2\ \underline{D}\ \underline{K}\ \underline{T}\ \underline{n}} \tag{31}$$

Thus, Equation (10) may be written as

$$\underline{Z}/2 = \sinh^{-1} \underline{P} \tag{32}$$

However, the inverse hyperbolic sine of $\underline{P}$ may be defined by the expression

$$\sinh^{-1} \underline{P} = \ln(\underline{P} + \sqrt{\underline{P}^2 + 1}) \tag{33}$$

Thus,

$$\underline{Z}/2 = \ln(\underline{P} + \sqrt{\underline{P}^2 + 1}) \tag{34}$$

and, from Equation (6),

$$\gamma = \frac{\underline{P} + \sqrt{\underline{P}^2 + 1} - 1}{\underline{P} + \sqrt{\underline{P}^2 + 1} + 1} \qquad (35)$$

$$\underline{P} = 4.26 \times 10^4 \sqrt{3.14/2(78.9)(1.380 \times 10^{-16})(296)(2.52 \times 10^{18})}$$

$$= 18.7$$

$$\gamma = \frac{18.7 + \sqrt{(18.7)^2 + 1} - 1}{18.7 + \sqrt{(18.7)^2 + 1} + 1} = 0.947$$

$$\gamma^2 = (0.947)^2 = 0.898$$

4. The calculation of $\underline{X}$

$$\underline{X} = \sqrt{8\pi n \epsilon^2 \underline{V}^2/\underline{D}\ \underline{K}\ \underline{T}} \qquad (8)$$

$$= \sqrt{\frac{(8)(3.14)(2.52 \times 10^{18})(4.80 \times 10^{-10})^2\ (1)^2}{(78.9)(1.380 \times 10^{-16})(296)}}$$

$$= 2.13 \times 10^6\ \text{cm.}^{-1}$$

5. The calculation of $(1 - \tanh \underline{Xd})$

$$\underline{Xd} = (2.13 \times 10^6)(3.0 \times 10^{-7}) = 0.639$$

$$\tanh \underline{Xd} = 0.565$$

$$1 - \tanh \underline{Xd} = 0.435$$

6. The calculation of $\underline{V_R}$

$$\underline{V_R} = (32\ \underline{n}\ \underline{K}\ \underline{T}\ \gamma^2/\underline{X})(1 - \tanh \underline{Xd}) \qquad (5)$$

$$= \frac{(32)(2.52 \times 10^{18})(1.380 \times 10^{-16})(296)(0.898)(0.435)}{(2.13 \times 10^{6})}$$

$$= 0.604 \text{ ergs/sq. cm.}$$

7. The calculation of $\underline{V}_{\underline{A}}$

$$\underline{A} = 4.0 \times 10^{-12} \text{ ergs} \quad \text{(page 117)}$$

$$\underline{V}_{\underline{A}} = -\underline{A}/48\,\pi\underline{d}^2 \qquad (4)$$

$$= -(4.0 \times 10^{-12})/(48)(3.14)(3.0 \times 10^{-7})^2$$

$$= -0.295 \text{ ergs/sq. cm.}$$

8. The calculation of the total potential energy

$$\underline{V}_{\underline{R}} + \underline{V}_{\underline{A}} = 0.604 - 0.295 = 0.309 \text{ ergs/sq. cm.}$$